Motor neuron differentiation in the developing and the regenerating adult spinal cord of zebrafish *Danio rerio* (HAMILTON, 1822)

Dissertation

zur Erlangung des
Doktorgrades der Naturwissenschaften
des Fachbereichs Biologie der Universität Hamburg

vorgelegt von
Dipl.-Biol. Michell Mario Reimer
aus Siegen

Hamburg/Edinburgh,
August 2008

Genehmigt vom Department Biologie
der Fakultät für Mathematik, Informatik und Naturwissenschaften
an der Universität Hamburg
auf Antrag von Frau Priv.-Doz. Dr. C. BECKER
Weiterer Gutachter der Dissertation:
Herr Professor Dr. K. WIESE
Tag der Disputation: 24. Oktober 2008

Hamburg, den 10. Oktober 2008

Professor Dr. Jörg Ganzhorn
Leiter des Departments Biologie

Gutachter:

Herr Prof. Dr. L. Renwrantz

Frau PD Dr. C.G. Becker

1 INTRODUCTION

1.1 Aims of the study

(aim 1) Adult zebrafish, in contrast to mammals, show an amazing capacity for functional spinal cord repair (Kirsche, 1950; Becker et al., 1997; van Raamsdonk et al., 1998; Becker et al., 2004). However, cellular regeneration of spinal neurons, such as motor neurons has not been analysed. Therefore, this study asks whether motor neurons that are lost due to spinal injury regenerate in adult zebrafish and if so, what are the cellular and molecular mechanisms of neuronal regeneration.

(aim 2) In order to analyse the molecular mechanism of axonal differentiation of motor neurons, which may be recapitulated during regeneration, the well established system of axon growth from so-called primary motor neurons in embryonic zebrafish was used (Beattie, 2000). It has been shown that cell recognition molecules are important for axon growth and pathfinding (Beattie, 2000; Giger et al., 2000; Feldner et al., 2005). Therefore, this study asks which specific cell recognition molecules are necessary for correct growth of primary motor axons during embryonic development.

Together, these aims are intended to increase our understanding of motor neuron differentiation in general and during successful regeneration of the adult spinal cord in particular. Ultimately, insights from zebrafish into these evolutionarily conserved mechanisms may help to cure human conditions, such as spinal cord injury and motor neuron disease.

1.2 Zebrafish (*Danio rerio*) as a model organism

The zebrafish (*Danio rerio*) is part of the family of *Cyprinidae*. It belongs to the class of *Actinopterygii*, in the infraclass of the *Teleostei*. These 2-4 cm long freshwater fish can be found in South Asia, Northern India, Bhutan, Pakistan and Nepal.

The genome of the zebrafish is partially duplicated in evolution (Taylor et al., 2001). Therefore a substantial number (up to 30%) of mammalian genes have two orthologs in the zebrafish genome. Conveniently, the zebrafish genome is now fully sequenced (www.ensembl.org, Sanger Institute), providing easy access to gene sequences in-silico. This facilitates the design of transgenic reporter lines, which are relatively easy to generate in zebrafish, and of morpholinos (antisense-oligo nucleotides) for gene knock-down studies. The possibility to inject RNA overexpression constructs as well as morpholinos from the one cell stage egg and the transparancy of embryos makes the zebrafish an ideal model system for studying developmental processes in vivo (Nasevicius and Ekker, 2000; Malicki et al., 2002).

Furthermore, zebrafish development is well characterised and a variety of transgenic reporter lines that express fluorescent proteins in motor neurons as well as antibodies that label motor neurons are available (Renoncourt et al., 1998; Higashijima et al., 2000; William et al., 2003; Flanagan-Steet et al., 2005).

1.3 Mammals, including humans, do not regenerate the lesioned or diseased CNS.

CNS injury or disease in mammals often causes irreversible loss of motor and sensory function (Dijkers, 2005). The properties of axonal regeneration and its failure in mammals has been extensively studied. It is thought that the lack of

axonal regeneration in mammals is due to inhibitory molecules, such as myelin-associated inhibitors (e.g. nogo-A), myelin-associated glycoprotein, and oligodendrocyte myelin glycoprotein, that prevent axon outgrowth (Spencer et al., 2003; Schwab, 2004). Other inhibitory molecules are part of the extracellular matrix, such as chondroitin sulfate proteoglycans, which are found in the glial scar (Carulli et al., 2005). Another reason for regeneration failure is inflammation, which often leads to a further increase of damage to the CNS (Bambakidis et al., 2008).

The regeneration and replacement of lost neurons in adult mammals is not so well-characterised. Studies have show that neuronal progenitor cells in the subventricular zone and dentate gyrus in the adult mammalian brain proliferate and differentiate into neurons (Johansson, 2007). In the spinal cord of rats, proliferation and differentiation of glial progenitor cells that give rise to astrocytes and oligodendrocytes has been demonstrated (Horner et al., 2000) but neurogenesis has never been observed. To find the signalling pathways that trigger endogenous progenitor cells to differentiate into neurons after a lesion or disease and replace lost neurons could be one way to ameliorate the devastating effects after CNS damage.

1.4 Anamniotes (amphibians and fish) have a high regenerative capacity, which includes the CNS

The zebrafish is well established as a model in developmental studies and interest in adult regeneration, e.g. of heart tissue (Poss et al., 2002) and spinal cord (Becker et al., 1997), is increasing.

Zebrafish show an impressive tissue regeneration capacity at the adult stage (Bernhardt, 1999; Becker et al., 2004). After a spinal cord lesion, zebrafish grow

an axonal bridge between the two ends of the fully transected spinal cord and regain swimming function (Becker et al., 2004). In tail regeneration paradigms in amphibians in which the tail, including the spinal cord is amputated (Echeverri and Tanaka, 2002; Beck et al., 2003) the tail is regenerating from an advancing blastema. This includes a completely regenerated spinal cord.

1.5 The zebrafish shows anatomical and functional spinal cord regeneration

In 1950, Walter Kirsche described in detail the morphological response to a complete spinal cord transection in adult teleosts (*Poecilia reticulata*) (Kirsche, 1950). Based on his morphological observations that large "ganglion cells" disappeared and later reappeared, he even hypothesized the replacement of lost neurons in response to a lesion event.

A complete transection of the spinal cord leads to loss of movement in the distal body part. Swimming performance in zebrafish has been tested in a tunnel with a constant water flow. Swimming behaviour recovered after a lesion and plateaued around 2.5 months post-lesion (van Raamsdonk et al., 1993). However, while significant recovery of swimming behaviour occurred, performance of the fish remained worse than in unlesioned fish. Another method to quantify functional recovery after a lesion is to measure spontaneous movement in an open-field setup. This test shows a recovery in swim distance at 6 weeks post-lesion, which was indistinguishable from sham (muscle)-lesioned controls (Becker et al., 2004). The difference in the results of these test paradigms may be that to be forced to swim against a flow is more challenging for the fish than to perform their normal swimming patterns. This indicates that while regeneration after spinal injury occurs, it is not perfect.

Anatomically, long-range axonal projections are destroyed after a complete transection. These include descending axons from the brainstem, intraspinal descending connections, ascending axons from dorsal root ganglia and intraspinal neurons providing sensory feedback to the brainstem. Substantial regrowth of spinal axons is only observed from brainstem neurons. Blocking the regrowth of these long-range axonal projections abolishes the capacity for functional recovery of the adult zebrafish (Becker et al., 2004). While this clearly demonstrates that axonal regrowth from the brainstem is essential for functional recovery after spinal cord injury, the plastic changes in the spinal cord, e.g. regeneration of target neurons, remain largely unknown.

The signalling cascade leading to motor neuron differentiation during development is well understood and is evolutionarily conserved. Progress in recent years in identifying extracellular signals and cell-intrinsic differentiation programs has led to a general model of early generation of different classes of neurons. Most of this data were obtained from studies with chick and mouse embryos, but motor neuron differentiation is very similar in embryonic zebrafish (Park et al., 2002). Generally, a gradient of the morphogen *sonic hedgehog* (*Shh*) regulates the expression of a set of transcription factors in progenitor cells of the ventral spinal cord. The pattern of transcription factor expression defines five domains of progenitor cells, termed p0, p1, p2, pMN and p3. Specific cell types are produced from each domain, leading to the generation of different types of interneurons and somatic motor neurons. The pMN domain gives rise to motor neurons (Fig. 1). Specifically, a high concentration of *sonic hedgehog* in combination with the transcription factors *nkx6.1*, *pax6* and *olig2* define the motor neuronal cell fate in progenitor cells (Jessell, 2000; Briscoe and Ericson, 2001; Shirasaki and Pfaff, 2002). The resulting immature neurons are positive

for the motor neuron marker *islet1/2* and *HB9* (Higashijima et al., 2000; Flanagan-Steet et al., 2005).

The question arises, whether some or all of these mechanisms are re-capitulated during adult motor neuron regeneration.

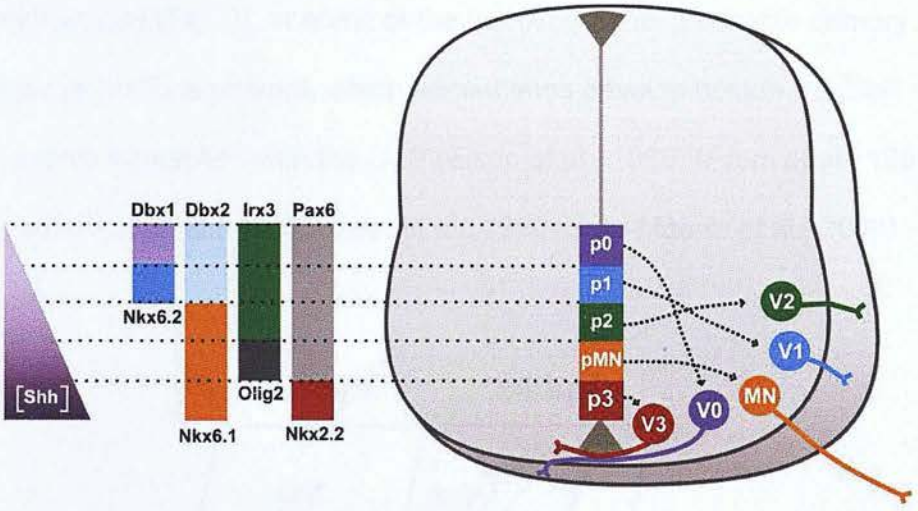

Fig. 1: Spinal cord neurons. Schematic diagram of the development of early classes of ventral spinal cord neurons in mice. A gradient of the morphogen *Sonic hedgehog* (*Shh*) regulates the expression of a set of transcription factors in progenitor cells of the ventral spinal cord. The pattern of transcription factor expression defines five domains of progenitor cells, termed p0, p1, p2, pMN, and p3. A specific cell type is produced from each domain, leading to the generation of V0, V1, V2, and V3 interneurons and somatic motor neurons (MN). After (Kullander, 2007).

1.6 Primary motor neurons in developing zebrafish provide a model for studying motor axon differentiation

A widely used model system to study signals for early motor axon growth, is the outgrowth of primary motor axons in zebrafish embryos (Beattie, 2000). This is because there are only three primary motor neurons per spinal hemi-segment. These neurons grow axons out of the spinal cord following a common path in the middle of each segment to the horizontal myoseptum. From there the axons paths diverge. The axon of the caudal primary motor neuron (CaP) grows

towards the ventral somite, pioneering the ventral motor nerve. The axon of the middle primary motor neuron (MiP) follows the CaP axon up to the horizontal myoseptum where it retracts and grows towards the dorsal somite. The rostral primary motor neuron (RoP) axon takes a lateral direction from the horizontal myoseptum (Fig. 2). In some of the hemisegments a variable primary motor neuron (VaP) is present, which somethimes develop beside the CaP and mostly die from interaction with the CaP (Eisen et al., 1986; Myers et al., 1986; Westerfield et al., 1986; Eisen et al., 1990; Sato-Maeda et al., 2008).

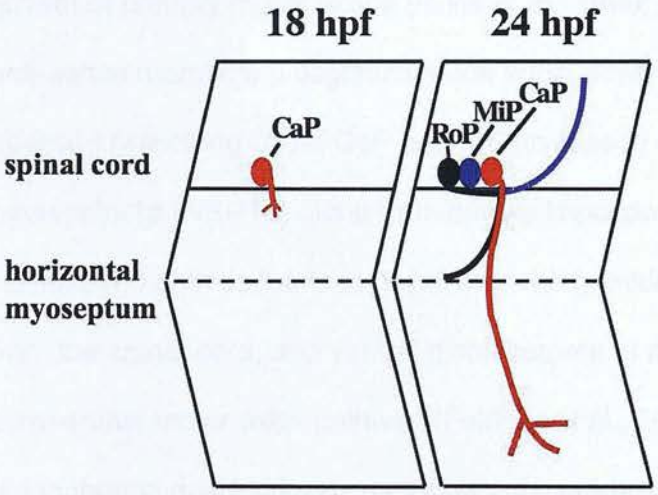

Fig. 2: Schematic illustration of primary motor axon outgrowth in embryonic zebrafish. A side view of zebrafish trunk segments at 18 and 24 hpf is given. At 18 hpf the caudal primary motor neuron (CaP) grows an axon out of the spinal cord. At 24 hpf, the axons of the middle (MiP) and rostral (RoP) primary motor neurons have followed on the common pathway to the horizontal myoseptum and the MiP has grown towards the dorsal somite. The CaP axon is the only one growing ventrally beyond the horizontal myoseptum.

1.7 Cell recognition molecules in axonal pathfinding

The molecular mechanisms underlying axonal pathfinding are pathway cues and axonal receptors. PlexinA1 to A4 are co-receptors for axon-repelling or

attracting class 3 extracellular semaphorins. It is thought that neuropilin-1 (NRP1) or neuropilin-2 (NRP2) is the ligand-binding part and plexins are the signal transducing part of semaphorin class 3 receptors (for recent review, see Kruger et al., 2005). Removing individual components from this guidance network leads to specific defects of nerve growth (Giger et al., 2000; Huber et al., 2005; Yaron et al., 2005), indicating distinct roles for different ligand/receptor combinations in the pathfinding of different axon populations. Sema3Aa and sema3Ab (zebrafish homologs of mammalian sema3A) are expressed in the trunk environment. Overexpression of either ligand reduces growth of primary motor axons (Roos et al., 1999; Halloran et al., 2000) and anti-sense morpholino oligonucleotide knockdown of sema3A1 leads mainly to aberrant branching of the CaP axon (Sato-Maeda et al., 2006). Knockdown of neuropilin-1a (NRP1a) alone or in double knockdown experiments with semaphorin ligands leads to nerve branching, additional exit points of axons from the spinal cord, and ventral displacement of neuronal somata along the extra-spinal motor axon pathway (Feldner et al., 2005). This suggests that semaphorins guide primary motor axons by repellent mechanisms via NRP1a containing axonal receptors. So far, the role of plexins has not been examined. The only class A member of the plexin family characterised in zebrafish is plexinA4, but it is not expressed in primary trunk motor neurons (Miyashita et al., 2004). Therefore, we have investigated the role of another plexinA, *plexinA3* in the outgrowth of primary motor axons. The knowledge of embryonic neurogenesis and axonal outgrowth of motor neurons may lead to further insights into mechanisms of adult spinal cord regeneration.

1.8 Summary

In this study I demonstrate for the first time that adult zebrafish are capable of regenerating motor neurons lost after spinal cord lesion. Evidence is provided that these neurons fully differentiate and are integrated into the spinal network. I identify the morphogen *shh* as one of the signals that is important for motor neuron differentiation and progenitor cell proliferation at the adult stage. Embryonic studies indicate that the cell recognition molecule *plexinA3* is pivotal for correct motor axon pathfinding. These findings provide insight into the differentiation processes of motor neurons, both in development and regeneration in a vertebrate.

2 MATERIAL AND METHODS

2.1 Materials

2.1.1 Enzymes

Restriction endonucleases	
various (5-20 U/µl)	New England Biolabs UK Ltd. (Hitchin, Hertfordshire, UK)
DNA polymerase	
PfuUltra™ HF DNA Polymerase	Stratagene (Amsterdam, NL)
Taq DNA Polymerase with Standard Taq Buffer	New England Biolabs UK Ltd. (Hitchin, Hertfordshire, UK)
Reverse Transcriptases	
SuperScript II™ RT	Invitrogen (Karlsruhe, D)
SuperScript III™ RT	Invitrogen Ltd. (Paisley, UK)
RNaseOUT™ Recombinant Ribonuclease Inhibitor	Invitrogen Ltd. (Paisley, UK)
RNasin®Plus RNase Inhibitor	Promega (Mannheim, D)
Miscellaneous	
T4 DNA Ligase	New England Biolabs UK Ltd. (Hitchin, Hertfordshire, UK)
Alkaline Phosphatase, shrimp (SAP)	Roche (Mannheim, D)
Alkaline Phosphatase	Roche Diagnostics Ltd. (Burgess Hill, UK)
Proteinase K	Roche Diagnostics Ltd. (Burgess Hill, UK)

2.1.2 Bacterial strains

XL1-Blue competent cells	Stratagene (UK)

NEB Turbo Competent *E. coli* (High Efficiency)	New England Biolabs UK Ltd. (Hitchin, Hertfordshire, UK)
dam⁻/dcm⁻ Competent E. coli	New England Biolabs UK Ltd. (Hitchin, Hertfordshire, UK)
E. Coli One Shot®TOP10	Invitrogen (Karlsruhe, D)
E. Coli DH5α	Invitrogen (Karlsruhe, D)

2.1.3 Bacterial media

All bacterial media were autoclaved before use. If nessecary Ampicillin or Kanamycin was added.

Bacterial growth media encapsulated media LB medium	QBIOgene, Fisher Scientific (UK)
LB Agar Miller Fisher BioReagents	Fisher Scientific (UK)
Antibiotics	
Ampicillin (50mg/ml in H_2O stock, 50µg/ml working solution)	
Kanamycin (50mg/ml in H_2O stock, 30µg/ml working solution)	

2.1.4 Vectors

pGEM®-T easy	Promega (Southamton, UK)	TA cloning vector
pCR®-Blunt II-TOPO®	Invitrogen (UK)	TOPO cloning vector
pCS2+MT	(Rupp et al., 1994)	mRNA overexpression vector
pBlueScript® II	Stratagene (UK)	

2.1.5 Kits

MEGAscript™ (T3/T7/SP6)	Ambion (Cambridge, UK)
mMESSAGE mMACHINE™	Ambion (Cambridge, UK)
Poly (A) Tailing Kit	Ambion (Cambridge, UK)

Rapid DNA Ligation Kit	Roche Diagnostics Ltd. (Burgess Hill, UK)
pGEM®-T easy vector system I	Promega (Southamton, UK)
Zero Blunt® TOPO® PCR Cloning Kit	Invitrogen (UK)
QIAquick™ Gel Extraction	Qiagen (Crawley, UK)
QIAquick™ PCR Purification	Qiagen (Crawley, UK)
MiniElute™ Gel Extraction Kit	Qiagen (Crawley, UK)
MiniElute™ PCR Purification Kit	Qiagen (Crawley, UK)
HiSpeed® Plasmid Midi Kit	Qiagen (Crawley, UK)
RNeasy® Midi Kit	Qiagen (Crawley, UK)
GFX™ Micro Plasmid Prep Kit	GE Healthcare (Little Chalfont, UK)
High Pure PCR Product Purification Kit	Roche (Mannheim, D)

2.1.6 DNA Standards

GeneRuler™DNA Ladder Mix, ready to use	Fermentas (York, UK)
Ready-Load™ 1Kb Plus DNA Ladder	Invitrogen (UK)
Quick-Load® 2-Log DNA Ladder(0.1-10.0 kb)	New England Biolabs UK Ltd. (Hitchin, Hertfordshire, UK)
100 bp DNA Ladder	New England Biolabs UK Ltd. (Hitchin, Hertfordshire, UK)
DNA sample buffer (10x)	Eppendorf (UK)

2.1.7 Oligonucleotides

Primer (purification: desalted)	metabion (Martinsried, D)
Primer (purification: RP-Column)	TAGN Ltd (Gateshead, UK)
Primer (purification: RP-Column)	VH Bio Ltd . (Gateshead, UK)

2.1.8 Primers

plexin A3 (BamHI) forward

5`- GTGGATCCATGAGGTCCTTGTGGCTG -3`

plexinA3 (BamHI) reverse

5`- TAGGATCCGCTGCTGCCAGACATCAG-3`

olig2 forward

5`- TCCAGCAGACCTTCTTCTCC -3`

olig2 reverse

5`- ACAACTGGACGGATGGAAACC -3`

patched 1 forward

5`- GTCTGCAAGCCACTTTTGATGC -3`

patched 1 reverse

5`- GGGGTAGCCATTGGGATAGT -3`

GAPDH forward

5`- ACTCCACTCATGGCCGTT -3`

GAPDH reverse

5`- TCTTCTGTGTGGCGGTGTAG -3`

2.1.9 Morpholinos

Synthetic antisense oligonucleotides (morpholino) were used to "knockdown" genes, Blocking eighter the translation of the mRNA or the splicing of the preRNA. Morpholinos were synthesised by Gene Tools LLC (Philomath, OR, USA), sequences see appendix.

2.1.10 Antibodies

anti-*HB9 /MNR2* (81.5C10)	Dr. T.M. Jessell (Columbia University, New York, USA), 1:400, Developmental Studies Hybridoma Bank (Tanabe et al., 1998)
anti-*islet-1/-2* (40.2D6)	Developmental Studies Hybridoma Bank(Iowa City, USA), 1:1000 (Tsuchida et al., 1994)

anti-acetylated tubulin (6-11B-1)	Sigma Aldrich (UK), 1:1000
anti-NCAM-PSA (735)	Prof. Dr. Rita Gerardy-Schahn (MHH, Hannover) 1:1000 (Kibbelaar et al., 1989)
anti-neurofilament-associated antigen (3A10)	Dr. T.M. Jessell (Columbia University, New York, USA), 1:50, Developmental Studies Hybridoma Bank
anti-myc epitope (9E10)	Santa Cruz Biotechnology, (Santa Cruz, USA), 1:600
rat anti-BrdU (BU 1/75)	AbD Serotec (Oxford, UK) 1:500
anti-*PCNA* (PC10)	Dako Cytomation (Glostrup, Denmark) 1:500
anti-*nkx6.1* (AB2024)	O.Madsen (Hagedorn Research Institute, Gentofte, Denmark)1:1000
anti-GFP (A11122)	Invitrogen (UK) 1:200
pax6 (MiniPerm 95)	Veronica van Heyningen (MRC, Edinburgh)

All Cy2-, Cy3-, Cy5 and HRP conjugated anti-rabbit, anti-rat and anti-mouse secondary antibodies were from Jackson ImmunoResearch Laboratories Inc. (West Grove, PA, USA) or Dianova (Hamburg, Germany),1:200. Goat Serum (ab7481) was used for blocking in immunohistochemistry, (Abcam,Cambridge, UK) and heat inactivated prior use for 30min at 60°C.

2.1.11 Buffers and solutions

Method-specific solutions that are not listed below are specified in the corresponding chapters.

blocking buffer (whole mount immunohistochemistry)	1x PBS 1% (v/v) DMSO 1% (v/v) normal goat serum (NGS) 1% (w/v) BSA 0.7% (v/v) Triton-X 100

blocking buffer (vibratome section immunohistochemistry)	1.5% (v/v) normal goat serum in PBSTx
blocking solution (whole mount in-situ hybridisation)	1% (w/v) blocking reagent (Boehringer) in PBST
Citrate buffer	10mM sodium citrate in 1x PBS, pH 6.0
DAB stock solution	6% (w/v) diaminobenzidine (DAB)
Danieau solution	58 mM NaCl 0.7 mM KCl 0.4 mM $MgSO_4$ 0.6 mM $Ca(NO_3)_2$ 5 mM HEPES pH 7.6
dNTP stock solution (100mM)	dATP, dCTP, dGTP, dTTP, 25 mM each
phosphate buffer saline (10x PBS)	1.36 M NaCl 0.1 M $Na_2HPO_4$27 mM KCl 18 mM KH_2PO_4 pH 7.4
PBST	0.1% (v/v) Tween 20 in 1x PBS
PBStx	0.1% (v/v) Triton X 100 in 1x PBS
PFA	4% paraformaldehyde (w/v) in 1 xPBS
Saline sodium citrate buffer (SSC) (20x stock)	3 M NaCl 0.3 M tri-sodium citrate pH 7.4
Tris-acetate-EDTA buffer (TAE) (50x stock)	2M Tris-acetate 100mM EDTA pH 8.5

2.1.12 Chemicals

Chemicals were purchased as *pro analysis* quality from Sigma-Aldrich (UK) and Fisher Scientific (UK).

2.1.13 Equipment

Apotome	Zeiss (Goettingen, D)
Axiophot	Zeiss (Goettingen, D)
Bench-top centrifuges 5417 R and 5804 R	Eppendorf (Hamburg, D)
Centrifuge RC 5C Plus Sorvall	Kendro (Hanau, D)
Centrifuge Sigma 3K30C	Sigma Laborzentrifugen GmbH (Osterode am Harz, D)
Cryostat CM3050	Leica (Bensheim, D)
E.A.S.Y. UV-light documentation	Herolab (Wiesloh, D)
Fishsystem	Aqua Schwarz (Goettingen, D)
Hotplate stirrer Fisherbrand® metal top	Fisher Scientific (UK)
Hybridizer UVP HB-1000	Jencons PLS (East Grinstead, UK)
Incubated shaker MaxQ Mini 4450	Fisher Scientific (UK)
Laser scanning microscope LSM510	Zeiss (Goettingen, D)
Microcentrifuge 5415 D	Eppendorf (Hamburg, D)
Microinjector Narishige Intracel + manipulator	Intracel Ltd. (Herts, UK)
MJ mini gradient thermal cycler	Biorad (UK)
MJ PTC-200 DNA ENGINE™ Peltier Thermal Cycler	Biozym (Hessisch Oldendorf, D)
Qualicool incubator 260	LTE Scientific Ltd (Oldham, UK)
Spectrophotometer Ultrospec 3000/DPV	APB (Freiburgh, D)
Sub-Cell GT / Power Pac Basic System	Biorad (UK)
Technico Mini centrifuge	Fisher Scientific (UK)
Vibratome Microm	Optech Scientific Instruments (Oxfordshire, UK)
Wide Mini-Sub Cell GT / Power Pac Basic System	Biorad (UK)

2.1.14 Zebrafish

Zebrafish (*Danio rerio*) were kept at 26.5°C, 14-hour light and 10-hour dark cycle. They were fed two times a day, with dry flakes, ZM pellets (ZM Ltd., UK) and *Artemia salina* larvae. The fish were breed and raised according to standard protocols (Westerfield, 1989; Nusslein-Volhard).

2.2 Molecular biological methods

Standard molecular biological methods were carried out according to (J Sambrook et al., 1989) unless otherwise indicated.

2.2.1 Standard Polymerase chain reaction (PCR)

The standard PCR (Saiki et al., 1985), an amplification of DNA by *in vitro* enzymatic replication, was performed in an MJ mini-gradient thermal cycler (Biorad, UK).

Reagents:

Template (cDNA, gDNA, Plasmid DNA)	10pg – 1ng
dNTPs	200 µM (each dNTP)
Primer (forward)	0.1 – 1 µM
Primer (reverse)	0.1 – 1 µM
Reaction buffer (10x)	1x
DNA Polymerase (1min/kb Taq DNA Polymerase, 2min/kb PfU Ultra DNA Polymerase)	2.5U
add ddH_2O to final volume 50 µl	

Program:

cycles	time	temperature
1	5 min	94 °C
	30 s	94 °C
25 - 40	45 s	Tm – 1 °C
	1 min per kb	72 °C
1	10 min	72 °C

Usually the reaction was carried out in a 0.2 ml PCR reaction tube. Taq polymerase was routinely used for the amplification of up to 2 kb long DNA fragments. Proof reading PfuUltra™ HF DNA Polymerase was used to amplify DNA for overexpression and full-length constructs. After the PCR reaction was finished, 5 µl of the product was analysed by agarose gel electrophoresis.

2.2.2 Nested PCR

The nested PCR approach was used to amplify sequences from genomic DNA (gDNA). A very low number of copies of a specific DNA template, e.g. a regulatory sequence from gDNA, leads often to the amplification of the wrong DNA sequence. This approach prevents the amplification of the wrong product by sequentially using two primer pairs for the same sequence. The first primer pair includes the sequence of the second primer pair and the first PCR reaction is used as a template of the second (1:40 dilution). The reaction mix is equal to the standard PCR.

2.2.3 Touchdown PCR

Another modification of the standard PCR to reduce non-specific amplicons is touchdown PCR: starting the PCR program using a higher annealing temperature than the optimum in early PCR cycles. At every cycle the annealing temperature was decreased by 1 °C until Tm – 1 °C was reached. At that

temperature 20 additional cycles were performed to allow the enrichment of the wanted product over any non-specific product.

Program:

cycles	time	temperature
1	5 min	94 °C
	30 s	94 °C
20	30 s	Tm + 14 (first) °C
	30 s	Tm – 1 (last) °C
	1 min per kb	72 °C
	30 s	94 °C
20	30 s	Tm – 1 °C
	1 min per kb	72 °C
1	10 min	72 °C

2.2.4 TA cloning

DNA, obtained using *Taq* DNA polymerase, contains a single 3'-adenosine overhang to each site of the PCR product. These PCR products can directly be cloned into a linearized vector with a 3'-thymidine overhang. For this ligation reaction T4 DNA ligase is used (pGEM®-T easy vector system I, Promega).

2.2.5 TOPO cloning

PCR with PfuUltra™ HF DNA Polymerase leads to a product without any overhang. Such PCR fragments with a blunt-end were ligated in the pCR-BluntII TOPO vector, using the Zero Blunt® TOPO® PCR Cloning Kit (Invitrogen, UK).

2.2.6 Purification of DNA fragments and PCR products

Silica-matrix based columns to purify DNA (MiniElute™ PCR Purification Kit, QIAquick™ PCR Purification and High Pure PCR Product Purification Kit) were used according to manufacturer´s protocol. The DNA was eluted in 50µl ddH_2O.

2.2.7 Restricition enzyme digestion of DNA

Double stranded DNA was digested with appropriate amounts of restriction enzymes (NEB) according to the manufacturer´s protocols. Control digestions were carried out in a 20 µl total volume reaction for 2-3 hours. For preparative digestions the total reaction volume was scaled up to 100 µl overnight at the recommended temperature.

2.2.8 Agarose gel electrophoresis of DNA fragments

To separate and analyse restriction digestions and PCR products, horizontal agarose gel electrophoresis was perfomed. Gels (0.8-1.5% w/v) were prepared by heating agarose (Fisher Scientific, UK) in 1x TAE buffer. The concentration was chosen depending on the size of the DNA sample to be separated. Before pouring the gel, Ethidium-bromide (Fisher Scientific, UK) was added (7µl/100ml). For loading the samples, loading buffer (Eppendorf, UK) was mixed to a final concentration of 1x fold. Electrophoresis was performed with 10 V/cm in BIORAD gel chambers with 1x TAE buffer. For documentation, pictures were taken in an E.A.S.Y. UV-light documentation system and if necessary, bands were cut out with a scalpel.

To extract DNA from agarose gels, the QIAquick™ Gel Extraction or MiniElute™ Gel Extraction Kit from Quiagen, UK was used according to the manufacturer´s protocol.

2.2.9 Dephosphorylation of DNA fragments

To prevent linearized DNA from religating in a ligation reaction using T4 DNA ligase, the 5'-phosphates of the DNA were removed. 1U of alkaline shrimp phosphatase (Roche) dephosphorylates approximately 50 ng of linearized DNA in 20 minutes at 37 °C.

2.2.10 Ligation of DNA fragments

To ligate DNA fragments into a vector, e.g. subcloning, 50 ng vector DNA was mixed with 5x molar amount of insert DNA for blunt end or 3x molar amount for sticky end ligation. 1 µl T4 DNA ligase and 2 µl of 2x reaction buffer was added to a final reaction volume of 20 µl. Incubation was performed for 2 hours at room temperature or overnight at 16 ˚C.

Alternatively, the Rapid DNA ligation kit (Roche Diagnostics Ltd. Burgess Hill, UK) was used according to manufacturer´s protocol.

After the ligation, an aliquot was directly used for transfomation in *E.coli*.

2.2.11 Transformation of plasmid DNA into bacteria

2-10 µl of the ligation mix or 0.5 µl of a plasmid DNA preparation was used to transform heat shock competent *E.coli*. The DNA was added to 100 µl of the competent bacteria in a 1.5ml reaction tube and gently mixed, incubated for 30 minutes on ice, followed by a 45-second heat shock at 42 ˚C. After the heat shock 800 µl LB medium were added and the tube was incubated on ice for 2 minutes. Further incubation for 1 hour on a shaker at 200 rpm at 37 ˚C was followed by plating the bacterial solution on LB agar plates with the required antibiotic. Bacterial colonies were picked after 12-14 hours at 37 ˚C.

2.2.12 Miniprep (small scale plasmid preparation)

One picked colony was transfered into a 15 ml reaction tube containing 5 ml of LB medium with the required antibiotic. After incubation overnight at 200 rpm and 37 ˚C the plasmid was cleaned-up with the GFX™ Micro Plasmid Prep Kit (GE Healthcare).

2.2.13 Midiprep (medium scale plasmid preparation)

For large scale plasmid preparation, one colony was picked off from the LB agar plate and transfered into a sterile 250 ml Erlenmeyer flask with 50 ml LB medium. The LB medium contained the required amount of antibiotics (ampicillin 50 – 100 µg/ml, kanamycin 30 µg/ml). After overnight incubation in a shaker with 200 rpm at 37 ˚C, the plasmid was harvested using HiSpeed® Plasmid Midi Kit (Qiagen, Crawley, UK), according to the manufacturer´s protocol.

2.2.14 Quantification of DNA

The quantification of DNA samples was carried out directly in the aqueous solution by measuring the adsorption at a wavelenth of 260 nm against blank (aquatous solution without DNA). An optical density (OD) of 1 absorption equals approximately 50g/ml dsDNA. Alternatively, the concentration was defined using agarose gel electrophoresis with a DNA mass ruler (Quick-Load® 2-Log DNA Ladder, NEB).

2.2.15 Sequencing of DNA

For sequencing, DNA samples were sent to the Sequencing Service, College of Life Sciences, MSI/WTB Complex University of Dundee, UK. Samples were prepared according the facilities protocols (http://www.dnaseq.co.uk) and obtained using their web interface.

2.2.16 Precipitation of DNA

Sodium acetate (3M, pH 4.9, 1:10 v/v) and 2.5x volumes cold (-20 ˚C) ethanol absolute were added to the DNA. After mixing, the reaction tubes were kept on ice for 30 minutes and centrifuged for 15 minutes at 16000x g (RT). The

supernatant was removed and the pellet was washed with 800 µl ethanol 70%. After centrifugation and removal of the supernatant the pellet was washed repeatedly with ethanol 70% in 400 µl and 200 µl. The pellet was dried for 15 minutes and resuspended in ddH_2O.

2.2.17 Total RNA extraction from zebrafish tissue

To extract total RNA from brain and spinal cord tissue or whole embryos, the animals were killed via a schedule 1 method (Home Office, UK). The tissue was removed quickly and total RNA was obtained using the RNeasy® Midi Kit (Qiagen, Crawley, UK), according to the manufacturer´s protocol.

2.2.18 First strand cDNA synthesis

First strand synthesis was carried out using the SuperScript III™ RT and the RNaseOUT™ Recombinant Ribonuclease Inhibitor (Invitrogen Ltd.,Paisley, UK) according to the manufacturer´s protocols. The reaction steps were performed in a MJ mini-gradient thermal cycler (Biorad, UK).

total RNA	11 µl
random primers	1 µl
dNTP mix (10mM)	1 µl in 0.2ml PCR reaction tubes
mix and spin down	
5 min	65 ˚C
1 min	on ice, spin down
5x First strand buffer	4 µl
DTT (0.1M)	1 µl
RNase OUT	1 µl
Super Script III	1 µl
pipette to mix and spin down	
5 min	25 ˚C
60 min	50 ˚C
15 min	70 ˚C, store at -20 ˚C

2.2.19 *In vitro* transcription

To generate DIG labelled probes for *in situ* hybridisation, an *in vitro* transcription was performed using the MEGAscript™ Kit (Ambion, Cambridge, UK). 10 µg of plasmid DNA containing the wanted insert, flanked by a T3, T7 or SP6 promotor were digested with restriction endonucleases overnight. Thereby, only the promotor sequence and the desired DNA insert was transcribed. The digested plasmid DNA was precipitated as described in Precipitation of DNA (see above). For the generation of DIG labelled RNAs, DIG-11-dUTP (Roche, UK) was used instead of UTP provided by Ambion. Alternatively, e.g. for double labeling experiments, fluorescein labelled RNA probes were used. For this purpose, reactions were carried out using Fluorescein-12-UTP (Roche, UK) instead of DIG-11-UTP.

DIG-UTP mix (10x)
10 mM ATP
10 mM CTP
10 mM GTP
6.5 mM UTP
3.5 mM DIG-11-dUTP (Roche, UK)

To generate mRNA for overexpression studies, Ambion's mMESSAGE mMACHINE™ Kit (Ambion, Cambridge,UK) was used. In both cases, 20 µl *in vitro* transcriptions were performed according to the manufacturer´s protocol. After the incubation time, the template DNA was destroyed by adding 1 µl DNase to the reaction mix and incubating it for 15 min at 37°C. Generated RNAs were purified by lithium chloride precipitation (part of the Kit) and stored at –80°C.

2.3 Histological Methods

2.3.1 Immunohistochemistry on cryosections

Immunohistochemistry on 14 µm cryosections was performed as described (Becker and Becker, 2001). Sections were cut on a cryostat and mounted on poly-L-lysine (0.1% PLL) covered glass slides. After drying for 10 min up to a few hours the sections were encircled with Pap Pen and fixed in Methanol at -20°C for 10 min. A single wash in PBS to remove the Methanol was followed by 30 min blocking in PBS with goat serum (15 µl serum / ml) in a wet chamber. Then the sections were incubated in the primary antibody in PBS at 4°C in a humid chamber overnight. The following day the unbound antibody was removed by washing in PBS 3 times for 15 min and detected with the secondary antibody for 45 min at RT. Finally, 3 times washing in PBS removed the unbound antibody and mounted with Elvanol (DuPont,Wilmington, Delaware, USA).

2.3.2 *In situ* hybridisation on cryosections

Non-radioactive detection of mRNAs was performed in 14 µm cryosections. The sections were cut from freshly frozen tissue on a cryostat and mounted on glass slides, dried for maximally 45 mins and fixed in 4% PFA overnight. The next day, sections were washed 3 times in 1x PBS, treated with 0.1 M HCl for 20 min, acetylated in 0.1 M triethanolamine containing 0.25% acetic anhydride, and dehydrated in an ascending ethanol series. Finally, sections were air-dried and prehybridized for 3 hours at 37°C with hybridization mix. Hybridization with the DIG-labelled probes was performed at 55°C overnight in humid chambers. DIG-labelled probes were diluted 1:500 - 1:1000 in hybridization buffer. After

hybridization, the sections were washed twice in 0.2x SSC at 55°C, followed by three washing steps in 0.2x SSC containing 50% formamide (each 90 minutes at 55°C). To prevent unspecific binding, sections were incubated in blocking buffer for 30 min prior to the antibody detection. Anti-Digoxigenin-AP antibodies (Roche, Mannheim, D), diluted 1:2000 in blocking buffer, were applied and incubated overnight at 4°C. To remove unbound antibody, sections were washed twice in Buffer1 for 15 min. The Buffer1 was removed and the sections were equilibrated for 5 min with BCIP/NBT tablets (Sigma-Aldrich) and developed with the same staining solution until signals became visible under a stereomicroscope. Finally, sections were washed in 1x PBS and coverslipped with Elvanol.

Hybridisation buffer:

25 ml deionized formamide
5 ml 10x "Grundmix"
3.3 ml 5M NaCl
2.5 ml 2M DTT
10 ml dextransulfate
4.7 ml RNase free H_2O

10x "Grundmix":

2 ml 1 M Tris pH 7.5
200 µl 0.5 M EDTA
2 ml 50x Denhardt's solution
2 ml tRNA (25 mg/ml)
1 ml poly A^+ RNA (10 mg/ml)
2.8 ml RNase free H_2O

Buffer 1:

100 mM Tris

150 mM NaCl

pH 7.5

Blocking buffer:

1% (w/v) Blocking Reagent

0.5% (w/v) BSA

in Buffer 1

2.3.3 Immunohistochemistry on vibratome sections of adult spinal cord

Immunohistochemistry on vibratome sections was carried out with rat anti-BrdU (BU 1/75, 1:500, AbD Serotec, Oxford, UK), mouse anti-*islet-1/-2* (Tsuchida et al., 1994) (40.2D6, 1:1000, Developmental Studies Hybridoma Bank, Iowa City, USA), mouse anti-*HB9* (MNR2, 1:400, Developmental Studies Hybridoma Bank) mouse anti-*PCNA* (PC10, 1:500, Dako Cytomation, Glostrup, Denmark) and goat anti-*ChAT* (AB144P, 1:250, Chemicon, Temecula, USA) antibodies. Secondary Cy3-conjugated antibodies were purchased from Jackson ImmunoResearch Laboratories Inc. (West Grove, PA, USA). Animals were transcardially perfused with 4% paraformaldehyde and post-fixed at 4°C overnight. Spinal cords were dissected and floating sections (50 µm thickness) were produced with a vibrating blade microtome (Zeiss, Goettingen, D). Antigen retrieval was carried out by incubating the sections for 1 hour in 2 M HCl for BrdU immunohistochemistry, or by incubation in citrate buffer (10mM sodium citrate in PBS, pH=6.0) at 85°C for 30 minutes for *HB9*, *islet-1/-2* and *PCNA* immunohistochemistry. All other steps were carried out in PBS (pH 7.4) containing 0.1% triton-X100. Sections were blocked in goat serum (15 µl/ml) for 30 minutes, incubated with the primary antibody at 4° overnight, washed three

times 15 minutes, incubated with the appropriate secondary antibody for 1h, washed again, mounted in 70% glycerol and analysed using a confocal microscope (Zeiss Axioskop LSM 510). Double-labeling of cells was always determined in individual confocal sections.

2.3.4 Stereological quantifications in spinal cord sections

Stereological counts (Coggeshall and Lekan, 1996) were performed in confocal image stacks of three randomly selected vibratome sections from the region up to 750 µm rostral to the lesion site and three sections from the region up to 750 µm caudal to the lesion site. Cell numbers were then calculated for the entire 1.5 mm surrounding the lesion site. Variability of values is given as standard error of the mean. Statistical significance was determined using the Mann-Whitney U-test ($p < 0.05$) or ANOVA with Bonferroni/Dunn post-hoc test for multiple comparisons.

2.3.5 Profile counts in spinal cord sections

PCNA$^+$ and BrdU$^+$ nuclear profiles in the ventricular zone (up to one cell diameter away from the ventricular surface) were determined in vibratome sections (50 µm thickness) in the same region of spinal cord. At least 6 sections were analysed per animal by fluorescence microscopy and values were expressed as profiles per 50 µm section. The observer was blinded to experimental treatments. Variability of values is given as standard error of the mean. Statistical significance was determined using the Mann-Whitney U-test ($p < 0.05$) or ANOVA with Bonferroni/Dunn post-hoc test for multiple comparisons.

2.3.6 Microinjection into zebrafish eggs

Freshly fertilized eggs were harvested 15 minutes after the light in the fish facility was switched on. Eggs were washed with autoclaved fishwater containing Methylene blue 10^{-5} % and arranged in a line in a petri dish containing 2% agarose in 1x PBS. To visualize the amount of injected liquid, 0.3 µl of 5% rhodamine dextran (MW = 10000) were added to a 1 µl aliquot of morpholino, mRNA, or Danieau solution. A glass micropipette (3 µm, GB 150F-8P, Science Products GmbH, Hofheim, D) was filled with the required solution by capillary force and attached to a micromanipulator (Microinjector Narishige, Intracel Ltd., Herts, UK). The solution was directly injected into the yolk of 1 - 4 cell staged eggs. Injected eggs were incubated in fishwater with Methylene blue at 28.5°C until the desired developmental stage was reached.

2.3.7 Whole mount immunohistochemistry

To detect proteins in 24 hpf zebrafish embryos, whole mount immunohistochemistry was performed. The chorions were removed and yolks were opened using an insect needle and fine forceps. Afterwards, embryos were fixed in 4% PFA containing 1% (v/v) DMSO for 45 min at RT. Then, embryos were washed in 1x PBS and incubated with blocking buffer to prevent unspecific binding of the primary antibody for 30 min at RT. Primary antibodies were diluted in blocking buffer and applied to the embryos and incubated overnight at 4°C. Three washing (1x PBS for 15 min) steps removed unbound primary antibody. To visualize primary antibodies, fluorescence- or HRP labelled secondary antibodies were diluted 1:200 in blocking buffer and applied to the embryos for 1h at RT. Unbound secondary antibody was removed by three washing steps with 1x PBS for 15 min each. To visualize the HRP signals,

embryos were incubated in 0.5 mg/ml diaminobenzidine (DAB) in 1x PBS for 20 min at 4°C. The dark brown precipitate was developed by adding 1/10 volume of a 0.035% H_2O_2 solution in 1x PBS. After 5 - 10 min, the staining solution was removed, embryos were washed 3 times in 1x PBS and cleared in an ascending glycerol series (30, 50 and 70% glycerol in 1x PBS). Embryos were mounted in 70% glycerol.

2.3.8 Whole mount *in situ* hybridisation

To detect the expression patterns of mRNAs in 16-24 hpf zebrafish embryos, whole mount *in situ* hybridization was performed. Embryos at the desired developmental stages were anesthetized in 0.1% aminobenzoic acid ethyl methyl ester (MS222, Sigma-Aldrich, UK), dechorionated and fixed overnight in 4% PFA at 4°C. The following day, the embryos were washed 4 times with PBST (Phosphate Buffered Saline + 1% Tween®40) and incubated in 100% methanol (-20 °C) for 30 min. Methanol was removed using a descending methanol series (75 %, 50 % and 25 % methanol in PBST) and washed twice in PBST. To enhance penetration of the DIG labelled RNA probes, embryos were digested with 1.4 µg/ml recombinant Proteinase K (Roche, UK) in PBST for 10 min at RT. Two wash steps in 2 mg/ml glycine in PBST followed. Embryos were post-fixed in 4% PFA for 20 min at RT and subsequently washed 4 times with PBST to remove residual PFA. Embryos were prehybridized in hybridization buffer at 55°C for at least 3 hours. Hybridization with the DIG-labelled probes occurred at 55°C overnight. DIG-labelled probes were diluted 1:250- 1:4000 in hybridization buffer. After hybridization, embryos were washed twice in with 2x SSCT containing 50% formamide for 30 min, followed by a washing step in 2x SSCT for 15 min and two washing steps with 0.2x SSCT for 30 min. All washing

steps were executed at 55°C. To prevent unspecific binding of the anti-DIG AP-conjugated antibodies, embryos were incubated for 30 min in 1% w/v Blocking Reagent (Roche, Mannheim, D) in PBST. Anti-Digoxigenin-AP antibodies (Roche, Mannheim, D) were diluted 1:2000 in Blocking Reagent and applied overnight at 4°C. To remove unbound antibody, embryos were washed 6 times in 1x PBST for 20 min. The washing solution was removed and the signal was developed in the dark with SIGMA FAST™ BCIP/NBT tablets (Sigma-Aldrich) until the reaction product became visible under a stereomicroscope. Sense probes were developed in parallel under the same conditions as the antisense probes and did not show any labeling. Finally, embryos were washed 3 times in 1x PBS and cleared in an ascending glycerol series (30, 50 and 70% glycerol in 1x PBS). The yolk sack was removed and embryos were mounted in 70% glycerol.

Whole mount hybridisation buffer:

5 ml deionized formamide
2.5 ml 20x SSC
10 µl Tween 20
100 µl 100 mg/ml yeast RNA (Sigma Aldrich, Deisenhofen, D)
2.38 ml DEPC-H_2O
10 µl 50 mg/ml heparin

2.4 Animal experiments

All fish are kept and bred in our laboratory fish facility according to standard methods and all experiments have been approved by the Home Office.

2.4.1 Perfusion fixation of adult zebrafish

After killing fish in 0.1% aminobenzoic acid ethylmethylester (MS222; Sigma, St. Louis, MO) they were transcardially perfused with 4% paraformaldehyde and post-fixed at 4°C overnight.

2.4.2 Spinal cord lesion of adult zebrafish

Before the spinal cord lesion, fish were kept for at least 24h in water with 1300 µS salt concentration to prevent bacterial or fungal infections. As described previously (Becker et al., 1997), fish were anesthetized by immersion in 0.033% aminobenzoic acid ethylmethylester in PBS for 5 min. A longitudinal incision was made at the side of the fish to expose the vertebral column. The spinal cord was completly transected under visual control 4 mm caudal to the brainstem-spinal cord junction. Afterwards the lesioned fish were kept in single tanks with high salt concentration and ESHA2000.

2.4.3 Retrograde tracing of adult zebrafish

Motor neurons in the spinal cord were retrogradely traced by bilateral application of biocytin to the muscle periphery at the level of the spinal lesion, as described previously (Becker et al., 2005),with the modification that biocytin was detected with Cy3-coupled streptavidin (Invitrogen) in spinal sections.

2.4.4 Intraperitoneal substance application

Animals were anaesthetised and intraperitoneally injected. We injected 5-bromo-2-deoxyuridine (BrdU, Sigma-Aldrich, UK) solution (2.5 mg/ml) at a volume of 50 µl at 0, 2, 4 days post-lesion. Analysis took place at 14 days post-lesion.

Cyclopamine was purchased from LC Laboratories (Woburn, MA, USA). The related control substance tomatidine (Sigma-Aldrich, UK). For intraperitoneal injections into adult fish cyclopamine and tomatidine were dissolved in HBC (45% (2-Hydroxypropyl)-beta-cyclodextrin) (Sigma-Aldrich, UK) and injected at a concentration of 0.2mg/ml in a volume of 25µl (equaling 10 mg/kg, Sanchez and Ruiz i Altaba, 2005) at 3, 6 and 9 days post-lesion. Analysis took place at 14 days post-lesion

3 RESULTS

3.1 Adult spinal cord regeneration

Zebrafish show functional regeneration after a lesion and the role of descending axons from the brainstem in this process has been studied extensively. Here we address the plastic changes occuring in the spinal cord. Specifically, I ask whether neurogenesis takes place in the lesioned spinal cord.

3.1.1 Spinal cytoarchitecture is not restored in a spinal lesion site

To determine in which spinal cord region neurons might regenerate, we analysed the overall organization of the regenerated spinal cord (Fig. 3 A) at 6 weeks post-lesion, when functional recovery plateaus. Electron-microscopic analysis, performed by Dr. Catherina G. Becker, indicates that both ends of the severed spinal cord fuse and form a thin tissue bridge which consists mainly of regenerated, partially re-myelinated, axons (Fig. 3 B). Therefore, substantial neurogenesis in the lesion site is unlikely.

The pre-lesioned spinal cord is still present after regeneration. Immediately adjacent to the axonal bridge the original cytoarchitecture is still found. Furthermore, white matter tracts are filled with myelin debris of degenerating fibres, indicating that this tissue was present before the lesion (Becker and Becker, 2001).

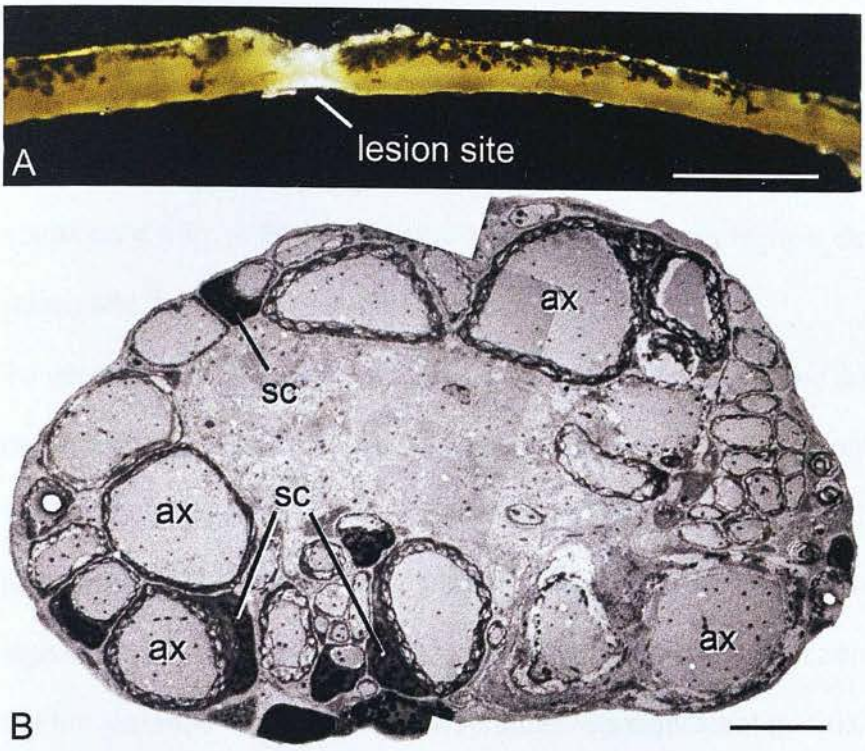

Fig. 3: The lesion site consists mainly of regenerated axons. **A:** A lateral stereo-microscopic view of a dissected spinal cord is shown (rostral is left). The dorsal aspect of the spinal cord is covered by melanocytes and the tissue bridging the lesion site appears translucent. **B:** An electron-microscopic cross-section through the lesion site is shown. The lesion site consists mainly of axons (ax), some of which are re-myelinated by Schwann cells (sc). Bar in A = 1 mm, in B = 5 µm.

3.1.2 A spinal lesion triggers ventricular proliferation

We analysed proliferation patterns in the lesioned spinal cord to determine in which region neuronal regeneration might take place. Proliferation activity in the spinal cord was studied by repeated injections of 5-bromo-2-deoxyuridine (BrdU). BrdU, a synthetic thymidine analogue, is incorporated into the DNA of dividing cells and later detected via immunohistochemistry. The injections were given at 0, 2 and 4 days post-lesion (dpl). Proliferation patterns were analysed at 2 weeks post lesion (wpl). In the unlesioned spinal cord only a few cells were labelled (Fig. 4, A left), indicating that cell division is a rare event. At 2 weeks post-lesion the number of newly generated cells in the spinal cord is

significantly increased (p=0.0001, n = 3 animals) compared to the unlesioned situation (Fig. 4, middle, right). This increase is detectable up to 3.6 mm rostral and 3.6 mm caudal from the lesion site. Thus, it spans up to 1/3 of the entire spinal cord (Fig. 4, B). Numbers of newborn cells were highest close to the lesion site and around the central canal.

To determine the location of acutely proliferating cells we used an antibody recognizing the Proliferating Cell Nuclear Antigen (*PCNA*). In contrast to BrdU, which labels dividing cells permanently, the *PCNA* antibody only labels acutely proliferating cells in the early G1 and S phase of the cell cycle. This showed a significant increase in proliferating cells only in the ventricular zone. Already at 3 dpl the increase in ventricular proliferation was significant ($p < 0.0001$, n = 3 animals/time point) and peaked at 2 wpl. At 6 wpl, the proliferation was reduced again to levels that were not significantly different from those in unlesioned animals. This corresponds to functional recovery, which is complete at the same time point.

These findings suggest that, after a spinal lesion, new cells were primarily generated at the ventricle and then migrated out in to the parenchymal region.

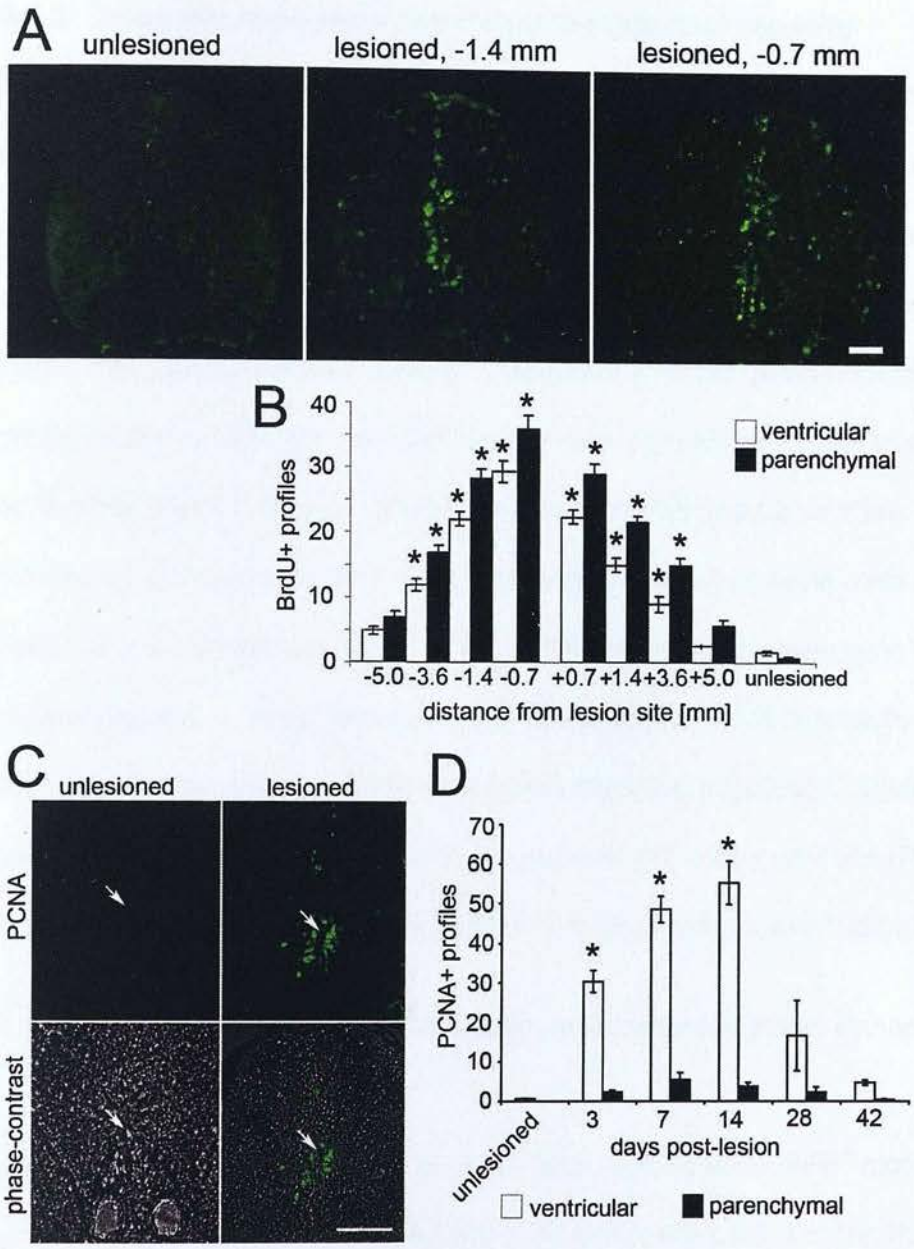

Fig. 4: Lesion-induced proliferation in the adult spinal cord. Confocal images of spinal cross-sections are shown (dorsal is up). **A:** BrdU labeling of spinal cross-sections shows a massive increase in labeling in the ventricular zone at 2 wpl (injections 0, 2, and 4 days post-lesion). The highest density of $BrdU^+$ cells is detectable in the ventricular zone close to the lesion site. **B:** Quantification of $BrdU^+$ profiles at 2wpl indicates significant proliferative activity up to 3.6 mm rostral and caudal to the lesion epicenter (n = 3 animals per treatment, $p < 0.0001$). **C:** *PCNA* immunohistochemistry indicates a strong increase in the number of proliferating cells in the ventricular zone (arrows) at 14 days post-lesion. **D:** The number of proliferating ventricular, but not parenchymal cell profiles/section was significantly increased after a lesion and peaked at 2 wpl (n = 3 animals per time point, $p < 0.0001$). Bar in A = 25 µm, in C = 50 µm.

3.1.3 Motor neurons show significant regenerative capacity

To determine whether neuronal death and/or regeneration occurs in the lesioned spinal cord, I focused on motor neurons, a cell type that never regenerates in mammals. To this end, numbers of GFP^+ motor neurons in *HB9:GFP* and *islet-1:GFP* transgenic animals were analysed (Higashijima et al., 2000; Flanagan-Steet et al., 2005). These lines express green fluorescent protein (GFP) under the control of the promotor for *HB9* or *islet-1*. In addition, antibodies against *islet-1/2*, *HB9* (also called *MNR2*) and transmitter synthesizing enzyme choline acetyltransferase (*ChAT*) proteins were utilised. *Islet-1/2* is a transcription factor of the LIM family and is expressed in various subpopulations of motor neurons in the spinal cord of adult zebrafish. The homeobox gene *HB9* is expressed in an overlapping population together with the *islet-1* and *islet-2* proteins as well as in *islet-1/2*$^-$ motor neurons (Renoncourt et al., 1998). The antibody against *ChAT* protein labels mature motor neurons.

3.1.3.1 Numbers of large and small motor neurons show dynamic changes after a lesion

Unlesioned *HB9:GFP* animals showed 132.5 ± 34.88 large GFP^+ motor neurons (diameter >12 µm, n = 4 animals) per 1500 µm spinal cord. Testing the specificity of the transgene with the corresponding antibody reveals that 97.8% (n = 3 animals) of the *HB9:GFP*$^+$ cells were also *HB9* immunopositive. Of the large *HB9:GFP*$^+$ cells, 80.6% (n = 3 animals) express choline acetyl transferase (*ChAT*), a marker of mature motor neurons. This indicated that most large GFP^+ cells were fully differentiated motor neurons. Furthermore, retrograde tracing from the muscle periphery in 8 weeks post-lesion animals with Biocytin, followed by detection with Streptavidin-Cy3, reveals that 52 of 55 traced cells

were *HB9:GFP*$^+$ (n=3). This indicates that large *HB9:GFP*$^+$ cells are innervating muscle tissue and therefore are mature motor neurons.

The response of small (< 12 µm diameter) and large (> 12 µm diameter) *HB9:GFP*$^+$ motor neurons to a lesion was determined (Fig. 5) in an area of 750 µm rostral and caudal to the lesion site. The number of large GFP$^+$ cells was significantly reduced at 1 wpl ($p = 0.0035$, n = 4 vs. 3 animals) and 2 wpl ($p = 0.0003$, n = 4 vs. 11 animals). After 6 to 8 weeks the number of large motor neurons was increased again to levels that were not significantly different from the unlesioned situation ($p = 0.0867$, n = 4 unlesioned vs. 6 lesioned animals). This showed that the original number of mature *HB9*$^+$ motor neurons is decreased in response to the lesion event. Furthermore it indicates a trend in recovery of the number of large cells.

Numbers of small *HB9:GFP*$^+$ motor neurons responded inversely to the transection of the spinal cord. A significant increase after 2 wpl ($p < 0.0001$, n = 4 unlesioned vs. 11 lesioned animals) was followed by a significant decrease in number of small neurons at 6 to 8 weeks ($p = 0.0002$, n = 11 animals at 2 wpl vs. 6 animals at 6 to 8 wpl).

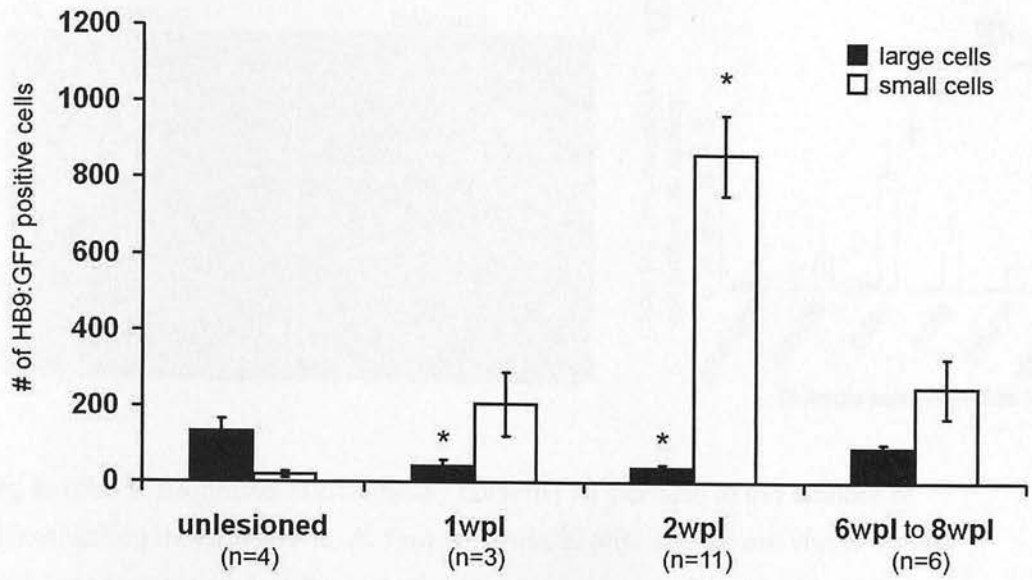

Fig 5: Dynamic changes in the numbers of *HB9:GFP*$^+$ motor neurons after a lesion. A spinal cord lesion induces an increase in the number of small and a decrease in the number of large motor neurons at 2 wpl. At 6 to 8 wpl, the population of large motor neurons partly recovers, while numbers of small *HB9:GFP*$^+$ cells return to original levels. Stereological counts of *HB9:GFP*$^+$ cells calculated to 1500µm around the lesion site are given.

This transient, more than 43-fold increase, in the number of small *HB9:GFP*$^+$ motor neurons indicates a highly dynamic response in the number of spinal motor neurons to the lesion event. In addition, the time course matches that of the functional recovery, indicating a possible link between motor neuron regeneration and functional recovery.

Using the *islet-1/2* antibody the spatial distribution of differentiating motor neurons was analysed in 14 µm cryosections at increasing distances from the lesion site (Fig. 6). Close to the lesion site (0-250 µm) the number of islet-1/2 positive cell profile counts is highest and significantly increased 2 wpl ($p = 0.0253$, $n = 5$ animals each group) compared to unlesioned controls. This corresponds to proliferative activity in the ventricular zone, which is also highest close to the lesion site (Fig. 4 D).

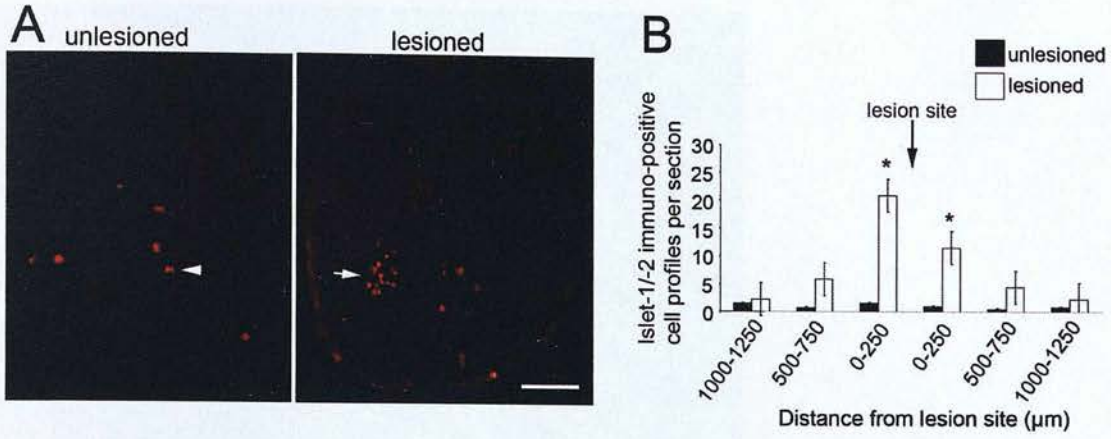

Fig 6: *Islet-1/-2* immunohistochemistry confirms an increase in the number of differentiating motor neurons. **A:** Few large nuclei (arrowhead) are visible in the unlesioned spinal cord. In the lesioned situation, clusters of small *islet-1/-2* immunopositive cell nuclei appear in the ventro-lateral spinal cord (arrow). **B:** Numbers of *islet-1/-2* immunopositive cell profiles were determined in cryosections (14 µm in thickness) for the regions indicated, showing a significant increase in *islet-1/-2* immunopositive cell profiles around the lesion site. (n = 5 unlesioned animals; n = 5 animals at 2 wpl; p = 0.0253). Bar = 50 µm.

3.1.3.2 Small motor neurons are newly generated after a lesion

To directly address whether motor neurons were newly generated, BrdU was injected into *HB9:GFP* and *islet-1:GFP* transgenic animals at 0, 2, and 4 dpl post-lesion and the number of double labelled neurons was determined at 2 wpl.

At 2 wpl there was an increase in the number of small *islet-1:GFP* positive cells, which was statistically significant compared with the unlesioned situation (unlesioned: 27 ± 3.9 cells, n = 5 animals, 2 wpl: 870 ± 244.9 cells, n = 4 animals, p = 0.0139). In BrdU injected animals, 184 ± 49.3 small cells (n = 3 animals, p = 0.0104) were double labelled with the transgene and BrdU immunohistochemistry. In the unlesioned controls no double-labelled cells (n = 5 animals) were found (Fig. 7).

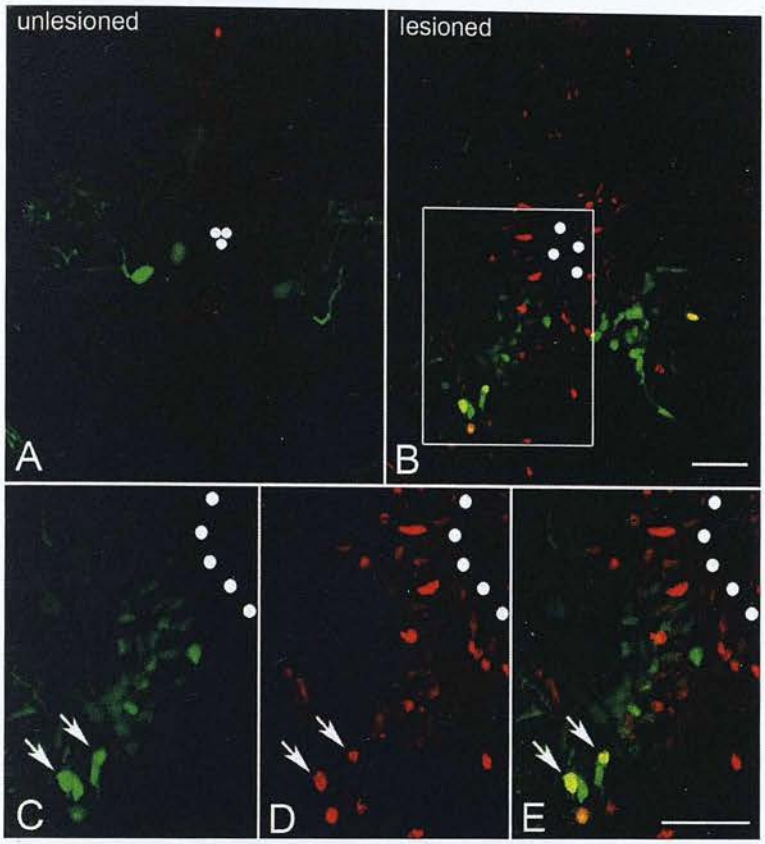

Fig 7: Newly generated small *islet-1:GFP*$^+$ cells in the lesioned spinal cord. Cross-sections through the spinal cord of unlesioned **A:** and lesioned **B-E:** animals at 2 weeks post-lesion are shown. In unlesioned animals only large GFP$^+$ cells are detectable, whereas many smaller GFP$^+$ cells are present in the ventrolateral aspect of the lesioned spinal cord. Many of these cells are also BrdU$^+$, as indicated by arrows in the higher magnification **C-E:** of the area boxed in B. Dots outline the ventricle. Bars = 25 µm.

The *HB9:GFP* transgenic fish confirms these observations: at 2 wpl the small *HB9:GFP*$^+$ cells were increased from 20.0 ± 7.66 in the unlesioned situation (n = 4 animals) to 869.5 ± 106.78 (n = 11 animals, $p < 0.0001$). In this transgenic fish, 200.0 ± 46.2 cells (n = 7 animals, $p = 0.0076$) were double-labelled by the transgene and BrdU at 2 wpl (Fig. 8). In the unlesioned spinal cord only one double-labelled motor neuron was observed (n = 4 animals). Even a BrdU injection protocol extended to the maximum number of injections tolerated by the fish (injections at 0, 2, 4, 6, 8 days post-lesion, analysis at 14 days post-

lesion) did not yield any *HB9:GFP*$^+$/BrdU$^+$ cells in unlesioned fish (n = 5 animals). Letting the fish swim in BrdU-treated water in order to label all newly generated cells over the entire time of the experiment does not show sufficient labeling of dividing cells (Dr. Thomas Becker, personal communication). Hence the unlesioned mature spinal cord appears virtually quiescent with respect to motor neuron generation. However, low rates of motor neuron formation may have been missed due to the limited metabolic availability of BrdU.

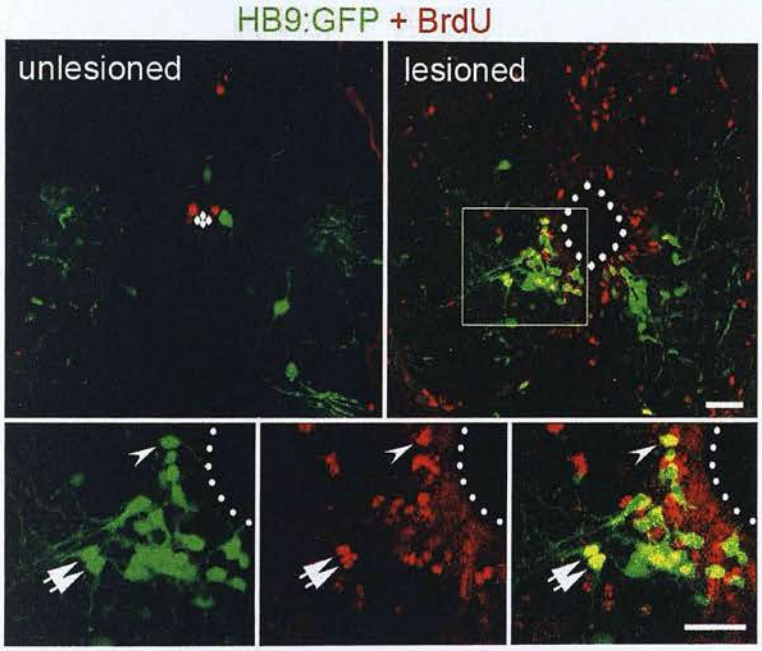

Fig. 8: Generation of new motor neurons in the lesioned spinal cord. *HB9:GFP*/BrdU double-labelled neurons are present in the lesioned, but not the unlesioned, ventro-lateral spinal cord. These cells (boxed in upper right and shown in higher magnification in bottom row) bear elaborate processes (arrows) or show ventricular contact (arrowhead). Bars = 25 µm.

3.1.3.3 Lesion induces cell death

The number of large *HB9*$^+$ motor neurons decreases significantly after a lesion. We performed TUNEL staining in *HB9:GFP* transgenic fish at 3 dpl and found TUNEL$^+$/*HB9:GFP*$^+$ cells (Fig. 9). The apoptosis marker TUNEL labels the nuclei of cells undergoing programmed cell death (Hewitson et al., 2006).

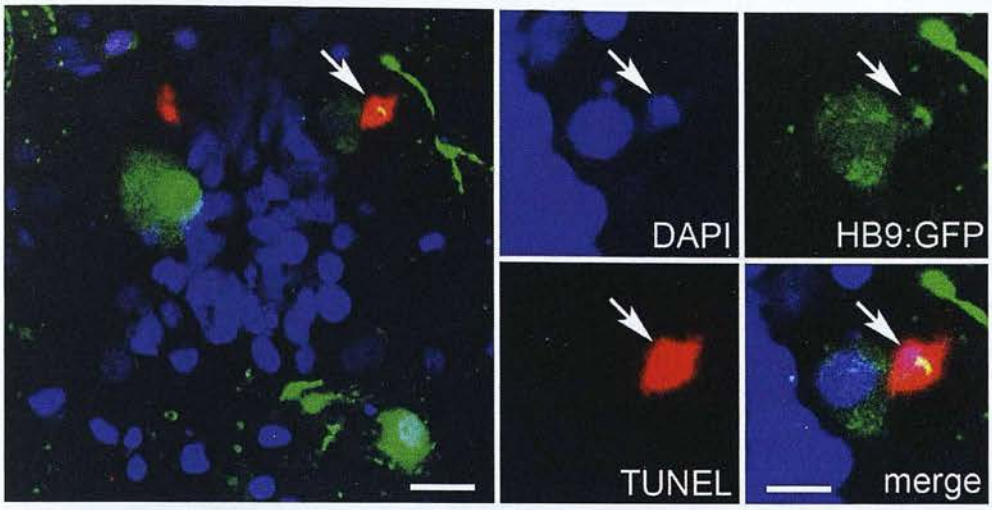

Fig. 9: Lesion induced apoptosis at 3 dpl. *HB9:GFP* (green), DAPI nuclear staining (blue) and TUNEL staining (red). Triple labelling indicates apoptotic motor neurons (arrow). Bars: left 15µm, right 8 µm.

3.1.3.4 Different subpopulations of newly generated motor neurons may be present in the lesioned spinal cord

The *islet-1:GFP* and the *HB9:GFP* transgenic animals show a similar distribution of small motor neurons in the ventral horn of the lesioned spinal cord. For *islet-1*, the transgene expression confirms the expression of the endogenous gene because 89.5 % of the *islet-1:GFP*$^{+}$ cells were *islet-1/2* immunopositive at 2 wpl. The small proportion of cells only labelled by GFP in *islet-1:GFP* animals may result from higher stability of the GFP than endogenous islet-1 detected by the antibody. In contrast, a substantial proportion, 51.7 %, of *HB9:GFP*$^{+}$ cells were not double-labelled by the *islet-1/2* antibody and many cells were exclusively labelled by the islet-1/-2 antibody in both transgenic lines (55.7 % in the *HB9:GFP* and 35.4 % in the *islet-1:GFP* fish) (Fig. 10). This suggests heterogeneity among newly generated motor neurons with respect to marker expression (William et al., 2003).

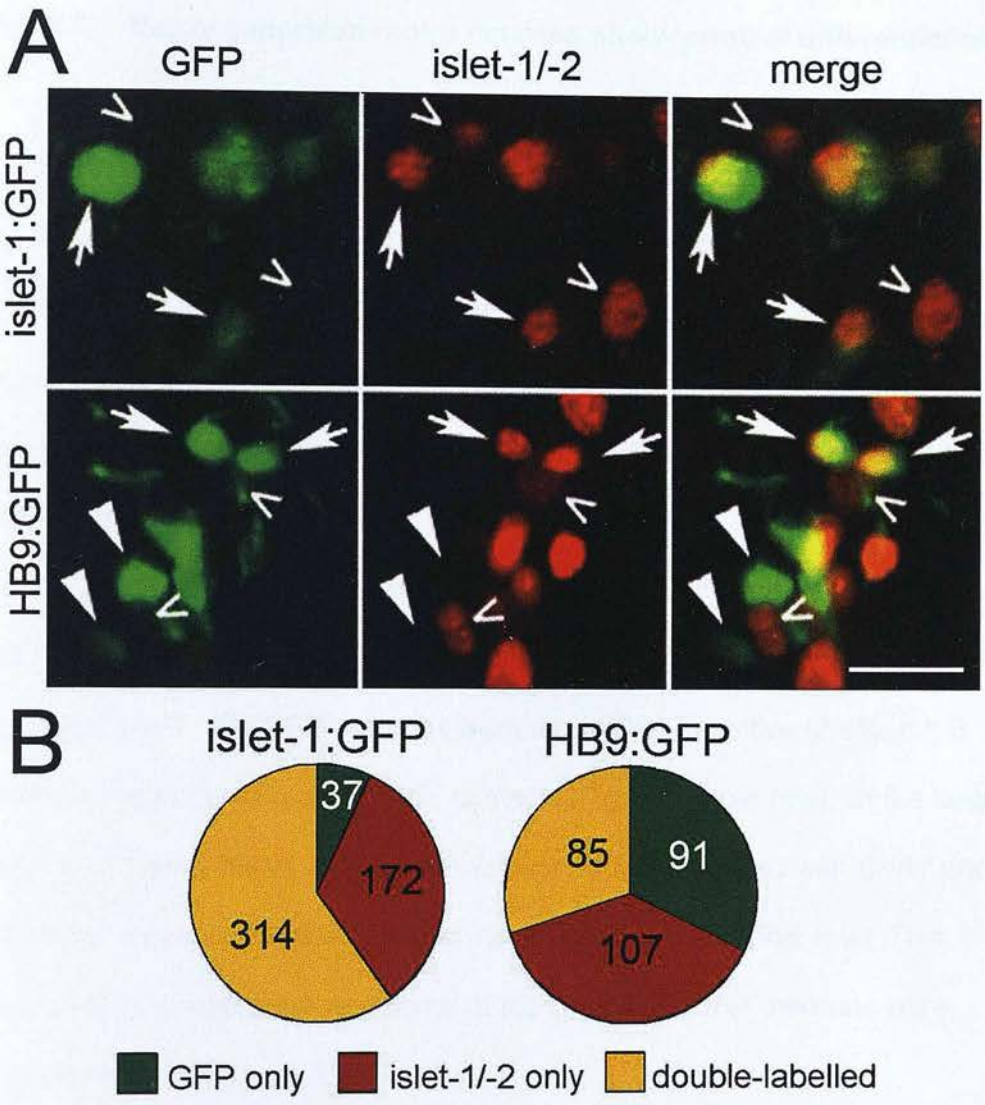

Fig. 10: Partial overlap of *islet-1/-2* immunohistochemistry and transgenic motor neuron markers in the lesioned spinal cord. **A:** *Islet-1:GFP*$^{+}$ cells are double-labelled by the *islet-1/-2* antibody, confirming specificity of transgene expression. A substantial proportion of *HB9:GFP*$^{+}$ cells are not double-labelled by the antibody and many cells are only labelled by the *islet-1/-2* antibody in both transgenic lines, suggesting that different types of cells were generated after a lesion. Arrows indicate double-labelled neurons, arrowheads indicate neurons only labelled by the transgene and open arrowheads point to cells only labelled by the antibody. **B:** Summations of all cells counted in six sections (50 µm thickness) per animal from the region of 1.5 mm surrounding the lesion site (n = 3 animals for each transgene) are indicated. Bar = 25 µm.

3.1.3.5 Newly generated motor neurons show terminal differentiation and may be integrated into the spinal network

To determine whether newly generated motor neurons fully matured, expression of *ChAT*, a marker for terminally differentiated motor neurons (Arvidsson et al., 1997), and coverage of motor neurons by $SV2^+$ contacts, a marker for synaptic coverage, was analysed. In the unlesioned situation 80.6% (n = 3 animals) of the large $HB9{:}GFP^+$ cells expressed *ChAT*, indicating that the majority of $HB9{:}GFP^+$ cells were mature motor neurons. Small $HB9{:}GFP^+$ cells were rarely found. Furthermore, all $ChAT^+$ cells were covered with synapses in the unlesioned spinal cord.

At 2 wpl, small $HB9{:}GFP^+$ neurons were rarely *ChAT* positive (2.8%, n = 3 animals) and did not receive $SV2^+$ contacts (Fig. 11, upper row). Of the large $HB9{:}GFP^+$ cells, 36.4% (n = 3 animals) were double labelled with *ChAT* and often not covered with *SV2* labelled synapses (Fig. 11, middle row). This indicates that most small and some of the large $HB9{:}GFP^+$ neurons were immature at 2 wpl.

To determine whether newly generated motor neurons show terminal differentiation and network integration at later stages of regeneration, BrdU injections at day 0, 2 and 4 were combined with anti-*ChAT* and anti-*SV2* immunohistochemistry. At 6 wpl 29.3 ± 23.14 $ChAT^+$ cells/1500µm (n = 3 animals) were also $BrdU^+$ and extensively covered with *SV2* labelled synapses. The inset in the lower row indicates that similar cells are part of the typical cytoarchitecture of the unlesioned spinal cord (Fig.11, lower row). These observations are consistent with the hyposthesis that newly generated motor neurons can fully mature and integrate into the spinal network.

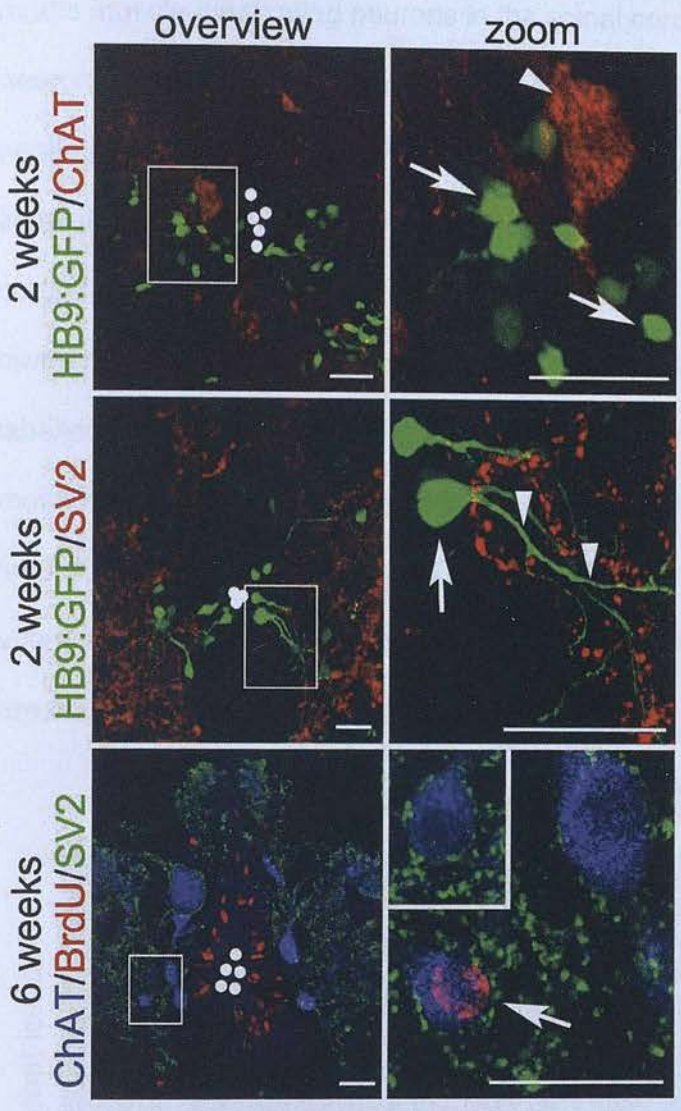

Fig. 11: Maturation of newly generated motor neurons. Confocal images of spinal cross-sections are shown (dorsal is up). Clusters of newly generated *HB9:GFP*$^+$ motor neurons are *ChAT*$^-$ (arrow in top row indicates a *ChAT*$^+$/*HB9:GFP*$^-$ differentiated motor neuron). Somata (arrow in middle row) and proximal dendrites (arrowheads in middle row) receive few *SV2*$^+$ contacts at 2 wpl. At 6 wpl, *ChAT*$^+$/BrdU$^+$ somata are decorated with *SV2*$^+$ contacts (arrow in bottom row), inset: unlesioned situation. Bars = 25 µm.

3.1.3.6 Evidence for motor axon growth out of the spinal cord

To determine whether newly generated motor neurons grow axons out of the spinal cord, we applied the retrograde neuronal tracer biocytin to the muscle tissue surrounding the lesion site of BrdU injected animals. Biocytin tracing

marks muscle-innervating neurons in the spinal cord, which are bona fide motor neurons. Fish were injected at 12, 13 and 14 dpl with BrdU and biocytin was applied at 42 dpl. Out of 4 fish, we found one $BrdU^+$/$biocytin^+$ cell (Fig.12), indicating that this newly generated cell extended an axon out of the spinal cord. The ventro-lateral position of the cell in the spinal cord is consistent with a motor neuron identity of this cell. One reason for the scarcity of these double-labelled cells may be that BrdU labels only a sub-population of newly generated motor neurons (approximately 25% at 14 dpl) and retrograde tracing does not label all motor neurons, such that overlap of the two markers may be a rare event. However, this observation suggests that newly generated motor neurons are capable of regenerating a peripheral axon.

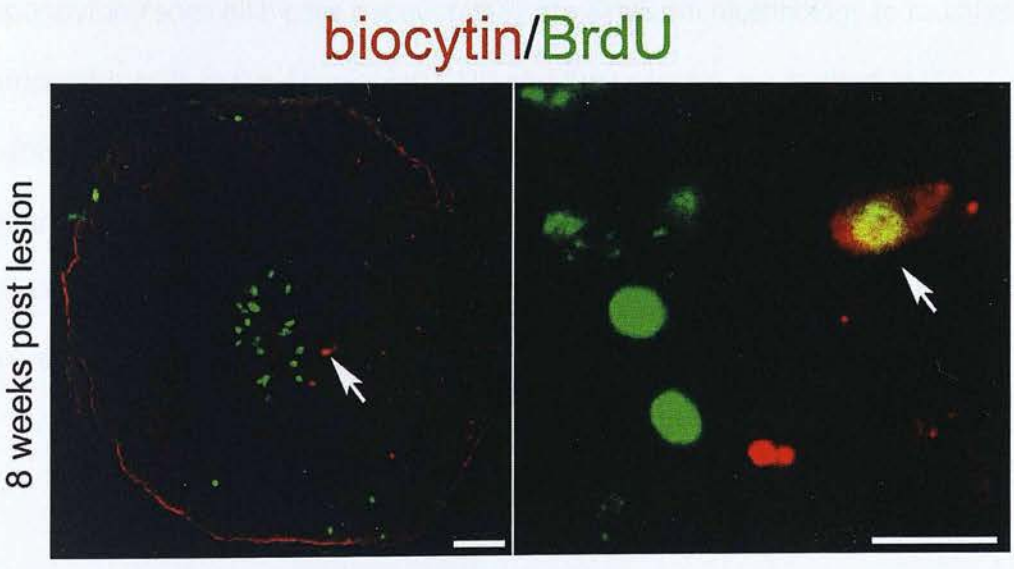

Fig.12: Retrograde tracing of a newborn motor neuron in the spinal cord from the muscle periphery. Confocal images of the same spinal cross-section are shown in low (left) and high (right) magnification (dorsal is up). Arrows point to the same biocytin/BrdU doubled labelled motor neuron at 8wpl. Bars = 50 µm (left), 15 µm (right).

3.1.4 *Olig2:GFP*$^{+}$ ependymo-radial glial cells are potential motor neuron stem cells in the adult spinal cord

Olig2 expressing cells give rise to motor neurons during development. To determine whether this cell type also exists during adult regeneration and plays a similar role, we investigated adult expression of *olig2*. A transgenic fish expressing GFP under the control of the *olig2* promoter outlines the entire morphology of the ventricle-contacting *olig2* positive cells, including long radial processes in unlesioned animals (Fig. 13, upper row). Additionally, the transgene marks *olig2*-expressing oligodendrocytes. These cells are morphologically distinguishable from *olig2*$^{+}$ ependymo-radial glial cells and are distributed in the parenchyma of the spinal cord. For this study, I focused on the ependymo-radial glial cells because they are similar in morphology to radial glial progenitor cells in the developing CNS and their somata are located at the ventricle, where lesion-induced proliferation takes place. Indeed, *olig2:GFP*$^{+}$ ependymo-radial glial cells respond to a spinal cord transection with proliferation, as demonstrated by immunohistochemistry for *PCNA*, which marks acutely proliferating cells (Fig. 13, lower row).

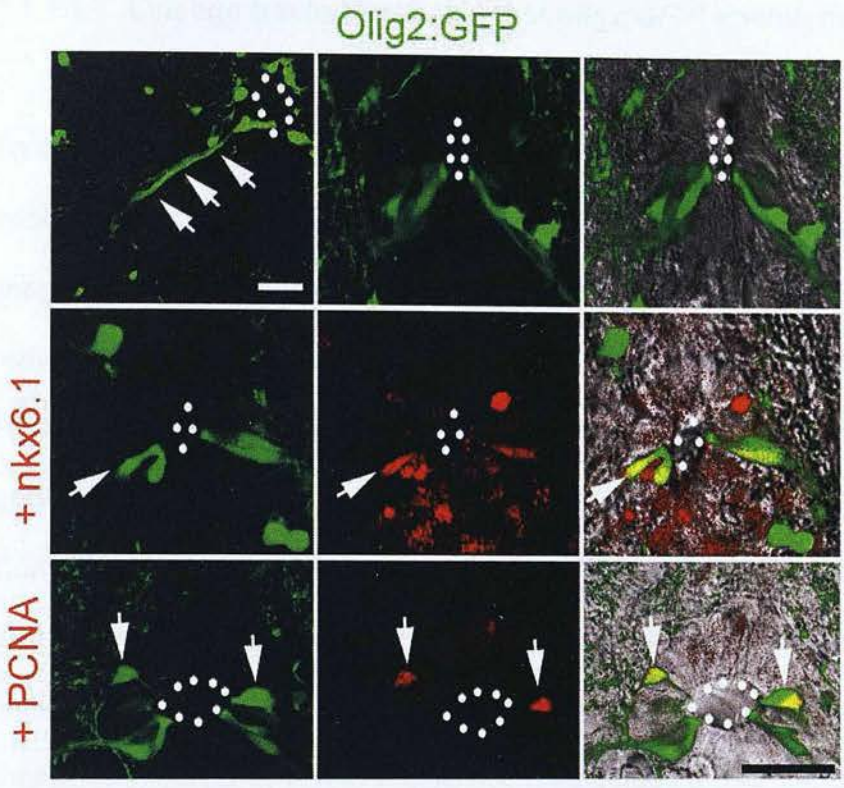

Fig. 13: *olig2:GFP*+ cells have long radial processes (arrows in upper left), contact the ventricle (upper row, middle and right), and are double-labelled (arrows) with *nkx6.1* and *PCNA* antibodies at 2 wpl. Confocal images of cross-sections are shown. Dots outline the ventricle. Bar = 25 µm.

To determine whether other transcription factors, known to be important for motor neuron development, are also expressed in *olig2:GFP*$^{+}$ ependymo-radila glial cells during regeneration, we double labelled with antibodies against *nkx6.1*. Developmentally, the homeodomain transcription factor *nkx6.1* is part of the mechanisms regulating *olig2* expression. It promotes *olig2* expression at an early stage in development and represses it at a later stage in chicken (Liu et al., 2003). In the adult spinal cord of zebrafish, *olig2:GFP*$^{+}$ ependymo-radial glial cells expressed *nkx6.1* at 2 wpl (Fig. 13, middle row). The presence of *nkx6.1* in *olig2*$^{+}$ ependymo-radial glial cells after a lesion indicates that during regeneration of motor neurons a gene expression program similar to development could occur.

3.1.4.1 Lineage tracing indicates that *olig2:GFP*$^+$ ependymo-radial glial cells are motor neuron progenitor cells.

To directly demonstrate that *olig2*$^+$ ependymo-radial glial cells are the progenitor pool for new motor neurons, I used GFP expression as a stable marker for linage tracing. *Olig2*$^+$ ependymo-radial glial cells that give rise to motor neurons may still be GFP$^+$ when starting to express the motor neuron specific markers *HB9* and *islet-1*. This is because GFP is a relatively stable protein (Tallafuss and Bally-Cuif, 2003).

Comparing unlesioned and lesioned spinal cord of *olig2:GFP* transgenic fish with anti-*HB9* immunohistochemistry reveals that after a lesion *olig2*$^+$ ventricular cells differentiate to *HB9* expressing motor neurons (Fig.14, middle row). In the unlesioned fish no *GFP*$^+$/*HB9*$^+$ cells could be detected (Fig. 14, upper row) versus 204.0 ± 32.29 *GFP*$^+$/*HB9*$^+$ cells per 1500 µm around the lesion site in the group of the lesioned animals (n = 3 animals per group).

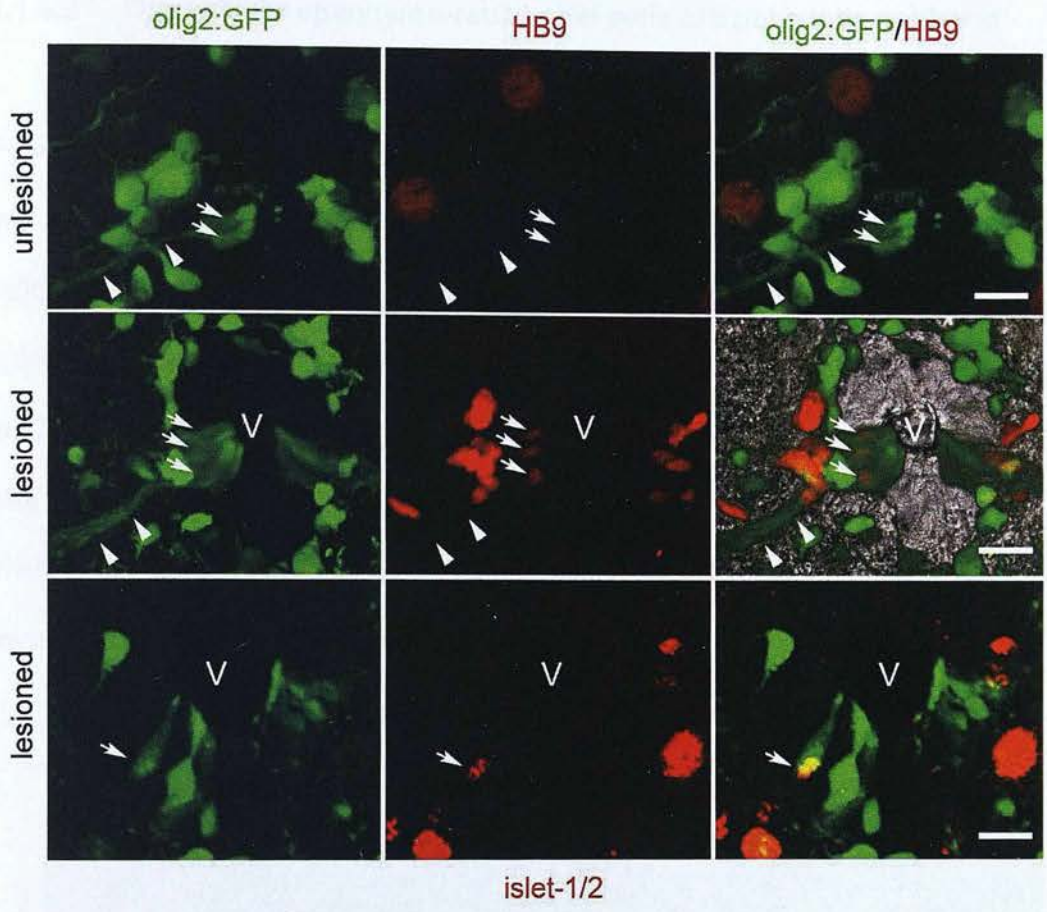

Fig. 14: Confocal images of spinal cross-sections unlesioned vs. 2 wpl are shown (dorsal is up). *Olig2:GFP*$^+$ progenitor cells (arrows) have long radial processes (arrowheads), contact the ventricle (outlined by dots), and are double-labelled with *HB9* or *islet-1/2* antibodies at 2 wpl, but not in the unlesioned spinal cord. Bars in A = 25 µm; Bars in B = 7.5 µm (upper row), 15 µm (middle and lower row).

Similarly, transgenic zebrafish showed ependymo-radial glial cells double-labelled for *olig2:GFP* and *islet-1/-2*$^+$ cells at 2 wpl (Fig. 14, lower row). In the 1500 µm around the lesion site, 34.3 ± 8.93 cells (n = 4 animals) were double labelled. This indicates that *olig2*$^+$ ependymo-radial glial cells have the capacity to proliferate and to give rise to cells expressing markers for motor neurons in response to a lesion. Moreover, this indicates a molecular switch of the *olig2* expressing ependymo-radial glial cells from a gliogenic to a motor neuron cell fate after a lesion.

3.1.4.2 *Olig2:GFP*+ ependymo-radial glial cells are polysialic acid and GFAP negative

Polysialic acid (PSA) and GFAP are progenitor cell markers (Rutishauser, 2008) and (Ninkovic and Götz, 2007). Surprisingly, *olig2:GFP*$^+$ ependymo-radial glial cells are selectively GFAP (data not shown) and PSA immuno-negative in unlesioned animals (Fig. 15). Other ependymo-radial glial cells around the entire ventricle express these antigens. However, *olig2:GFP*$^+$ ependymo-radial glial cells express another progenitor cell marker, brain lipid binding protein (Park et al., 2007). This indicates that *olig2:GFP*$^+$ ependymo-radial glial cells express a unique set of progenitor cell markers.

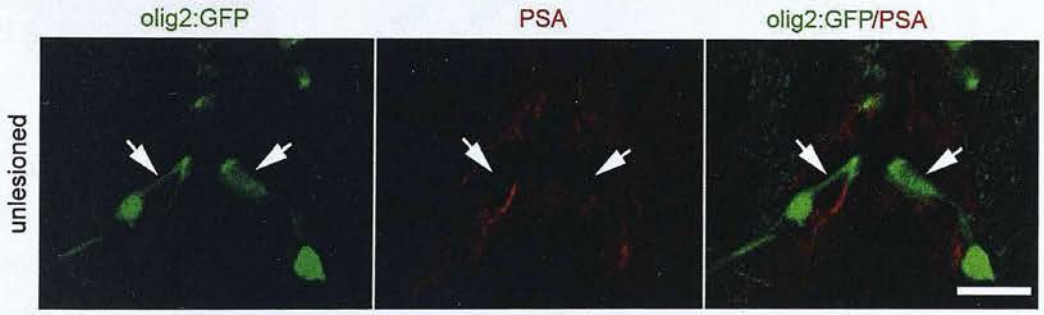

Fig 15: Anti-PSA immunohistochemistry in unlesioned fish. *Olig2:GFP*$^+$ ependymo-radial glial cells (arrows) are PSA$^-$. Cross sections of the spinal cord at the ventricular zone are shown. Bar = 10 µm.

3.1.4.3 Ependymo-radial glial cells, including *olig2:GFP*$^+$ cells, in the spinal cord are label-retaining cells

To determine whether ventricular cells have stem cell characteristics, I tested for BrdU retention over an extended time period, an indicator of slow proliferation (Chapouton et al., 2006). Lesioned animals were injected with a single pulse of BrdU at 14 days post-lesion and the number of ventricular BrdU$^+$ cells was assessed around the entire ventricle at 4 hours and 14 days post-

injection (Fig.16). There was no significant difference in the number of BrdU labelled cells at both time points (p = 0.7237), indicating the presence of slowly proliferating cells in the ventricular zone.

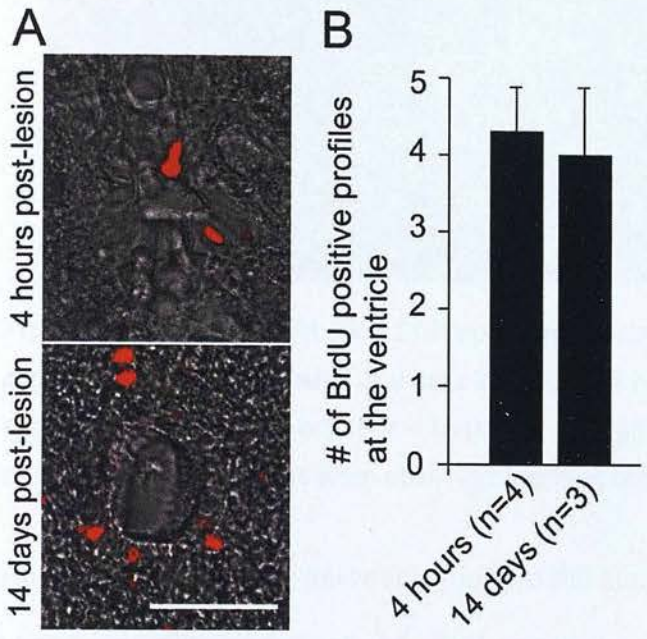

Fig 16: The ventricular zone contains label-retaining cells. **A:** After a single injection of BrdU at 2 wpl and subsequent immunohistochemical analysis at 4 hours or 14 days after injection, BrdU labelled cell profiles were found at the ventricle. **B:** Numbers of $BrdU^+$ cell profiles around the ventricle (up to two nuclei away from the ventricular surface) were determined in confocal image stacks of three randomly selected vibratome sections each from the region up to 750 µm rostral and caudal to the lesion site. This analysis indicates no significant differences in the number of BrdU labelled cells at both time points (p = 0.7237). Bar = 50 µm.

To examine whether the *olig2:GFP*$^+$ ventricular zone also contained label-retaining cells, I repeated the same experiment in *olig2:GFP* transgenic animals. Numbers of *olig2:GFP*$^+$/$BrdU^+$ ependymo-radial glial cells were not significantly different between the two time points (4 hours: 60 ± 11.5 cells, n = 5 animals; 14 days: 53 ± 13.3 cells, n = 4 animals, p = 0.6). This indicates that *olig2:GFP*$^+$ cells did indeed retain label (Fig. 17).

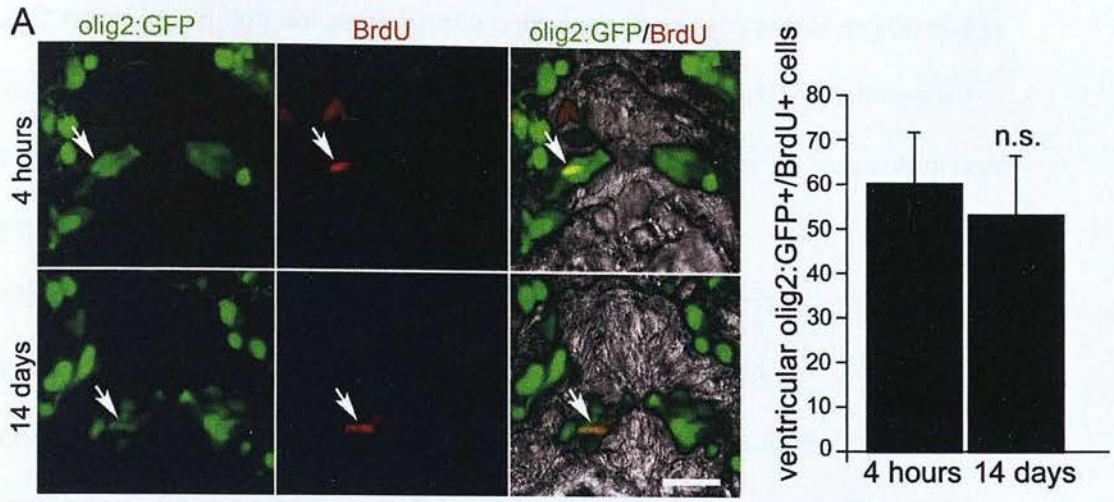

Fig. 17: Label retention in *olig2:GFP* ependymo-radial glial cells. **A:** A subpopulation of *olig2:GFP*$^+$ ependymo-radial glial cells is BrdU$^+$ at 4 hours and 14 days after a single application of BrdU at 2 wpl. Bar = 15 µm. **B:** No significant differences in the number of *olig2:GFP*$^+$/BrdU$^+$ cells were observed between both time points of analysis.

Both label-retention experiments indicate the stem cell characteristics of ventricular cells, specifically of *olig2*$^+$ ependymo-radial glial cells.

Thus far I was able to show that in response to spinal cord lesion new motor neurons were generated. Some of these small motor neurons matured and integrated in the intraspinal circuitry. Evidence suggests that the origin of these new motor neurons is the *olig2*$^+$ ependymo-radial glial cell domain. These ventricular cells even possess stem cell characteristics.

3.1.5 Expression of ventral neural tube markers is increased in a developmentally appropriate pattern

To determine the signals that may induce motor neuron regeneration we analysed expression of *sonic hedgehog* (*shh*), a key player in the organisation of spinal cord patterning in development (Lewis and Eisen, 2001). Transgenic zebrafish, expressing green fluorescent protein (GFP) under the promotor of *shh* revealed an increase in *shh* expression in response to a spinal cord lesion

at 2 wpl (Fig. 18, left column). These cells form the very ventral region of the ventricle. In situ hybridisation with a probe against *shh* mRNA confirms the localization of the transcript and the upregulation in response to a spinal cord transection.

Olig2 is a downstream gene of *shh* signalling. In situ hybridisation showed a lesion induced upregulation of *olig2* expression at the enlarged ventricle, conterminous to the *shh* domain (Fig. 18, right column), suggesting that increased *shh* expression induced increased *olig2* expression in the neighbouring ventricle zone.

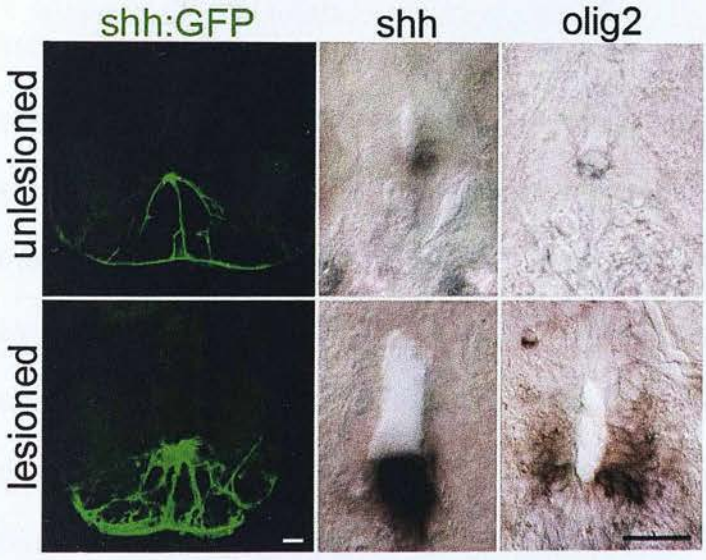

Fig. 18: Lesion-induced expression of *shh* and *olig2* at the ventricle of the lesioned spinal cord. *Shh:GFP* and in situ hybridisation signals are increased at 2 wpl. Cross-sections are shown. Bars = 25 µm.

Combination of the *shh:GFP* transgenic animals with immunohistochemistry detecting *PCNA* reveals that the ventricular *shh:GFP*$^+$ cells are proliferating at 2 weeks post-lesion (Fig. 19). This finding is consistent with the increase in the density of *shh:GFP*$^+$ cells and the intensity and region of *shh* RNA expression (Fig. 18, middle column).

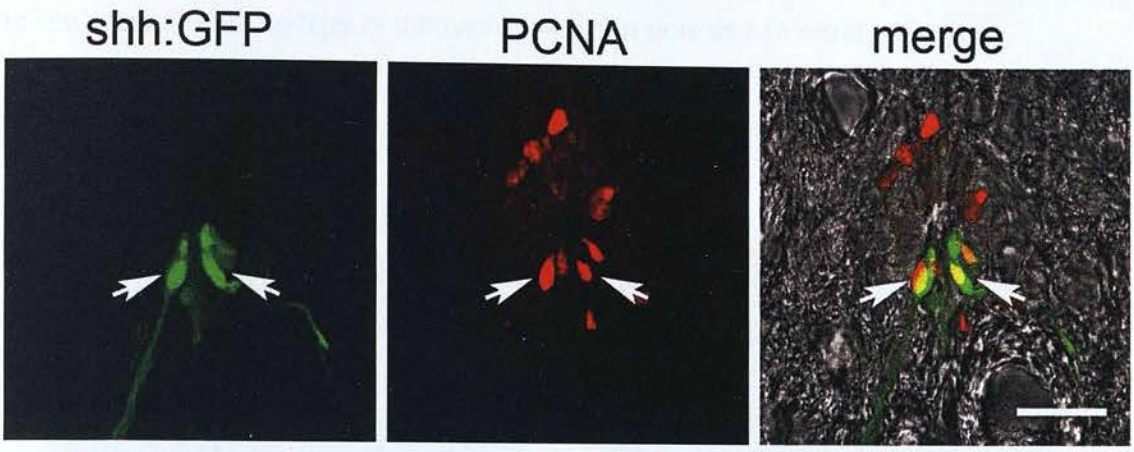

Fig. 19: *Shh:GFP*$^{+}$ ependymo-radial glial cells proliferate after a lesion. GFP^{+} cells have a radial morphology, contact the ventricle at its ventral edge and are labelled by a *PCNA* antibody (arrows) at 2 wpl. Bar = 20 µm.

The increase in the expression of *shh* after a lesion and the increase of *olig2* expression in the adjacent *olig2* domain is consistent with the assumption that *shh* could be a key player in motor neuron regeneration.

Further important transcription factors that determine the cell fate of progenitor cells in the developing spinal cord are the ventrally expressed *nkx6.1* in combination with the *olig2:GFP* expression and the medio-dorsally expressed *pax6* (Becker and Becker, 2007).

Both *nkx6.1* and *pax6* were upregulated after a spinal cord lesion in the adult fish. Low levels of *nkx6.1* observed in the unlesioned ventral spinal cord were increased at 2 weeks post-lesion, but expression was still restricted to the ventral ventricular zone (Fig. 20, upper rows). At 1 wpl *pax6* was expressed in the lateral and dorsal domain of the ventricular zone and was upregulated in response to a spinal cord lesion in the same domain (Fig. 20). Double labelling of *nkx6.1* in *olig2:GFP* transgenic fish (Fig. 21) indicates that the *olig2:GFP*$^{+}$ ventricular zone is included in the *nkx6.1*$^{+}$ zone, with the *nkx6.1*$^{+}$ zone extending slightly more dorsally than the *olig2:GFP*$^{+}$ zone. This is comparable

to the spatial relationships of the two expression domains in the developing neural tube.

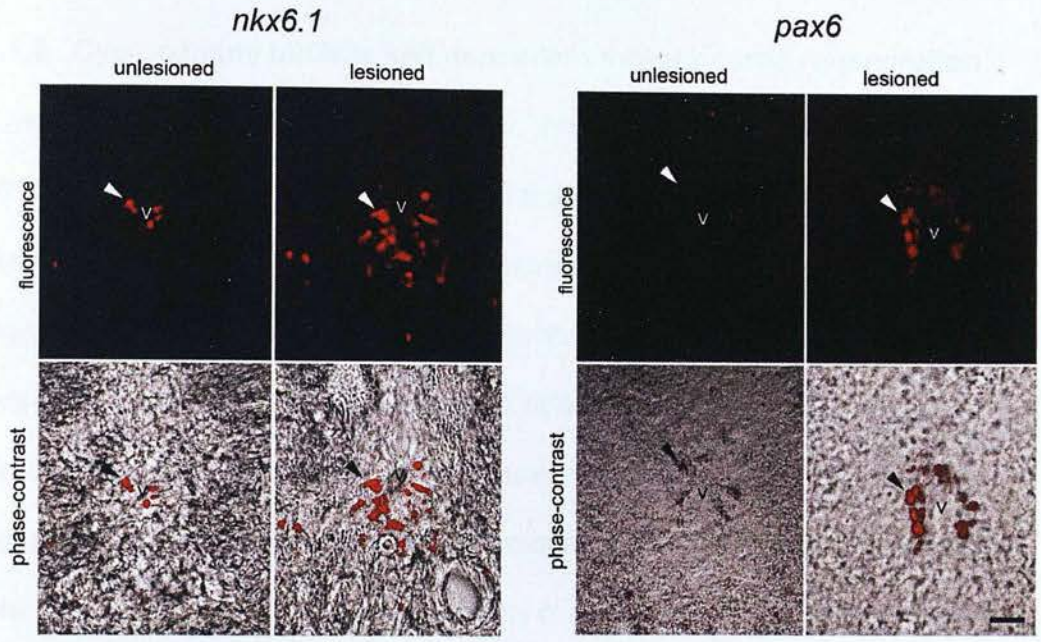

Fig 20: *Nkx6.1* and *pax6* expression is increased in the lesioned spinal cord. Labeling intensity of *nkx6.1* is increased around the ventral ventricle (arrows) at 2 wpl. *Pax6* immunohistochemistry shows upregulation of *pax6* after spinal cord lesion in the upper ventral and dorsal part of the spinal cord. 14 µm cryosections, unlesioned (overexposed to show low levels of immunoreactivity) vs. 1 wpl. Bar 20 µm.

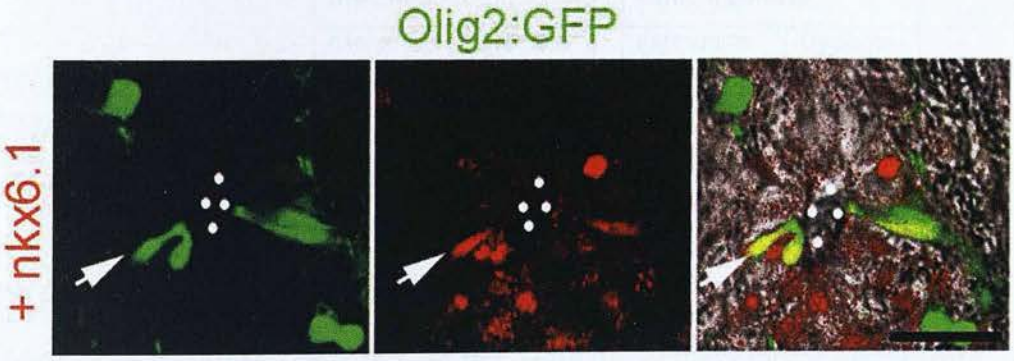

Fig. 21: *olig2:GFP*$^{+}$ ependymo radial glial cells are *nkx6.1* immunopositive in the lesioned adult spinal cord. Double-labelled (arrows) with *nkx6.1* antibody at 2 wpl. Confocal images of cross-sections are shown. Dots outline the ventricle. Bar = 25 µm.

These data indicate that transcription factors are expressed in different dorso-ventral domains of the neural tube. Additionally, the patterns in the ventricular

zone of the unlesioned adult spinal cord are comparable to the lesioned situation, but the expression is increased after a spinal lesion.

3.1.6 Cyclopamine inhibits *shh* dependent motor neuron regeneration

If increased *shh* expression is involved in the generation of new motor neurons after a lesion, a pharmacoligical block of this signaling pathway should reduce the number of newly generated motor neurons. To test this hypothesis, the *shh* signal was experimentally reduced by injections of cyclopamine, a specific small molecule inhibitor of *shh* signalling (Park et al., 2004).

To control the specific activity of cyclopamine I incubated embryos with the substance. This treatment resulted in cyclopia and loss of motor axons (Tab.1), which is consistent with published actions of cyclopamine in zebrafish (Park et al., 2004) . In vehicle treated controls none of the animals showed cyclopia.

Tab. 1: Cyclopamine activity. 24 hpf *HB9:GFP* embryos were analysed after Cyclopamine treatment (n = 6 animals/group were analysed).

	treatment			**vehicle control**	
	axons/fish	Cyclopia		axons/fish	Cyclopia
100 µM Cyclopamine/EtOH	1.2 ± 0.54	7 of 15		46.3 ± 0.95	0 of 15
50 µM Cyclopamine/EtOH	2.3 ± 0.61	5 of 15		46.3 ± 1.09	0 of 15
5 µM Cyclopamine/EtOH	9.7 ± 2.35	1 of 14		48.0 ± 0.52	0 of 14

The loss of motor axons was analysed in the transgenic line *HB9:GFP* after cycopamine incubation from 6 to 24 hpf. Here the primary motor axons were massively effected. For *islet-1:GFP* embryos incubated from 24 to 72hpf the loss of motor neurons in the spinal cord is clearly visible (Fig. 22). This indicates that the *shh* pathway is necessary for the formation and development of motor neurons in development.

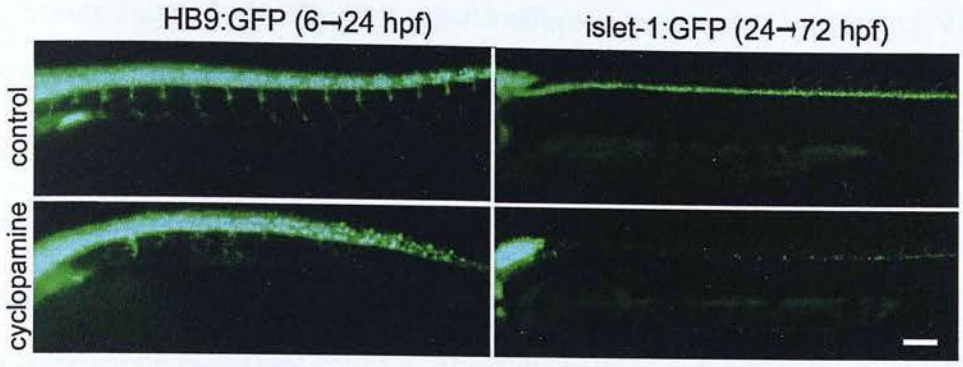

Fig. 22: Specific activity of Cyclopamine in transgenic lines *HB9:GFP* and *islet-1:GFP*. Control animals show normal axon growth, 5 µM Cyclopamine show severe effect on motor axon outgrowth (*HB9:GFP*) and loss of motor neurons (*islet-1:GFP*). Rostral is left, Bar = 25 µm.

Adult spinal cord lesioned zebrafish were repeatedly injected with the *sonic hedgehog* inhibitor cyclopamine at 10 mg/kg, a mouse specific non toxic concentration (Ecke et al., 2008), 3, 6 and 9 days post operation. To avoid the toxic effects of ethanol, I used (2-Hydroxypropyl)-β-cyclodextrin (HBC) as solvent. This solvent has negligible effects on the activity of cyclopamine (Tab.2).

Tab. 2: Cyclopamine activity in HBC at 24 hpf. *HB9:GFP* embryos were analysed after Cyclopamine treatment (n = 6 animals/group were analysed).

	treatment			**vehicle control**	
	axons/fish	Cyclopia		axons/fish	Cyclopia
100 µM Cyclopamine/ HBC	3.7 ± 0.88	6 of 15		47.7 ± 0.95	0 of 15
50 µM Cyclopamine/ HBC	6.0 ± 1.91	4 of 15		46.7 ± 1.33	0 of 12
5 µM Cyclopamine/ HBC	30.8 ± 2.15	0 of 14		46.0 ± 1.15	0 of 15

Injecting cyclopamine into spinal-lesioned adult animals highly significantly reduced the number of newly generated motor neurons within 1.5 mm surrounding the lesion site (377 ± 45.7 cells; n = 9 animals) compared with

animals injected with the related but ineffective substance tomatidine (747 ± 42.2 cells; n = 10 animals; p = 0.0004) at 2 wpl (Fig. 23 A, upper row). Moreover, *shh* is a mitogen (Fuccillo et al., 2006) and I tested whether cyclopamine reduces ventricular proliferation in this region of the lesioned spinal cord by determining the numbers of *PCNA*$^+$ ventricular cells after the same cyclopamine treatment scheme. The number of *PCNA*-labelled cell profiles at the ventricle in cyclopamine-injected animals (45 ± 2.8 profiles/section; n =16 animals) was significantly lower compared with tomatidine-injected control animals (60 ± 7.0 profiles/section; n = 10 animals; p = 0.027; one-tailed test; Fig. 23 A, lower row). Thus, *shh* signalling appears to play a role for progenitor cell proliferation and motor neuron differentiation.

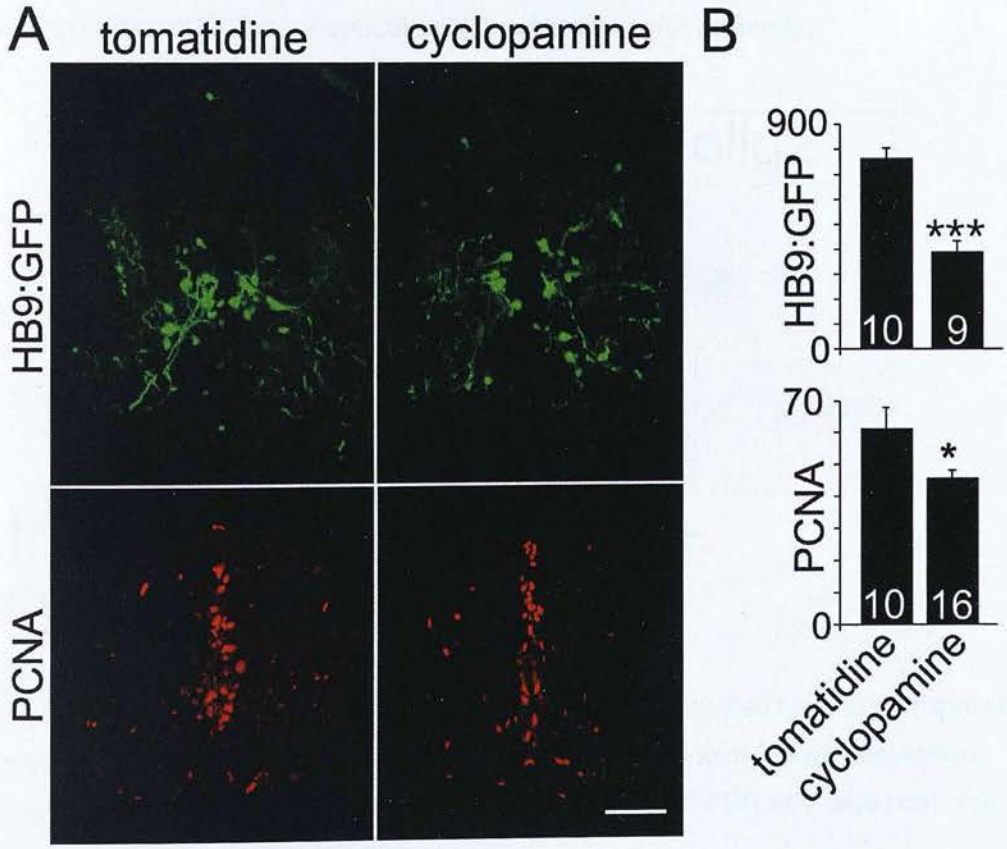

Fig 23: Cyclopamine treatment reduces the number of differentiating motor neurons and ventricular proliferation. **A:** Spinal cross-sections show reduced numbers of *HB9:GFP*$^+$ cells and *PCNA*$^+$ cells after cyclopamine treatment at 2 wpl. **B:** Numbers of

HB9:GFP$^+$ cells and *PCNA*$^+$ profiles are significantly reduced in cyclopamine injected animals. Numbers of animals/treatment are given. Bar = 50 µm.

To assess whether cyclopamine injections specifically influence expression of *shh* target and down-stream genes in the adult spinal cord, I performed RT-PCR to analyse expression of the *shh* target gene *patched1* (Sanchez and Ruiz i Altaba, 2005) and of *olig2*, expression of which depends on *shh* during development (Lu et al., 2000). Expression of both *patched1* and *olig2* mRNA was clearly reduced in the lesioned spinal cord after the cyclopamine treatment, compared to tomatidine treatment (Fig. 24). The PCR was normalized against the housekeeping gene *glyceraldehyde-3-phosphate dehydrogenase* (*GAPDH*). This suggests that cyclopamine affects ventricular proliferation and motor neuron differentiation by specifically blocking the *shh* pathway.

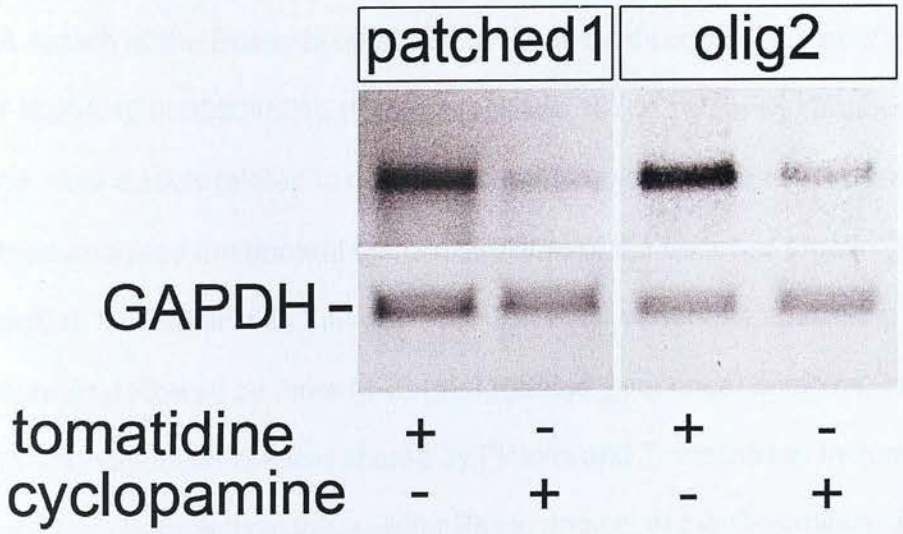

Fig 24: Intraperitoneal injection of cyclopamine reduces *patched1* and *olig2* expression in the lesioned spinal cord. A single injection of cyclopamine at 3 days post-lesion strongly reduces detectability of *patched1* and *olig2* by RT-PCR at 4 days post-lesion compared with tomatidine injection.

3.2 Motor axon pathfinding during development

To analyse the molecular mechanism of axonal differentiation of motor neurons, I turned to the axon growth of so-called primary motor neurons in embryonic zebrafish. The pioneering primary motor axons in the zebrafish trunk are guided by multiple cues along their pathways. We decided to analyse the function of plexins. Plexins are receptor components for semaphorins that influence motor axon growth and pathfinding. This study was a cooperation with Dr. Julia Feldner and is published (Feldner et al., 2007). I contributed mainly to cloning of *plexinA3* overexpression construct, localization of *plexinA3* mRNA in primary motor neurons during axon outgrowth and rescue experiments of morpholino phenotypes.

3.2.1 Cloning of *plexinA3*

A search of the Ensembl database (www.ensembl.org/Danio_rerio/) predicted ENSDARG00000016216 (Ensembl release 19) on zebrafish chromosome 8 to be most closely related to mouse and human *plexinA3* gene sequences. We then analysed the general domain structure of the deduced protein (1892 amino acids). It is identical to that of *plexinA3* in other vertebrate species: a Sema domain, followed by three MRS (Met Related Sequence) domains, four IPT (Immunoglobulin-like fold shared by Plexins and Transcription factors) motifs, and the characteristic intracellular Plexin domain at the C-terminus. The transmembrane domain of the zebrafish protein is located between the IPT motifs and the Plexin domain and comprises amino acids 1241-1263 (Fig. 26A). The protein sequence of the cloned gene has significant structural homology and overall amino acid identity (73%) with human (Maestrini et al., 1996) and mouse (Kameyama et al., 1996) *plexinA3*. Dr. J. Feldner showed in a

phylogenetic tree, constructed using the Clustal method (Chenna et al., 2003), that zebrafish *plexinA3* segregated with *plexinA3* homologs of other species (Fig. 26, B). These data strongly suggest that we cloned a species homolog of *plexinA3*.

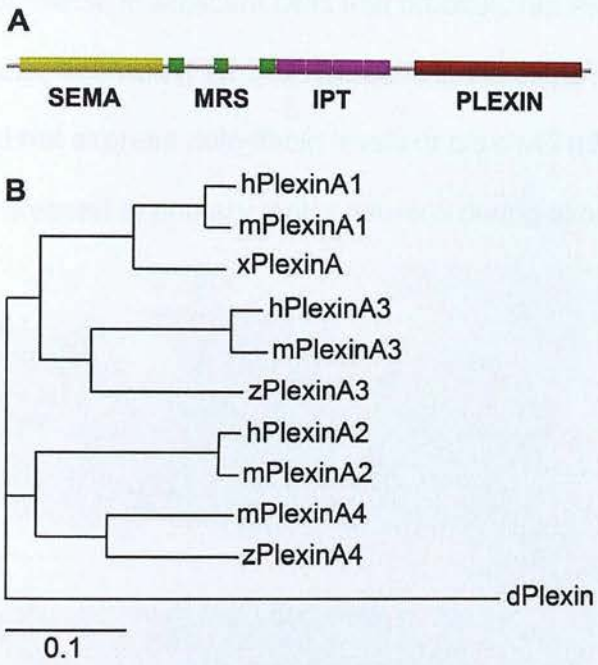

Fig. 26: Structual features and identitiy of *plexinA3* in zebrafish. **A:** Domain strucutre of *plexinA3*. SEMA, Sepmaphorin domain; PLEXIN, plexin domain; MRS, Met-related sequence. **B:** Multiple comparisons in a phylogenetic tree group zebrafish *plexinA3* with *plexinA3* homologs in other vertebrates. *Dosophila* was added as an outgroup. The scalebar represents 10 substitutions per 100 aa. z, zebrafish; m, mouse; h, human; x, *Xenopus*; d, *Drosophila*. (Feldner et al., 2007).

3.2.2 *PlexinA3* is strongly expressed in spinal motor neurons

In situ hybridization indicated expression of *plexinA3* mRNA mainly in the developing nervous system (Fig. 27 A, B). A particularly strong signal was found in regular clusters of cells at the ventral edge of the spinal cord at 16 and 24 hpf, i.e. during the time of axon outgrowth of primary motor neurons. Double labeling of the mRNA with GFP immunohistochemistry in HB9:GFP transgenic

animals at 24 hpf revealed co-localization of the mRNA in GFP$^+$ motor neuron clusters from which the CaP axon started to grow in developmentally younger caudal segments. Conspicuous *plexinA3* mRNA expression was also found in more dorsal GFP negative spinal neurons (Fig. 27 C-E). In more rostral segments in which the MiP axon could be seen to grow out, the mRNA was detectable in adjacent cells that probably represent the CaP and MiP primary motor neurons (Fig. 27 F-H). Cells in the extra-spinal pathway of motor axons did not express detectable levels of *plexinA3* mRNA. Thus, *plexinA3* mRNA is expressed in primary motor neurons during axon outgrowth.

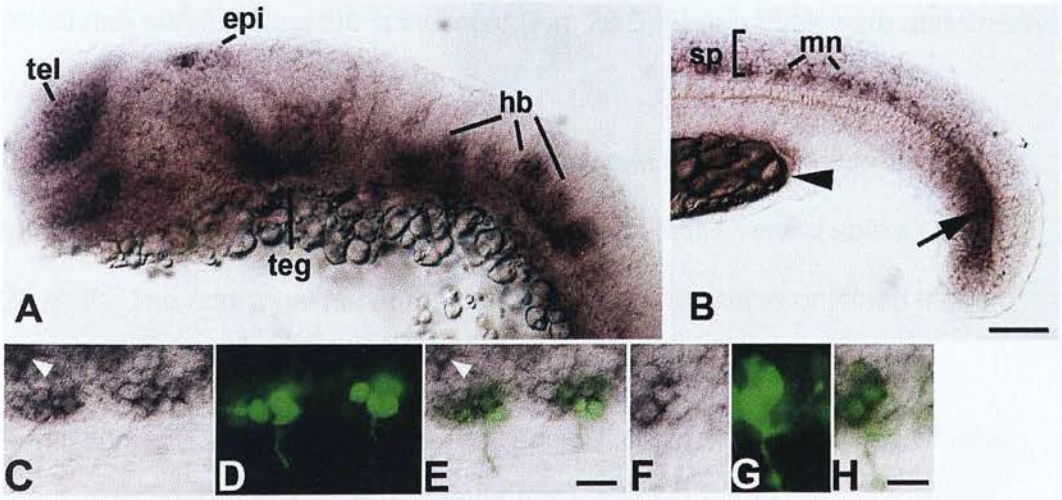

Fig 27: Expression pattern of *plexinA3* mRNA. Lateral views of whole mounted 24 hpf embryos are shown, rostral is left. **A,B:** *PlexinA3* mRNA is present in the telencephalon (tel), epiphysis (epi), tegmentum (teg), hindbrain neurons (hb) in the head (A), as well as in spinal cord (sp) and motor neurons (mn) (B). Additional expression is found in the tip of the tail (arrow in B). Yolk droplets (arrowhead in B) show non-specific staining. **C–H:** In situ hybridization of *plexinA3*-mRNA shows expression in clusters of GFP-immunopositive motor neurons of *HB9:GFP* transgenic fish in lateral views at 24 hpf. C–E, A caudal region in which CaP axons (D, arrowheads) are just growing out. The arrowhead in C and E depicts a more dorsal, GFP-immuno negative cell that shows strong expression of *plexinA3*-mRNA. At higher magnification in **F–H**, two adjacent intensely *plexinA3* mRNA$^+$ neurons in a more rostral segment are depicted. These are likely the CaP (right cell) and MiP (left cell) motor neurons, judging by the trajectories of

the GFP$^+$ MiP (arrow) and CaP (arrowhead) axons. Bars A,B = 100 µm, C-E = 25 µm, F-H = 12.5 µm.

3.2.3 *PlexinA3* is necessary for motor axon pathfinding

Ventral motor nerve growth in *plexinA3* morpholino injected embryos was analysed at 24 hpf using anti-tubulin immunohistochemistry (Fig. 28, A-F). Injection of 1 mM *plexinA3* morpholino1 led to abnormal growth of primary motor axons. Aberrations of ventral motor nerves, which have normally grown as one unbranched nerve beyond the ventral edge of the notochord at 24 hpf (Fig. 28 A,D), can be grouped into two categories: hemisegments showed an additional nerve exiting the spinal cord (Fig. 28 E, F) or nerves were abnormally branched (Fig. 28 B, C).

In 64% of the affected hemisegments, mostly one additional nerve of variable length grew ventrally from an additional exit point in the ventral spinal cord (Fig. 28 E, F). The additional nerve ran parallel to the main nerve or joined it at variable positions dorsal to the horizontal myoseptum. In 68% of the hemisegments showing additional exit points it could not be resolved whether the nerve emanated rostral or caudal to the segment border because the nerves grew very close to it. In the remaining hemisegments, 73% of the additional exit points were located in the posterior half of the somites, 25% were in the anterior half of the somites, or in both the anterior and posterior somite half (2%). On average, 4.7 ± 0.4 hemisegments/embryo had multiple exits in affected embryos.

Ventral motor nerves were aberrantly branched in 35% of the affected hemisegments (Fig. 28 C, D). The vast majority of these branches (82%) were directed caudally. Bifurcated (10%), rostrally (5%) and bilaterally (3%) branched

nerves were observed less frequently. On average, 3.4 ± 0.2 hemisegments/embryo showed aberrant branching in affected embryos.

The effects were dose dependent with 26%, 43%, 64% of the embryos showing aberrant nerve branching and 18%, 56%, 94% of the embryos showing additional exit points from the spinal cord following injections of 0.25, 0.5, and 1 mM morpholino1, respectively. Injecting 1 mM morpholino2 phenocopied these effects (83% embryos affected by abnormal branching; 95% embryos affected by additional exits). Injections of 1 mM of a morpholino in which 5 bases were mismatched had no effect (14% embryos affected by branching, 12% embryos affected by additional exits).

Thus, knockdown of *plexinA3* induces both branching of ventral motor nerves and additional exit points from the spinal cord preferentially in the posterior half of the trunk segments.

To elucidate whether dorsal motor axons, which are obscured in anti-tubulin labelled embryos, were affected by the morpholino treatment we analysed *HB9:GFP* transgenic fish at 31 hpf. At this time point, GFP^+ axons had grown into the dorsal MiP pathway at the level of the yolk extension in uninjected animals (Fig. 28, G). In 1 mM *plexinA3* morpholino1 (n = 10 embryos) or morpholino2 (n = 13 embryos) injected *HB9:GFP* embryos, axons were also present in the MiP pathway, including the segments with multiple exits (n = 47 segments). Interestingly, in nine of these segments, the additional exit points of ventral motor axons also produced additional axons that grew dorsally (Fig. 28, H). Most of these dorsally growing axons were located more laterally than the normal MiP axons as determined in confocal image stacks (not shown). This indicates that these ectopic axons did not simply follow a MiP pathway.

Branching away from the normal MiP pathway was also slightly increased by

the morpholino treatment (Fig. 28 H). The frequency of dorsal motor nerves that were branched ventral to the level of GFP^+ ventral spinal neurons was 33.4% ± 2.84% hemisegments/embryo (n = 327 hemisegments) in morpholino treated animals and 12.1% ± 2.04% hemisegments/embryo (n = 215 hemisegments, Mann-Whitney U-test, $P < 0.0001$) in *HB9:GFP* embryos injected with 5 miss-match (mm) morpholino (n=14 embryos). Thus, additional nerves and increased nerve branching occur in both ventral and dorsal primary motor axon paths.

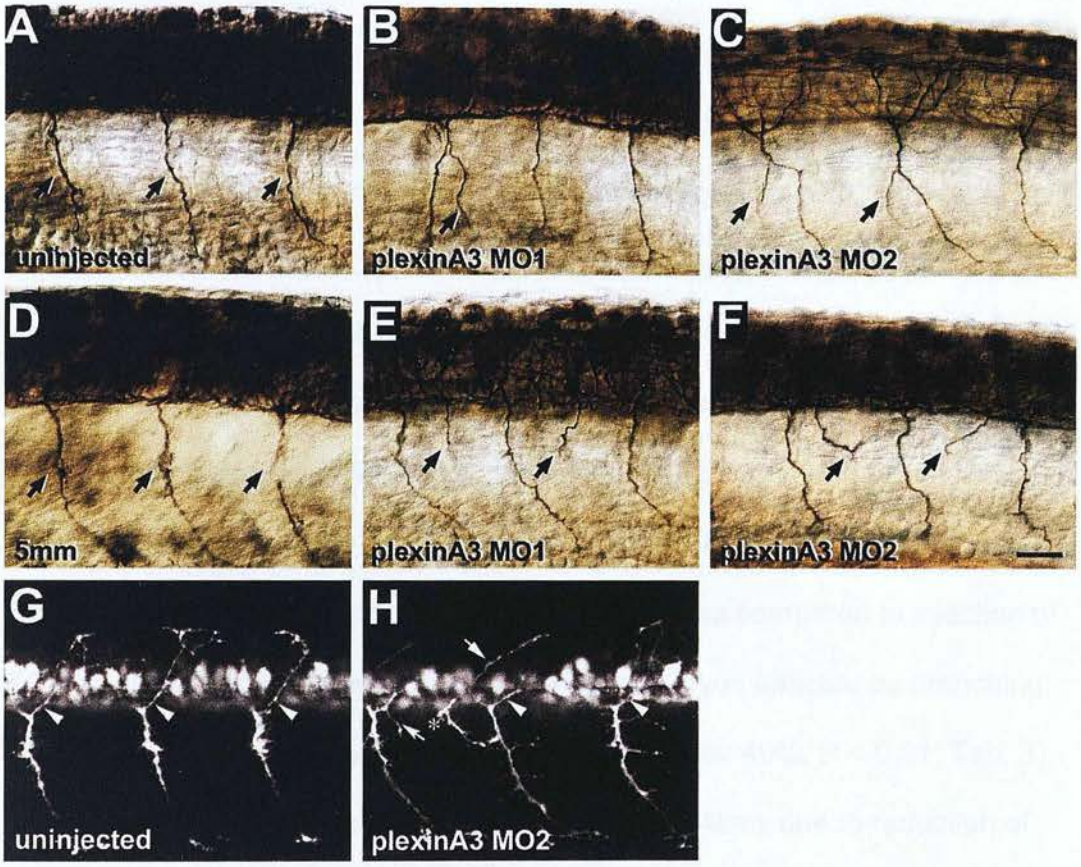

Fig. 28: Function of *plexinA3* in primary motor neurons. **A–F:** Lateral views at midtrunk levels of anti-tubulin-labelled whole mounted 24 hpf embryos are shown. In uninjected embryos (A) or those injected with 1 mM *plexinA3*, 5 mm morpholino (5 mm; D), single unbranched motor nerves (arrows in A and D) grow ventrally out of the spinal cord. Injection of 1mM *plexinA3* morpholino1 (MO1) induces branching (arrow in B) or a second spinal exit point for motor nerves per hemisegment (arrows indicate additional nerves in E). Injection of 1 mM *plexinA3* morpholino2 (MO2) also induced aberrant branching (arrows in C) of the ventral motor nerve and additional nerves exiting the spinal cord (arrows in F). **G,H:**, Axons in the dorsal MiP pathway are visualized in

HB9:GFP transgenic fish in selected confocal image stacks at 31 hpf, indicating normal growth in uninjected embryos (arrowheads in G), and excessive branching (curved arrow in H) and supernumerary nerves (straight arrow in H) in 1 mM *plexinA3* morpholino2-injected embryos. The asterisk in H indicates an additional nerve exit point with a dorsal and ventral nerve branch exiting the spinal cord. Arrowheads in H point to normal appearance of axons in the dorsal motor axon pathway. Rostral is left in A to P. Bar 25µm.

3.2.4 *PlexinA3* morpholino phenotypes are specific.

Morpholino phenotypes need to be carefully controlled. One of the best controls is to rescue the morpholino-induced phenotype with a co-injected full length RNA of the targeted gene, which does not include a binding sequence for the morpholino. Overexpression of a full length myc-tagged *plexinA3* mRNA alone had no effect on motor axon growth as determined by anti-tubulin immunohistochemistry at 24 hpf (data not shown). However, co-injection of *plexinA3* morpholino2 (titrated to 0.3 mM), with *plexinA3* mRNA, which does not have a binding sequence for the morpholino, led to a strong and significant reduction in the frequency of both abnormal branching (13% affected embryos) and additional exits (16% affected embryos). This was compared to injection of 0.3 mM *plexinA3* morpholino2 alone at 24 hpf (embryos affected by branching: 87%, $P < 0.0001$; embryos affected by additional exits: 49%, $P < 0.01$; Tab. 3). This indicates that morpholino phenotypes are most likely due to reduction of *plexinA3* expression.

Tab. 3: Effects of morpholino treatment on ventral motor nerves:

Injection type PLEXINA3 MORPHOLINOS	n	Embryos with aberrant ventral motor nerve branching (%)	Embryos with additional exits of ventral motor nerves (%)
Vehicle	53	11.5 ± 7.3	4.4 ± 2.4
PlexinA3 5mm MO (1 mM)	51	13.8 ± 5.3	12.0 ± 0.3
PlexinA3 MO1 (0.25 mM)	53	26.0 ± 10.4	17.5 ± 5.2
PlexinA3 MO1 (0.5 mM)	65	43.2 ± 14.7 **	56.0 ± 11.7 ***
PlexinA3 MO1 (1 mM)	68	63.8 ± 7.3 ***	93.9 ± 2.7 ***
PlexinA3 MO2 (1 mM)	66	82.9 ± 6.5 ***	94.7 ± 2.5 ***
„RESCUE" EXPERIMENTS			
PlexinA3 MO2 (0.3 mM) alone	42	87.3 ± 3.5	48.8 ± 12.5
PlexinA3 MO2 (0.3 mM) + PlexinA3 mRNA	47	12.7 ± 4.4***	15.7 ± 15.7**

Morpholino doses are indicated in brackets. n = numbers of embryos analyzed, MO = morpholino, plexinA3 MO1/MO2: morpholino1/2 against plexinA3, plexinA3 5mm MO: morpholino with 5 mismatched bases based on plexinA3 morpholino1, ** = P < 0.01, *** = P < 0.001 (Fisher's Exact Test).

In situ hybridization already indicated that *plexinA3* is mainly expressed in the spinal motor neurons and not in cells in other axonal pathways. However to analyse whether changes in the axonal pathways might have induced aberrant axon growth, we analysed other spinal neurons and trunk structures. Analysis of markers of the horizontal and vertical myosepta, as well as spinal floorplate, motor neuron somata, commissural primary ascending interneurons in the spinal cord and Mauthner neurons with their spinal axons, indicated normal differentiation of these structures after injection of 1mM *plexinA3* morpholino1, including those hemisegments with aberrant motor axon growth (Feldner et al. 2007). Thus, the spinal environment of primary motor axons was not detectably altered by the morpholino injections. Hence, we identified *plexinA3* as a crucial receptor in motor neurons for correct pathfinding of primary motor axons in embryonic zebrafish.

4 DISCUSSION

4.1 Adult zebrafish are capable of motor neuron regeneration

In adult zebrafish, a spinal lesion triggers neural stem cells in the spinal cord to produce motor neurons. These cells are added to pre-existing spinal tissue adjacent to a spinal lesion site, as evidenced by the presence of myelin debris at these levels and increased ventricular proliferation in a region covering more than a third of the entire spinal cord around the actual lesion site. In the lesion site itself, normal cytoarchitecture appears not to be restored. Thus, this model differs significantly from tail regeneration paradigms in amphibians in which the entire spinal cord tissue is completely reconstructed from an advancing blastema (Echeverri and Tanaka, 2002).

Two proliferation studies, one with the permanent marker BrdU and the other with a marker for acute proliferation (*PCNA*), revealed the time course and the distribution of newborn cells in the lesioned spinal cord. Both proliferation markers showed a strong increase in the number of labelled cells after a lesion. While BrdU labelled cells were found at the ventricle and in the parenchyma, the increase of *PCNA* labelled cells was only significant in the ventricular zone. These findings suggest that ventricular cells give rise to the majority of newborn cells after a lesion. Newborn cells at the ventricle may subsequently migrate into the parenchyma. Highest proliferative activity was detected close to the lesion site, which is consitent with proliferation being a specific lesion-induced response of the zebrafish spinal cord.

I focused on motor neurons in order to limit the scope of the analysis of different cell types that could theoretically could be newly generated after a lesion. This was because motor neuron loss is the major problem in amyotrophic lateral sclerosis (ALS) and other motor neuron diseases (Ryu and Ferrante, 2007), as well as one of the first problems that needs to be solved after a spinal cord injury. Moreover, the sequence of motor neuron differentiation during development is well-established and markers for motor neuron differentiation are available, such as antibodies (against *ChAT*, *HB9* and *islet-1/-2*) and two independent transgenic reporter lines in which motor neurons are labelled (*HB9:GFP* and *islet-1:GFP*) (Higashijima et al., 2000; Flanagan-Steet et al., 2005).

Looking at the transgenic *HB9:GFP* line we expected that the numbers of the GFP^+ motor neurons would be transiently reduced after a lesion and increase again to levels comparable to those in unlesioned animals. However, *HB9:GFP*$^+$ motor neurons had more complex reaction patterns than originally anticipated. In the unlesioned situation the majority of *HB9:GFP*$^+$ motor neurons were large (> 12 µm diameter) and mostly immunopositive for the mature motor neuron marker *ChAT*. Only very few smaller motor neurons (< 12 µm diameter) where present. The situation changed drastically after a lesion; the number of large motor neurons decreased significantly within the first week. In contrast small *HB9:GFP*$^+$ motor neurons gradually increased from 20.0 ± 7.66 in the unlesioned situation to a maximal value of 869.5 ± 106.78 at 2 wpl. These small motor neurons were rarely *ChAT*$^+$ or decorated by *SV2*$^+$ contacts and were reduced in number in the following weeks. At the same time the number of large *HB9:GFP*$^+$ motor neurons increased again. This result was confirmed with the transgenic *islet-1:GFP* line, in which motor neurons also express GFP. In this

line, the number of small motor neurons likewise increased transiently after a lesion while large neurons disappeared. These observations led us to hypothesize that small *HB9:GFP* or *islet-1:GFP* positive neurons were immature motor neurons that were derived from the proliferating ventricular cells and in the process of regeneration matured to large differentiated motor neurons. Indeed, intraperitoneal BrdU injections indicated that small motor neurons were newly generated after a lesion. The injections labelled 23% of the small, GFP^+ motor neurons with BrdU. Repeated BrdU injections kills the fish, therefore only three injections could be administered, one every other day. However, the bioavailability of BrdU has been estimated to be only 4 hours after injection (Zupanc and Horschke, 1995). This is one explanation why less than a quarter of the small motor neurons were double labelled. Another reason might be that after labelling with BrdU the number of cell divisions that occurred diluted the BrdU labelling below the detection level of immunohistochemistry. Nevertheless, the numbers of small *HB9:GFP*$^+$ motor neurons increased from 20 in unlesioned animals to 870 at 2 wpl, which represents a 43-fold increase. Moreover, a large proportion of these cells were $BrdU^+$. This suggests that nearly all small motor neurons at 2 wpl were newly generated.

Islet-1 and *HB9* are markers for different subpopulations and/or differentiation stages of motor neurons in the developing spinal cord of amniotes (William et al., 2003). In this study I found evidence that this may also be the case for the regenerating spinal cord of adult zebrafish, by using combinations of the *islet-1:GFP* and *HB9:GFP* transgenic reporter lines and antibodies to *islet-1/-2* and *HB9*. In the lesioned situation, the *islet-1/-2* antibody recognizes the majority of all *islet-1:GFP* labelled small motor neurons and additionally a huge population of cells that do not express the *islet1* transgene. These are thought to be *islet-2*$^+$

neurons. Combining the *HB9:GFP* line with the *islet-1/-2* antibody revealed that there is a large populations of motor neurons that are only labelled with the *HB9:GFP* transgene. Similarly, the *HB9* antibody labelled mainly GFP^- cells in the *islet-1:GFP* line (data not shown). This suggests heterogeneity among the newly generated motor neurons in terms of their marker expression profile. These findings indicate that spinal cord lesion in zebrafish may induce the generation of diverse motor neuron cell types.

One important question is whether newborn motor neurons are integrated into the spinal cord circuitry and fulfill their purpose as motor neurons. According to a time course study of *ChAT* immunohistochemistry conducted by a postgraduate student in our laboratory, Veronika Kuscha, the number of fully differentiated, $ChAT^+$ cells drops from 478.0 ± 111.12 (n = 3 animals) cells in unlesioned animals to 234.7 ± 111.12 (n = 3 animals) at 2 wpl and recovers by 6 wpl to 348.4 ± 67.27 (n = 4 animals) in the 1500 µm around the lesion site. Hypothesizing that the increase in $ChAT^+$ cells is due to the maturation of the newborn motor neurons (e.g. small $HB9:GFP^+$ cells), 114 $ChAT^+$ cells must have been newly generated between 2 and 6 wpl. Taking into account that the BrdU injection scheme labels almost a quarter of all newborn motor neurons, we expect to find 28.5 $ChAT^+$/$BrdU^+$ double labelled cells within 1500 µm around the lesion site. Confirming this expectation, a triple-immunohistochemisty experiment using antibodies against *ChAT*, BrdU and the synaptic marker *SV2* reveals that at 6 wpl 29.3 ± 23.14 (n = 3 animals) cells are double labelled for *ChAT* and BrdU and are decorated by $SV2^+$ contacts within 1500 µm around the lesion site. This suggests that after a spinal cord lesion the loss of mature motor neurons is compensated for by maturation and integration of newly generated motor neurons. The presence of $SV2^+$ contacts on these

neurons indicates that they may receive synaptic input and may thus be integrated into the spinal circuitry. Furthermore, double labelling with BrdU and retrograde tracing from the muscle tissue reveals that a newborn motor neuron contacted muscle tissue at 8 wpl, which is consistent with a motor neuron function of these newly generated cells. All these lesion induced morphological changes match the time course of functional recovery which plateaus at 6 wpl (Becker et al., 2004). Therefore, it is possible that newly generated fully mature motor neurons replace lost motor neurons and contribute to functional recovery after a spinal cord lesion.

4.2 *Olig2*$^+$ ependymo-radial glial cells are the putative stem cells in adult motor neuron regeneration

Some observations suggest that *olig2*$^+$ ependymo-radial glial cells are neural stem cells. Continued low level proliferation in the unlesioned adult (Park et al., 2007) and increased proliferation after a lesion do not lead to significant changes in the number of *olig2:GFP*$^+$ cells, suggesting asymmetric cell divisions and some potential for self-renewal. Using a BrdU label retention experiment, I was able to confirm that *olig2:GFP*$^+$ ependymo-radial glial cells were label-retaining, which is another stem cell characteristic (Grandel et al., 2006). Moreover, these cells express the stem cell markers *BLBP* and *atypical protein kinase C* protein (Park et al., 2007). A stem cell role for olig$^+$ ependymo-radial glia cells would be in agreement with that of several other radial glia cell types in developing mammals and in adult zebrafish (Pinto and Götz, 2007). For example, Müller cells, the radial glia cell type in the adult retina, can produce different cell types in adult zebrafish, depending on which of these are lost after specific lesions (Bernardos et al., 2007; Fimbel et al., 2007).

Furthermore, lineage tracing experiments showed *olig2:GFP*$^+$ ependymo-radial glial cells already expressed *HB9* and were BrdU$^+$ in a triple labelling experiment and were *islet-1/-2*$^+$ in double labelling experiments. This was only observed after lesion as *olig2:GFP*$^+$ ependymo-radial glial cells were never found to produce neurons in the unlesioned situation. Therefore, *olig2* expressing ependymo-radial glial cells switch from a gliogenic phenotype to motor neuron production, indicating that these are the likely adult stem cells. So far a fate switch for spinal progenitor cells has only been described for generating neurons to generating glial cells during development in different vertebrates (Götz and Barde, 2005).

4.3 Mechanisms of motor neuron regeneration in adult zebrafish are similar to developmental mechanisms

Comparing developmental mechanisms of motor neuron formation with motor neuron regeneration revealed similarities. In the development of vertebrate spinal cord motor neurons the morphogen *Sonic Hedgehog* (*shh*) sets a dorso-ventral gradient which leads to five progenitor domains. Each of these domains is defined by the expression of a unique set of transcription factors (Jessell, 2000). The *olig2*$^+$ domain in combination with the transcription factors *nkx6.1* and *pax 6* defines the pMN progenitor cell domain that gives rise to motor neurons.

The ventricular zone of the adult spinal cord in zebrafish retains its embryonic polarity. The expression domains of *shh*, *nkx6.1* and *olig2* around the ventral ventricle are comparable to those in the embryonic neural tube (Fuccillo et al., 2006). Even though expression of these markers was strongly increased after a lesion, they were expressed in a comparable pattern in unlesioned animals. The

transcription factor *olig2* is detectable as a transgene but is below the detection threshold of in situ hybridization in unlesioned animals (Park et al., 2007).

The polarized increase of *shh* profoundly influences motor neuron regeneration. I tested this by using small molecule perturbation of *shh* function. We used the well established inhibitor cyclopamine, which also abrogates differentiation of motor neurons in developing zebrafish (Park et al., 2004; Fuccillo et al., 2006). Injecting the substance into adult zebrafish specifically reduced expression of the *shh* target gene *patched1* and the down-stream gene *olig2* in semi-quantative PCR, indicating specific action of the compound on the *shh* pathway. Cyclopamine reduced ventricular proliferation and the number of regenerated motor neurons, suggesting that *shh* signaling is necessary for motor neuron regeneration.

So far, marker expression and *shh* signaling is remarkably similar between regeneration and developmental processes. However, the fate switch from gliogenesis to motor neuron production in progenitor cells appears to be specific for regeneration (Raya et al., 2003).

4.4 Implications of motor neuron regeneration in zebrafish for spinal cord regeneration in mammals

We were able to investigate proliferation of endogenous progenitor cells, neuronal differentiation signals and motor neuron regeneration in the injured spinal cord of the adult zebrafish, which shows successful recovery of function. In mammals, spinal cord injury leads to extensive secondary cell loss around the lesion site (Demjen et al., 2004). In the lesioned spinal cord of mammals, proliferation and expression of nestin, an intermediate filament marker for progenitor cells, is increased around the ventricle and in parenchymal

astrocytes, some of which carry radial processes (Yamamoto et al., 2001; Shibuya et al., 2002). Exogenous administration of *shh* to the lesioned spinal cord increases precursor cell proliferation (Bambakidis and Miller, 2004). Expression of *pax6*, a transcription factor of progenitor cells in the embryonic spinal cord (Fuccillo et al., 2006), is increased in the ependymal layer of the lesioned adult mammalian spinal cord. However, contrary to development, this expression is not polarized. *Olig2* and several other factors are not re-expressed (Yamamoto et al., 2001) and no neurons were formed. One report (Chen et al., 2005) showed a surprisingly wide spread increase in *shh* mRNA expression in the entire ependyma and several parenchymal cell types in mice. Overall, these observations suggest that spinal progenitors in mammals show some plasticity after a lesion and could be induced to produce new motor neurons. This might be achieved by combining *shh* with other growth factors (Ohori et al., 2006).

It will be very interesting to elucidate whether other signaling pathways are involved in neuronal regeneration in the adult spinal cord (i.e. notch pathway, retinoic acid pathway and wnt pathway), either directly or indirectly by stimulating *shh* expression. Identifying signals that trigger and control neuronal replacement from endogenous progenitor cells in fish may inform future cell therapies for spinal cord injury, but also for neurodegenerative diseases, such as ALS (Roskams and Tetzlaff, 2005).

4.5 *PlexinA3* is crucial for motor axon pathfinding

To understand motor neuron regeneration in the adult spinal cord it is important also to analyse motor neuron differentiation during development. We analysed the role of *plexinA3* for axonal differentiation of motor neurons. Morpholino

knockdown experiments suggest that *plexinA3* in dorsal and ventral motor axons may be necessary to correctly read repellent cues from semaphorins during axon outgrowth. The observed phenotypes are consistent with those observed for knockdown of NRP1a in our lab (Bovenkamp et al., 2004), indicating that NRP/plexin receptor complexes are likely to exist in primary motor axons. The receptor knockdown phenotypes observed, additional exits from the spinal cord and branching of the ventral and dorsal motor nerve, are consistent with a release of axon growth from environmental restrictions. Indeed, class 3 semaphorins are expressed in the trunk environment and are thought to signal through plexin receptors (Birely et al., 2005; Gulati-Leekha and Goldman, 2006).

Up to 95% of *plexinA3* morpholino-injected embryos show specific types of motor axon aberrations and 30% of all hemi-segments analysed were aberrant. This is more than in comparable studies of other proteins in motor axon growth (Feldner et al., 2005; Sato-Maeda et al., 2006). Two sequence-independent morpholinos yielded identical results and I was able to rescue all of the phenotypes to a significnat degree by supplementing *plexinA3* using mRNA overexpression. Using various markers, we could not find detectable changes in the spinal cord and trunk structures of morpholino treated embryos. This suggests a major and specific function of *plexinA3* in primary motor neurons. We conclude that growth and pathfinding of primary motor axons in zebrafish is governed by a complex interplay of different semaphorin ligands and receptors of which *plexinA3* is a crucial component. Shortly after completion of our *plexinA3* knockdown study, two independent publications reported *plexinA3* mutant zebrafish with almost identical phenotypes (Palaisa and Granato, 2007; Tanaka et al., 2007). This shows that forward and reverse genetics approaches

have the potential to elucidate motor axon differentiation in this in vivo model in unprecedented detail. It will be interesting to determine to what degree adult regenerating motor neurons recapitulate embryonic gene expression.

4.6 Conclusion

We conclude that the zebrafish, a powerful genetic model which is accessible to pharmacological manipulations, provides an opportunity to identify the evolutionarily conserved signals that control embryonic motor neuron differentiation and massive regeneration of motor from endogenous stem cells in the adult spinal cord.

5 SUMMARY

Zebrafish, in contrast to mammals, are capable of functional spinal cord regeneration. Spinal motor neurons are major targets for axons regenerating from the brainstem. Using immunohistochemical markers and transgenic reporter fish for motor neuron markers (*HB9*, *islet-1*), this study demonstrates that large differentiated motor neurons are transiently lost after a spinal lesion, suggesting that these cells undergo cell death after a lesion and may be replaced by proliferation. Indeed, a massive and transient increase in the number of small, undifferentiated motor neurons, which were labelled by the proliferation marker bromodeoxyuridine, was observed. Proliferation and lineage tracing studies indicated significant proliferation only at the spinal ventricle and that a subset of *olig2* expressing ependymo-radial glial cells are the likely motor neuron progenitor/stem cells in the lesioned spinal cord.

A spinal lesion increased expression of *sonic hedgehog* (*shh*), an embryonic differentiation signal for motor neurons. Blocking this signal with an antagonist reduced progenitor cell proliferation and motor neuron differentiation. This suggests that *shh* is an important signal for motor neuron differentiation during adult motor neuron regeneration.

To learn more about axonal differentiation of motor neurons, the role of the cell recognition molecule *plexinA3* was investigated during the outgrowth of embryonic primary motor axons. The molecule is selectively expressed in primary motor neurons. Knockdown of expression led to ectopic exiting from the spinal cord and excessive branching of motor axons. Over-expression of full length *plexinA3* rescued this effect, indicating specificity of experimental

manipulations. Thus, *plexinA3* expression is crucial for motor axon pathfinding during development.

Overall, this study demonstrates that adult zebrafish are capable of motor neuron regeneration from endogenous progenitor/stem cells and that *shh* is an important regulator of motor neuron regeneration. *PlexinA3* is crucial for motor axon differentiation in embryonic zebrafish. This study establishes adult spinal cord lesion as a model system for motor neuron regeneration, which may ultimately help to find ways to promote motor neuron regeneration also in human conditions, such as spinal cord injury or motor neuron disease.

6 ZUSAMMENFASSUNG

Im Gegensatz zu Säugetieren besitzt der Zebrafisch die Fähigkeit zur funktionellen Rückenmarksregeneration. Dabei sind Motorneurone ein wichtiger postsynaptischer Zelltyp für Axone die vom Hirnstamm her regenerieren. Das Ziel dieser Arbeit war es zu analysieren, ob Motorneurone im lädierten Rückenmark regenerieren und die Differenzierungssignale für Motorneurone während der adulten Regeneration und der Embryonalentwicklung zu erforschen. Es konnte gezeigt werden, dass grosse, differenzierte Motorneurone nach einer kompletten Rückenmarksdurchtrennung vorübergehend verloren gehen und nach erfolgter Regeneration wieder nachweisbar sind. Um dies zu zeigen, wurden transgene Tiere mit Reportergenen für die Motorneuronmarker *HB9* bzw. *islet-1* und immunhistochemische Marker zur Darstellung von Motorneuronen verwendet. Diese Beobachtungen legen die Vermutung nahe, dass Motorneurone durch verletzungsbedingten Zelltod verloren gehen und dann im Zuge der Regeneration ersetzt werden. Tatsächlich kann eine transiente, massive Zunahme kleiner, undifferenzierter Motorneurone beobachtet werden. Mit Hilfe des Proliferationsmarkers Bromodeoxyuridine (BrdU) konnte nachgewiesen werden, dass diese undifferenzierten Motorneurone neu gebildet wurden. Eine signifikante verletzungsbedingete Prolifertation wurde nur am Ventrikel festgestellt. Ferner zeigte sich durch „lineage tracing", dass eine *olig2* exprimierende Subpopulation der ventrikulären Ependymo-Radialgliazellen die vermutlichen Stammzellen oder Progenitorzellen für Motorneurone im Rückenmark darstellen.

Eine Rückenmarksdurchtrennung im adulten Zebrafisch führt zu einer Erhöhung der Expression von *sonic hedgehog* (*shh*), einem Differenzierungssignal für Motorneurone während der Embryonalentwicklung. Intraperitoneale Injektion des *shh* -Antagonisten Cyclopamin während der Regeneration blockiert diesen Signalweg und führt zu einer signifikanten Reduktion der Proliferation von Progenitorzellen sowie der Motorneurondifferenzierung. Diese Ergebnisse legen den Schluss nahe, dass *shh* eine zentrale Rolle für die Regeneration von Motorneuronen im adulten Zebrafisch einnimmt.

Um die axonalen Differenzierung von Motorneuronen genauer zu erforschen, wurde die Funktion des Zellerkennungsmoleküls *plexinA3* bei dem Auswachsen embryonaler primärer Motoraxone untersucht. Es konnte gezeigt werden, dass *plexinA3* spezifisch von primären Motorneuronen exprimiert wird. Eine experimentelle Verringerung der Expression dieses Proteins mittels Injektion von anti-sense Morpholino-Oligonukleotiden bewirkt ein ektopisches Auswachsen aus dem Rückenmark sowie exzessives Verzweigen der Axone primärer Motorneurone. In einem "Rescue-Experiment" konnte durch Überexpression von *plexinA3* der Morpholino-Effekt neutralisiert werden. Dies belegt die Spezifität der genetischen Manipulation und zeigt das *plexinA3* äußerst wichtig für die axonale Wegfindung während der Entwicklung ist.

Abschließend kann festgestellt werden, dass der adulte Zebrafisch unter Kontrolle von *shh* zur Regeneration von Motorneuronen fähig ist. Als Quelle für diese neu entstehenden Motorneurone dienen endogene Progenitor- oder Stammzellen. Bei der axonalen Wegfindung von primären Motorneuronen während der Embryogenese spielt *plexinA3* eine Schlüsselrolle. Die in dieser Arbeit gewonnen Erkenntnisse über Motorneuronendifferenzierung im Zebrafisch, können schlussendlich helfen, neue Strategien für die Regeneration

von Motorneuronen nach Rückenmarksverletzungen oder Behandlungen für Erkrankungen der Motorneuronen, wie beispielsweise der amyotrophen Lateralsklerose, zu entwickeln.

7 LITERATURE

Bambakidis NC, Miller RH (2004) Transplantation of oligodendrocyte precursors and sonic hedgehog results in improved function and white matter sparing in the spinal cords of adult rats after contusion. Spine J 4:16-26.

Bambakidis NC, Butler J, Horn EM, Wang X, Preul MC, Theodore N, Spetzler RF, Sonntag VK (2008) Stem cell biology and its therapeutic applications in the setting of spinal cord injury. Neurosurg Focus 24:E20.

Beattie CE (2000) Control of motor axon guidance in the zebrafish embryo. Brain Res Bull 53:489-500.

Beck CW, Christen B, Slack JM (2003) Molecular pathways needed for regeneration of spinal cord and muscle in a vertebrate. Dev Cell 5:429-439.

Becker CG, Becker T, eds (2007) Model Organisms in Spinal Cord Regeneration.

Becker CG, Lieberoth BC, Morellini F, Feldner J, Becker T, Schachner M (2004) L1.1 is involved in spinal cord regeneration in adult zebrafish. J Neurosci 24:7837-7842.

Becker T, Becker CG (2001) Regenerating descending axons preferentially reroute to the gray matter in the presence of a general macrophage/microglial reaction caudal to a spinal transection in adult zebrafish. J Comp Neurol 433:131-147.

Becker T, Lieberoth BC, Becker CG, Schachner M (2005) Differences in the regenerative response of neuronal cell populations and indications for plasticity in intraspinal neurons after spinal cord transection in adult zebrafish. Mol Cell Neurosci 30:265-278.

Becker T, Wullimann MF, Becker CG, Bernhardt RR, Schachner M (1997) Axonal regrowth after spinal cord transection in adult zebrafish. J Comp Neurol 377:577-595.

Bernardos RL, Barthel LK, Meyers JR, Raymond PA (2007) Late-stage neuronal progenitors in the retina are radial Muller glia that function as retinal stem cells. J Neurosci 27:7028-7040.

Bernhardt RR (1999) Cellular and molecular bases of axonal regeneration in the fish central nervous system. Exp Neurol 157:223-240.

Birely J, Schneider VA, Santana E, Dosch R, Wagner DS, Mullins MC, Granato M (2005) Genetic screens for genes controlling motor nerve-muscle development and interactions. Dev Biol 280:162-176.

Bovenkamp DE, Goishi K, Bahary N, Davidson AJ, Zhou Y, Becker T, Becker CG, Zon LI, Klagsbrun M (2004) Expression and mapping of duplicate neuropilin-1 and neuropilin-2 genes in developing zebrafish. Gene Expr Patterns 4:361-370.

Briscoe J, Ericson J (2001) Specification of neuronal fates in the ventral neural tube. Curr Opin Neurobiol 11:43-49.

Carulli D, Laabs T, Geller HM, Fawcett JW (2005) Chondroitin sulfate proteoglycans in neural development and regeneration. Curr Opin Neurobiol 15:116-120.

Chapouton P, Adolf B, Leucht C, Tannhauser B, Ryu S, Driever W, Bally-Cuif L (2006) her5 expression reveals a pool of neural stem cells in the adult zebrafish midbrain. Development 133:4293-4303.

Chen J, Leong SY, Schachner M (2005) Differential expression of cell fate determinants in neurons and glial cells of adult mouse spinal cord after compression injury. Eur J Neurosci 22:1895-1906.

Chenna R, Sugawara H, Koike T, Lopez R, Gibson TJ, Higgins DG, Thompson JD (2003) Multiple sequence alignment with the Clustal series of programs. Nucleic Acids Res 31:3497-3500.

Coggeshall RE, Lekan HA (1996) Methods for determining numbers of cells and synapses: a case for more uniform standards of review. J Comp Neurol 364:6-15.

Demjen D, Klussmann S, Kleber S, Zuliani C, Stieltjes B, Metzger C, Hirt UA, Walczak H, Falk W, Essig M, Edler L, Krammer PH, Martin-Villalba A (2004) Neutralization of CD95 ligand promotes regeneration and functional recovery after spinal cord injury. Nat Med 10:389-395.

Dijkers MP (2005) Quality of life of individuals with spinal cord injury: a review of conceptualization, measurement, and research findings. J Rehabil Res Dev 42:87-110.

Echeverri K, Tanaka EM (2002) Ectoderm to mesoderm lineage switching during axolotl tail regeneration. Science 298:1993-1996.

Ecke I, Rosenberger A, Obenauer S, Dullin C, Aberger F, Kimmina S, Schweyer S, Hahn H (2008) Cyclopamine treatment of full-blown Hh/Ptch-associated RMS

partially inhibits Hh/Ptch signaling, but not tumor growth. Mol Carcinog 47:361-372.

Eisen JS, Myers PZ, Westerfield M (1986) Pathway selection by growth cones of identified motoneurones in live zebra fish embryos. Nature 320:269-271.

Eisen JS, Pike SH, Romancier B (1990) An identified motoneuron with variable fates in embryonic zebrafish. J Neurosci 10:34-43.

Feldner J, Reimer MM, Schweitzer J, Wendik B, Meyer D, Becker T, Becker CG (2007) PlexinA3 restricts spinal exit points and branching of trunk motor nerves in embryonic zebrafish. J Neurosci 27:4978-4983.

Feldner J, Becker T, Goishi K, Schweitzer J, Lee P, Schachner M, Klagsbrun M, Becker CG (2005) Neuropilin-1a is involved in trunk motor axon outgrowth in embryonic zebrafish. Dev Dyn 234:535-549.

Fimbel SM, Montgomery JE, Burket CT, Hyde DR (2007) Regeneration of inner retinal neurons after intravitreal injection of ouabain in zebrafish. J Neurosci 27:1712-1724.

Flanagan-Steet H, Fox MA, Meyer D, Sanes JR (2005) Neuromuscular synapses can form in vivo by incorporation of initially aneural postsynaptic specializations. Development 132:4471-4481.

Fuccillo M, Joyner AL, Fishell G (2006) Morphogen to mitogen: the multiple roles of hedgehog signalling in vertebrate neural development. Nat Rev Neurosci 7:772-783.

Giger RJ, Cloutier JF, Sahay A, Prinjha RK, Levengood DV, Moore SE, Pickering S, Simmons D, Rastan S, Walsh FS, Kolodkin AL, Ginty DD, Geppert M (2000) Neuropilin-2 is required in vivo for selective axon guidance responses to secreted semaphorins. Neuron 25:29-41.

Götz M, Barde YA (2005) Radial glial cells defined and major intermediates between embryonic stem cells and CNS neurons. Neuron 46:369-372.

Grandel H, Kaslin J, Ganz J, Wenzel I, Brand M (2006) Neural stem cells and neurogenesis in the adult zebrafish brain: origin, proliferation dynamics, migration and cell fate. Dev Biol 295:263-277.

Gulati-Leekha A, Goldman D (2006) A reporter-assisted mutagenesis screen using alpha 1-tubulin-GFP transgenic zebrafish uncovers missteps during neuronal development and axonogenesis. Dev Biol 296:29-47.

Halloran MC, Sato-Maeda M, Warren JT, Su F, Lele Z, Krone PH, Kuwada JY, Shoji W (2000) Laser-induced gene expression in specific cells of transgenic zebrafish. Development 127:1953-1960.

Hewitson TD, Bisucci T, Darby IA (2006) Histochemical localization of apoptosis with in situ labeling of fragmented DNA. Methods Mol Biol 326:227-234.

Higashijima S, Hotta Y, Okamoto H (2000) Visualization of cranial motor neurons in live transgenic zebrafish expressing green fluorescent protein under the control of the islet-1 promoter/enhancer. J Neurosci 20:206-218.

Horner PJ, Power AE, Kempermann G, Kuhn HG, Palmer TD, Winkler J, Thal LJ, Gage FH (2000) Proliferation and differentiation of progenitor cells throughout the intact adult rat spinal cord. J Neurosci 20:2218-2228.

Huber AB, Kania A, Tran TS, Gu C, De Marco Garcia N, Lieberam I, Johnson D, Jessell TM, Ginty DD, Kolodkin AL (2005) Distinct roles for secreted semaphorin signaling in spinal motor axon guidance. Neuron 48:949-964.

J Sambrook, E F Fritsch, Maniatis T (1989) Molecular Cloning. In: New York Cold Spring Harbour Laboratory Press.

Jessell TM (2000) Neuronal specification in the spinal cord: inductive signals and transcriptional codes. Nat Rev Genet 1:20-29.

Johansson BB (2007) Regeneration and plasticity in the brain and spinal cord. J Cereb Blood Flow Metab 27:1417-1430.

Kameyama T, Murakami Y, Suto F, Kawakami A, Takagi S, Hirata T, Fujisawa H (1996) Identification of plexin family molecules in mice. Biochem Biophys Res Commun 226:396-402.

Kibbelaar RE, Moolenaar CE, Michalides RJ, Bitter-Suermann D, Addis BJ, Mooi WJ (1989) Expression of the embryonal neural cell adhesion molecule N-CAM in lung carcinoma. Diagnostic usefulness of monoclonal antibody 735 for the distinction between small cell lung cancer and non-small cell lung cancer. J Pathol 159:23-28.

Kirsche W (1950) Die regenerativen Vorgaenge am Rueckenmark erwachsener Teleostier nach operativer Kontinuitaetstrennung. In, pp 190-260. Berlin.

Kruger RP, Aurandt J, Guan KL (2005) Semaphorins command cells to move. Nat Rev Mol Cell Biol 6:789-800.

Kullander K (2007) Genetic Approaches to Spinal Locomotor Function in Mammals. In: Model Organisms in Spinal Cord Regeneration.

Lewis KE, Eisen JS (2001) Hedgehog signaling is required for primary motoneuron induction in zebrafish. Development 128:3485-3495.

Liu R, Cai J, Hu X, Tan M, Qi Y, German M, Rubenstein J, Sander M, Qiu M (2003) Region-specific and stage-dependent regulation of Olig gene expression and oligodendrogenesis by Nkx6.1 homeodomain transcription factor. Development 130:6221-6231.

Lu QR, Yuk D, Alberta JA, Zhu Z, Pawlitzky I, Chan J, McMahon AP, Stiles CD, Rowitch DH (2000) Sonic hedgehog--regulated oligodendrocyte lineage genes encoding bHLH proteins in the mammalian central nervous system. Neuron 25:317-329.

Maestrini E, Tamagnone L, Longati P, Cremona O, Gulisano M, Bione S, Tamanini F, Neel BG, Toniolo D, Comoglio PM (1996) A family of transmembrane proteins with homology to the MET-hepatocyte growth factor receptor. Proc Natl Acad Sci U S A 93:674-678.

Malicki J, Jo H, Wei X, Hsiung M, Pujic Z (2002) Analysis of gene function in the zebrafish retina. Methods 28:427-438.

Miyashita T, Yeo SY, Hirate Y, Segawa H, Wada H, Little MH, Yamada T, Takahashi N, Okamoto H (2004) PlexinA4 is necessary as a downstream target of Islet2 to mediate Slit signaling for promotion of sensory axon branching. Development 131:3705-3715.

Myers PZ, Eisen JS, Westerfield M (1986) Development and axonal outgrowth of identified motoneurons in the zebrafish. J Neurosci 6:2278-2289.

Nasevicius A, Ekker SC (2000) Effective targeted gene 'knockdown' in zebrafish. Nat Genet 26:216-220.

Ninkovic J, Götz M (2007) Signaling in adult neurogenesis: from stem cell niche to neuronal networks. Curr Opin Neurobiol 17:338-344.

Nusslein-Volhard C (2002) Zebrafish (Practical Approach). In: Oxford University Press.

Ohori Y, Yamamoto S, Nagao M, Sugimori M, Yamamoto N, Nakamura K, Nakafuku M (2006) Growth factor treatment and genetic manipulation stimulate neurogenesis and oligodendrogenesis by endogenous neural progenitors in the injured adult spinal cord. J Neurosci 26:11948-11960.

Palaisa KA, Granato M (2007) Analysis of zebrafish sidetracked mutants reveals a novel role for Plexin A3 in intraspinal motor axon guidance. Development 134:3251-3257.

Park HC, Shin J, Appel B (2004) Spatial and temporal regulation of ventral spinal cord precursor specification by Hedgehog signaling. Development 131:5959-5969.

Park HC, Mehta A, Richardson JS, Appel B (2002) olig2 is required for zebrafish primary motor neuron and oligodendrocyte development. Dev Biol 248:356-368.

Park HC, Shin J, Roberts RK, Appel B (2007) An olig2 reporter gene marks oligodendrocyte precursors in the postembryonic spinal cord of zebrafish. Dev Dyn 236:3402-3407.

Pinto L, Götz M (2007) Radial glial cell heterogeneity--the source of diverse progeny in the CNS. Prog Neurobiol 83:2-23.

Poss KD, Wilson LG, Keating MT (2002) Heart regeneration in zebrafish. Science 298:2188-2190.

Raya A, Koth CM, Buscher D, Kawakami Y, Itoh T, Raya RM, Sternik G, Tsai HJ, Rodriguez-Esteban C, Izpisua-Belmonte JC (2003) Activation of Notch signaling pathway precedes heart regeneration in zebrafish. Proc Natl Acad Sci U S A 100 Suppl 1:11889-11895.

Renoncourt Y, Carroll P, Filippi P, Arce V, Alonso S (1998) Neurons derived in vitro from ES cells express homeoproteins characteristic of motoneurons and interneurons. Mech Dev 79:185-197.

Roos M, Schachner M, Bernhardt RR (1999) Zebrafish semaphorin Z1b inhibits growing motor axons in vivo. Mech Dev 87:103-117.

Roskams AJ, Tetzlaff W (2005) Directing stem cells and progenitor cells on the stage of spinal cord injury. Exp Neurol 193:267-272.

Rupp RA, Snider L, Weintraub H (1994) Xenopus embryos regulate the nuclear localization of XMyoD. Genes Dev 8:1311-1323.

Rutishauser U (2008) Polysialic acid in the plasticity of the developing and adult vertebrate nervous system. Nat Rev Neurosci 9:26-35.

Ryu H, Ferrante RJ (2007) Translational therapeutic strategies in amyotrophic lateral sclerosis. Mini Rev Med Chem 7:141-150.

Saiki RK, Scharf S, Faloona F, Mullis KB, Horn GT, Erlich HA, Arnheim N (1985) Enzymatic amplification of beta-globin genomic sequences and restriction site analysis for diagnosis of sickle cell anemia. Science 230:1350-1354.

Sanchez P, Ruiz i Altaba A (2005) In vivo inhibition of endogenous brain tumors through systemic interference of Hedgehog signaling in mice. Mech Dev 122:223-230.

Sato-Maeda M, Obinata M, Shoji W (2008) Position fine-tuning of caudal primary motoneurons in the zebrafish spinal cord. Development 135:323-332.

Sato-Maeda M, Tawarayama H, Obinata M, Kuwada JY, Shoji W (2006) Sema3a1 guides spinal motor axons in a cell- and stage-specific manner in zebrafish. Development 133:937-947.

Schwab ME (2004) Nogo and axon regeneration. Curr Opin Neurobiol 14:118-124.

Shibuya S, Miyamoto O, Auer RN, Itano T, Mori S, Norimatsu H (2002) Embryonic intermediate filament, nestin, expression following traumatic spinal cord injury in adult rats. Neuroscience 114:905-916.

Shirasaki R, Pfaff SL (2002) Transcriptional codes and the control of neuronal identity. Annu Rev Neurosci 25:251-281.

Spencer T, Domeniconi M, Cao Z, Filbin MT (2003) New roles for old proteins in adult CNS axonal regeneration. Curr Opin Neurobiol 13:133-139.

Tallafuss A, Bally-Cuif L (2003) Tracing of her5 progeny in zebrafish transgenics reveals the dynamics of midbrain-hindbrain neurogenesis and maintenance. Development 130:4307-4323.

Tanabe Y, William C, Jessell TM (1998) Specification of motor neuron identity by the MNR2 homeodomain protein. Cell 95:67-80.

Tanaka H, Maeda R, Shoji W, Wada H, Masai I, Shiraki T, Kobayashi M, Nakayama R, Okamoto H (2007) Novel mutations affecting axon guidance in zebrafish and a role for plexin signalling in the guidance of trigeminal and facial nerve axons. Development 134:3259-3269.

Taylor JS, Van de Peer Y, Meyer A (2001) Revisiting recent challenges to the ancient fish-specific genome duplication hypothesis. Curr Biol 11:R1005-1008.

Tsuchida T, Ensini M, Morton SB, Baldassare M, Edlund T, Jessell TM, Pfaff SL (1994) Topographic organization of embryonic motor neurons defined by expression of LIM homeobox genes. Cell 79:957-970.

van Raamsdonk W, Smit-Onel MJ, Diegenbach PC (1993) Metabolic profiles of white and red-intermediate spinal motoneurons in the zebrafish. Acta Histochem 95:129-138.

van Raamsdonk W, Maslam S, de Jong DH, Smit-Onel MJ, Velzing E (1998) Long term effects of spinal cord transection in zebrafish: swimming performances, and metabolic properties of the neuromuscular system. Acta Histochem 100:117-131.

Westerfield M (1989) The zebrafish book, a guide for the laboratory use of zebrafish (*Brachydanio rerio*). In: University of Oregon Press.

Westerfield M, McMurray JV, Eisen JS (1986) Identified motoneurons and their innervation of axial muscles in the zebrafish. J Neurosci 6:2267-2277.

William CM, Tanabe Y, Jessell TM (2003) Regulation of motor neuron subtype identity by repressor activity of Mnx class homeodomain proteins. Development 130:1523-1536.

Yamamoto S, Nagao M, Sugimori M, Kosako H, Nakatomi H, Yamamoto N, Takebayashi H, Nabeshima Y, Kitamura T, Weinmaster G, Nakamura K, Nakafuku M (2001) Transcription factor expression and Notch-dependent regulation of neural progenitors in the adult rat spinal cord. J Neurosci 21:9814-9823.

Yaron A, Huang PH, Cheng HJ, Tessier-Lavigne M (2005) Differential requirement for Plexin-A3 and -A4 in mediating responses of sensory and sympathetic neurons to distinct class 3 Semaphorins. Neuron 45:513-523.

Zupanc GK, Horschke I (1995) Proliferation zones in the brain of adult gymnotiform fish: a quantitative mapping study. J Comp Neurol 353:213-233.

8 APPENDIX

8.1 Abbreviations

aa	amino acid
A	adenine
Amp	ampicillin
ATP	adensoin triphosphate
bp	base pairs
BSA	bovine serum albumine
C	cytosine
°C	degree celsius
cDNA	complementary deoxyribonucleic acid
CTA	cytosine triphosphate
dATP	2`-desoxyadenosine triphosphate
dpf	days post fertilisation
dCTP	2`-desoxycytosine triphosphate
dGTP	2'-desoxyguanosine triphosphate
DMSO	dimethylsulfoxide
DNA	deoxyribonucleic acid
DNase	desoxyribonuclease
dNTP	2'-desoxyribonucleotide-5'-triphosphate
dpf	days post fertilization
dpl	days post-lesion

DTT	dithiothreitol
E. coli	Escherichia coli
Fig.	figure
EDTA	ethylendiamintetraacetic acid
g	gram
G	guanosine
h	hour
h	human
hpf	hour post fertilisation
kan	Kanamycin
kb	kilo base pairs
l	litre
LB medium	Luria Bertani medium
m	milli (10^{-3})
min	minute
mRNA	messenger ribonucleic acid
n	number of animals, nano (10^{-9})
PBS	phosphate buffer saline
PCR	polymerase chain reaction
RNA	ribonucleic acid
RNase	ribonuclease
RT	room temperature
s	second
T	thymine
Tab.	table

T_m	melting temperature
v/v	volume per volume
w/v	weight per volume
wpl	weeks post lesion
x g	g-force
µ	micro (10^{-6})

8.2 Morpholinos

PlexinA3 MO1:

5'-ATACCAGCAGCCACAAGGACCTCAT-3'

PlexinA3 MO2:

5'-AGCTCTTCCCTCAAGCGTATTCCAG-3'

PlexinA3 5mm MO:

5'-ATACCACCACCCAGAACGACCTGAT-3'

8.3 Overexpression-construct *plexinA3*

8.3.1 Primers used to clone *plexinA3* overexpression construct:

plexin A3 (BamHI) forward

5`- GTGGATCCATGAGGTCCTTGTGGCTG -3`

plexinA3 (BamHI) reverse

5`- TAGGATCCGCTGCTGCCAGACATCAG-3`

8.3.2 Sequence of the overexpression construct for *plexinA3*:

5'-GTGGATCCATGAGGTCCTTGTGGCTGCTGGTATTTTCCTTCTCTGTTTTG
ACTGGGACCAACATGGCATTTCCAATGATTCTGTCGGAGCGCCCTGAAGT
CACCGGGAGCTTCAAGGTTAAAGACACGAGTCTCACTCACCTCACAGTGC
ACCGCAAAACTGGTGAGGTGTTCGTGGGTGCTATAAACCGAGTCTACAAG
CTTTCTGCCAATCTCACCGAAACGCGTTCTCACCAGACCGGTCCCGTGGA
AGACAACGCCAAGTGCTATCCACCCCCCAGTGTACGAGCTTGCACGCAGA
AACTGGAGTCTACAGACAACGTCAACAAATTGCTGCTGGTTGATTATGCGG
GCAACCGTCTGGCGGCCTGTGGAAGCATCTGGCAGGGCGTGTGCCAGTT
CCTGCGGTTGGAAGATCTGTTCAAGCTTGGTGAACCACATCACCGTAAAG
AGCACTACCTCTCGGGAGCCAAAGAGTCTGATGGGATGGCTGGAGTCGTG
GTGGGTGATGATGACGGAGACTTGAAGAAGAAAAAGAAAGGTGGCAGTCG
ACTCTTCATTGGTGCTGCAATCGATGGCAAATCAGAGTATTTTCCAACCCT
CTCTAGCCGTAAACTGGTGGCGGATGAGGAAAGTGTTAACATGTTCAGTTT
GGTCTACCAAGATGAGTTTGTGTCTTCTCAAATCAAGATACCTTCAGACAC
CCTCTCTCAGTATCCCGCATTTGATATCTACTACGTCTACGGGTTCTCCAG
CCGGACTTACATCTATTTCCTCACTTTGCAACTGGATACTCAGCTCACTCA
GGTGGATGTGACGGGGGAGAAGTTCTTCACCTCAAAAATAGTCCGCATGT
GCTCCAATGACACTGAGTTTTACTCCTACGTAGAGTTCCCGCTTGGGTGCA
CCAAGGATGGCGTGGAATACAGACTTGTTCAAGCTGCCTACAAGCATCGT
CCTGGAAAGATTCTGGCACAGGCTTTGGGCCTGTCTGAGGATGAGGATGT
CCTGTTCGTGATCTTCTCCCAGGGTCAGAAGAACAGGGCTAACCCACCGA
GAGAAACAGTGCTGTGCCTCTTCACACTGCACCAGATTAACCTGGCCATG
CGAGAGAGGATCAAGTCATGCTACCGCGGAGAGGGAAAGCTGTCTCTGC
CGTGGTTGCTCAACAAGGAGCTGCCTTGCATTAATACGCCCAAGCAGATT
GGTGATGATTTCTGCGGCCTGGTCTTGAATCAGCCCCTTGGGGGATTGAT
GGTGATCGAGGGCATTCCTCTGTTTGACGACCGCACTGACGGCATGGCAT
CAGTGGCTGCATACACATACGGAGACCATTCGGTGGTGTTTGTGGGCACT
CGCAGCGGCCACCTCAAGAAGATTCGAGTGAATGGTGTTCCTCCGCCGTC
AGAAAACGCTTTGCTGTACGAGACCGTGACCGTTGTGGAGGGAAGCCCCA
TCCTGAGGGACATGGTGTTCAGTCCAGACTATCAGTACATCTATCTGCTGA
GCGACAAACAGGTGAGTCGTCTGCCGGTGGAGAGCTGTTCTCAGTACAGC
AGCTGTAAGACGTGTCTGGGCTCTGGAGATCCTCACTGCGGCTGGTGTGT

CCTGCATAACAAGTGCTCCAGAAAGGAGGCCTGTGAGAAGTGGGCCGAG
CCGCTTCACTTCAGTACAGAGCTGAAGCAGTGTGTGGACATTACCGTCACT
CCGGATAACATGTCTGTGACCTCCGTGTCTACACAGCTGAGTGTGAAGGT
GGCGAACGTCCCGAACCTCTCTGCGGGGGTGACGTGTGTGTTTGAGGAG
CTCACCGAGAGTCCAGGAGAAGTGCTGGCTGAAGGACAAATCCTCTGCAT
GTCCCCTTCCCTTCGGGACGTCCCGTCTGTCACTCAGGGATATGGCGATA
AACGGGTCGTGAAGCTTTCTCTGAAGTCCAAAGAGACGGGGCTCAAATTC
ATCACCACCGACTTCGTCTTCTACAACTGCAGCGTTCTGCAATCGTGTTCA
TCGTGTGTTAGCAGTTCTTTCCCTTGCAACTGGTGTAAATATCGCCACATC
TGCACTAATAATGTAGCCGAGTGCTCTTTCCAGGAAGGTCGGGTGAGCAG
TGCAGAGGGCTGCCCACAGATTTTGCCCAGCAGTGACATCCTGGTACCGG
CGGGGATCGTTCGGCCAATCACATTGCGAGCCCGAAACTTGCCCCAGCCT
CAGTCTGGACAGAAGAACTATGAGTGCGTCTTTAACATCCAGGGAAAAGT
GCAGCGTATTCCTGCGGTCCGCTTCAACAGTTCCTGCATCCAGTGTCAGA
ACACCTCGTACTGGTATGAAGGGAACGAGATGGGGGATCTGCCTGTGGAT
TTCTCCATCGTGTGGGACGGTGACTTTCCCATCGACAAACCCTCATCCATG
AGAGCTCTCCTGTATAAGTGTGAGGCTCAGAGGGACAGCTGTGGACTATG
TCTGAAGGCTGACAGCACATTTGAGTGTGGCTGGTGTTTGGCCGATAAGA
AGTGTCTCCTAAAGCAACACTGTCCATCAGCCGAACACAACTGGATGCATC
AGGGACGACGCAACATTCGCTGCAGCCATCCGCGCATTACCAAGATTCGT
CCTCTGACGGGCCCGAAAGAAGGAGGCACACGCGTCACCATTGAAGGGG
AGAATCTGGGGCTGCAGGTTCGAGAAATCACTCACGTGCGTGTGGCTGGA
GTTCGCTGTAACCCTGCTGCAGCTGAATACATCAGCGCTGAGAGGATTGT
GTGTGATATGGAGGAGTCCCTGATGTCCAGTCCTCCCGGAGGTCCGGTG
GAGCTGTGTATCGGAGACTGCAGCGCTGAGTACAGGACTCAATCCACACA
GACTTACTCCTTTGTGATGCCGAGCTTCAGTCGAGTGCGCCCTGAGAAAG
GCCCGGTGTCCGGCGGGACGAGGCTGACCATCTCAGGCCGACATCTGGA
CGCCGGCAGCGCTGTGACCGTGTTTTTGGCCCAGGAGGAGTGTCTGTTC
GTCAGGAGGACGGTGCGTGAGATTGTGTGTGTGACGCCTCCATCAGCTTC
AGGATCTGGACCTTCATCTGTGAAGCTGTTTATTGATAAAGCAGAGATCAC
CAGCGACACCCGCTACATCTACACTGAAGACCCAAATATCTCCACCATCGA
GCCCAACTGGAGCATCATCAACGGCAGCACAAGCCTCACGGTCACAGGAA
CCAACCTGCTCACCATTCAGGAGCCCAAAGTCAGAGCCAAATATGGAGGA
GTGGAGACCACAAACATCTGTAGTCTGGTCAATGACTCTGTGATGACGTG

CTTGGCTCCGGGCATCATCTACACTAAACGTGAGGCTCCAGAAAGCGGCG
TTCACCCGGACGAGTTCGGCTTCATCCTGGATCACGTCTCTGCCCTCCTC
ATCCTCAACGGGACTCCGTTCACTTACTATCCCAACCCGACCTTTGAACCT
CTTGGGAATGCCGGGATTCTGGAGGTCAAACCAGGATCACCCATCATCCT
GAAGGGCAAGAACCTGATTCCTCCTGCGCCTGGGAACATCCGTCTGAATT
ACAGCGTGACGATCGGAGAAACGCCCTGCCTGCTAACAGTCTCTGAATCT
CAGCTGCTCTGCGATTCGCCAGATCTGACCGGAGAACAGCGAGTGATGAT
TCTTGTCGGCGGTCTGGAATATTCCCCCGGAATGCTTCACATTTATTCGGA
CAGCACTCTCACGTTGCCTGCCATCATCGGGATCGGAGCAGGTGGAGGA
GTCCTCCTCATCGCCATCATCGCTGTGCTCATCGCTTACAAGCGCAAGAC
GCGGGACGCCGACCGCACACTCAAACGCCTGCAGCTGCAGATGGACAAC
CTGGAGTCCCGGGTTGCGCTGGAGTGCAAGGAAGCATTCGCTGAGCTGC
AGACAGACATCCAAGAGCTGACGAATGACATGGACGGTGTGAAAATCCCT
TTCCTGGAGTATCGTACCTACACCATGAGAGTGATGTTCCCTGGCATCGAG
GAGCACCCGGTTCTGAAGGAGCTGGACTCTCCAGCTAATGTGGAGAAGGC
CCTGCGCTTGTTCAGTCAGCTGCTGCACAACAAGATGTTCCTGCTGACCTT
CATCCACACGCTGGAGGCGCAAAGGTCCTTCTCCATGCGGGATCGTGGCA
ATGTGGCCTCCCTCCTCATGGCGGCACTGCAGGGACGGATGGAGTACGC
CACTGTGGTTCTCAAACAGCTGCTAGCCGACCTGATCGAGAAGAACTTGG
AGAACCGAAACCACCCTAAACTACTGCTTAGACGAACTGAATCTGTGGCAG
AGAAGATGCTCACCAACTGGTTCACGTTCCTTCTGCACCGCTTCCTCAAGG
AGTGTGCGGGCGAGCCTCTGTTTATGCTGTACTGTGCTATAAAACAGCAG
ATGGAGAAAGGCCCCATAGACGCCATCACAGGAGAGGCCAGATACTCCCT
GAGCGAAGACAAGCTCATCCGACAGCAAATCGACTACAAGCAGCTGACGC
TGATGTGTATTCCTCCTGAAGGAGAAGCCGGGACAGAAATCCCTGTTAAG
GTGCTAAACTGTGACACGATCACTCAGGTGAAGGACAAGCTGTTGGACGC
TGTTTATAAAGGCATCCCGTACTCGCAGAGACCACAGGCGGACGACATGG
ACCTGGAATGGCGGCAGGGTCGACTGACCAGAATCATCCTCCAAGATGAA
GACGTCACCACAAAGATCGAGAGCGACTGGAAGAGACTGAACACACTGGC
ACATTACCAGGTGACAGATGGGTCTTTGGTGGCTTTGGTTCAGAAGCAAGT
ATCCGCTTACAACATCGCCAACTCTTTCACGTTCACTCGCTCTCTCAGTCG
ATACGAGAGCCTCTTGAGGACGTCCAGTAGTCCAGACAGCCTGCGCTCCA
GGGCTCCCATGATCACTCCTGACCAGGAAACGGGTACCAAACTCTGGCAC
CTGGTGAAGAACCATGAGCATGCAGACCAGCGGGAAGGAGACCGCGGCA

GCAAGATGGTGTCTGAGATTTACCTCACACGCTTACTAGCTACCAAGGGCA
CTCTGCAGAAGTTTGTGGACGATCTGTTTGAGACGGTCTTCAGTACAGCTC
ACCGCGGCAGCGCTCTCCCGCTGGCCATCAAATACATGTTTGATTTCCTG
GATGAACAGGCGGACAAGAGGCAGATCACCGACCCAGACGTACGGCACA
CCTGGAAGAGCAACTGCCTTCCTCTGCGGTTTTGGGTCAACGTGATCAAA
AACCCTCAGTTTGTGTTTGACATCCACAAGAACAGTATTACAGATGCCTGT
CTGTCGGTGGTGGCTCAGACATTTATGGACTCCTGCTCCACGTCTGAGCA
TCGTCTGGGAAAAGACTCTCCGTCAAACAAACTGCTCTACGCTAAAGACAT
CCCCAACTACAAGAGCTGGGTGGAGAGATATTACCGTGACATCAGCAAGA
TGCCAAGTATCAGTGATCAGGATATGGATGCCTATCTGGTCGAGCAGTCTC
GTCTCCATGGCAACGAGTTCAACACACTGAGCGCGCTCAGTGAACTGTAT
TTCTACATCAACAAGTACAAAGAAGAGATTTTGACAGCGCTGGACAGAGAC
GGTTACTGTCGCAAACACAAGCTACGACACAAACTGGAACAAGCCATTAAC
CTGATGTCTGGCAGCAGCGGATCCTA-3'

8.3.3 Restriction enzyme map for *plexinA3* overexpression construct

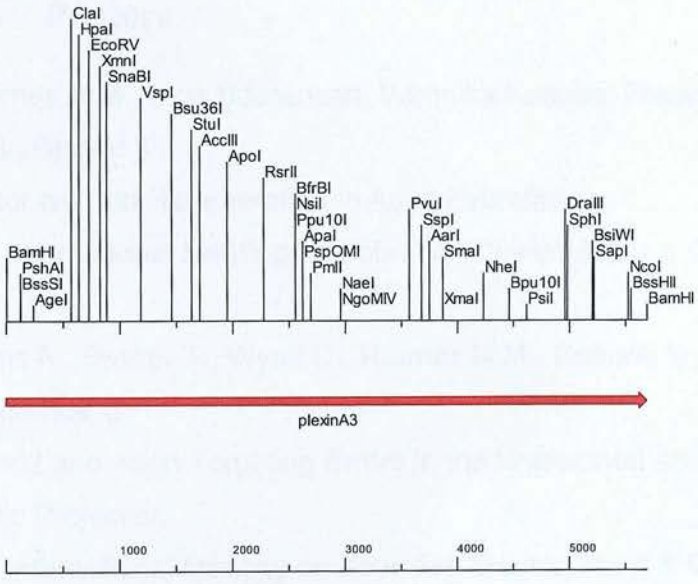

plexinA3 with BamHI sites (5692 bps)

8.4 Publications

Reimer M.M., Sörensen I., Frank R.E., Chong, L., Becker C.G.*, Becker T.* (2008) Sonic hedgehog dependent motor neuron regeneration in adult zebrafish. J Neurosci. (in press).

Feldner J., **Reimer M.M.**, Schweitzer J., Wendik B., Meyer D., Becker T., Becker C.G. (2007) PlexinA3 restricts spinal exit points and branching of trunk motor nerves in embryonic zebrafish. J Neurosci. 27:4978-83.

Siebert, S.*, Thomsen, S.*, **Reimer, M.M.**, Bosch, T.C.G. (2005) Control of foot differentiation in *Hydra*: Phylogenetic footprinting indicates interaction of head, bud and foot patterning systems. Mech. Dev. 122:998-1007.

* These authors contributed equally

8.5 Posters

Reimer M.M., Inga Soerensen, Veronika Kuscha, Frank R.E., Chong L., Becker C.G., Becker T.
Motor Neuron Regeneration in Adult Zebrafish
(8th International Meeting on Zebrafish Development & Genetics, Madison 2008)

Ebert A., Becker T., Wyatt C., **Reimer M.M.**, Roerink S., Rasband K., Chien C.-B., Becker C.
Robo2 and Axon Targeting Errors in the Unlesioned and Regenerated Adult Optic Projection
(8th International Meeting on Zebrafish Development & Genetics, Madison 2008)

Reimer M.M., Frank R.E., Chong L., Becker C.G., Becker T.
Sonic hedgehog dependent motor neurone regeneration in adult zebrafish.
(Scottish Neuroscience Group Meeting, Edinburgh 2007)

Reimer M.M., Frank R.E., Chong L., Becker C.G., Becker T.
Sonic hedgehog dependent motor neurone regeneration in adult zebrafish.
(Translational Research Symposium: Moving Forward with Motor Neurone Disease, Royal Society, Edinburgh 2007)

Reimer M.M., Sörensen I., Schweitzer J., Becker C.G., Becker T.
Progenitor cell-related gene expression and neurogenesis in the lesioned spinal cord of adult zebrafish.
(7th International Meeting on Zebrafish Development & Genetics, Madison 2006)

Sedlacek L., **Reimer M.M.**, Rifai M., Feldmann K., Bange F.C.
Differentiation of *Mycobacterium abscessus* (type I and II) and *Mycobacterium chelonae* based on LightCycler technology.
(DGHM meeting, Münster 2004)

Reimer M.M., Jäger T., Sedlacek L., Joost I., Maass S., Bange F.C.
The role of *narGHJI* and *nirB* in nitrate assimilation by *Mycobacterium tuberculosis*.
(DGHM meeting, Münster 2004)

8.6 Danksagung

Hiermit möchte ich mich ganz herzlich bei den Menschen bedanken, die mir bei der Durchführung meiner Doktorarbeit geholfen haben.

Herrn Prof. L. Renwrantz danke ich für die Zweitbetreuung meiner Arbeit.

Ganz besonders möchte ich den Einsatz und die Hilfe meiner Doktoreltern PD Dr. Catherina G. Becker und PD Dr. Thomas Becker hervorheben. Die konstante Diskussion und vertrauensvolle Atmosphäre in ihrer Arbeitsgruppe hat mir geholfen immer das Beste zu geben. Danke dafür!

Ein Laborumzug von Hamburg nach Edinburgh am Anfang einer Doktorarbeit ist natürlich spannend und sehr arbeitsintensiv, dass dies alles so reibungslos verlief verdanke ich neben den Beckers meinem „Mitstreiter" Anselm Ebert.

Die Gruppe wuchs im Laufe der Jahre und ich freue mich besonders darüber mit Bénédicte Autin, Cameron Wyatt, Sudeh Riahi, Veronika Kuscha, Tatyana Dias und Zheng Zhong zusammengearbeitet zu haben. Nicht zu vergessen meine Kollegen aus dem ZMNH: Julia Feldner, Inga Sörensen, Jörn Schweitzer und Eugen Kludt.

Meinen Eltern und Großeltern gilt meine Liebe und mein Dank für all die Zeit die sie mich während Studium und Doktorarbeit unterstützt haben.

Eine junge Frau las mein Poster, das im Flur zu unserem Labor hing. So lernte ich in Edinburgh meine Ehefrau kennen. Dafür und für ihre unermüdliche Geduld und Unterstützung möchte ich Rebecca von Herzen danken.

Brief Communications

Motor Neuron Regeneration in Adult Zebrafish

Michell M. Reimer,[1] Inga Sörensen,[2] Veronika Kuscha,[1] Rebecca E. Frank,[1] Chong Liu,[1] Catherina G. Becker,[1]* and Thomas Becker[1]*

[1]Centre for Neuroscience Research, Royal (Dick) School of Veterinary Studies, University of Edinburgh, Summerhall, Edinburgh EH9 1QH, United Kingdom, and [2]Medizinische Hochschule Hannover, Molekularbiologie, 30625 Hannover, Germany

The mammalian spinal cord does not regenerate motor neurons that are lost as a result of injury or disease. Here we demonstrate that adult zebrafish, which show functional spinal cord regeneration, are capable of motor neuron regeneration. After a spinal lesion, the ventricular zone shows a widespread increase in proliferation, including slowly proliferating olig2-positive (olig2$^+$) ependymo-radial glial progenitor cells. Lineage tracing in olig2:green fluorescent protein transgenic fish indicates that these cells switch from a gliogenic phenotype to motor neuron production. Numbers of undifferentiated small HB9$^+$ and islet-1$^+$ motor neurons, which are double labeled with the proliferation marker 5-bromo-2-deoxyuridine (BrdU), are transiently strongly increased in the lesioned spinal cord. Large differentiated motor neurons, which are lost after a lesion, reappear at 6–8 weeks after lesion, and we detected ChAT$^+$/BrdU$^+$ motor neurons that were covered by contacts immunopositive for the synaptic marker SV2. These observations suggest that, after a lesion, plasticity of olig2$^+$ progenitor cells may allow them to generate motor neurons, some of which exhibit markers for terminal differentiation and integration into the existing adult spinal circuitry.

Key words: **endogenous stem cells; radial glia; BrdU; PCNA; SV2; adult neurogenesis**

Introduction

Damage to the spinal cord by injury or motor neuron diseases is devastating because lost neurons are not replaced in the adult mammalian spinal cord (Pinto and Götz, 2007; Bareyre, 2008). Adult zebrafish have an impressively high regenerative capacity, including heart (Poss et al., 2002), retina (Fausett and Goldman, 2006; Bernardos et al., 2007; Fimbel et al., 2007), and functional spinal cord regeneration (Becker et al., 2004). Hence, we asked whether they might be able to regenerate spinal motor neurons, because this might help to elucidate the signals relevant for adult CNS regeneration.

There is significant neurogenesis in specific neurogenic zones even in the unlesioned brain of adult zebrafish (Zupanc et al., 2005; Adolf et al., 2006; Chapouton et al., 2006; Grandel et al., 2006). This is similar to mammals, which probably have fewer of these zones (Gould, 2007). However, the unlesioned adult zebrafish spinal cord shows very little, if any, proliferation and neurogenesis (Zupanc et al., 2005; Park et al., 2007). Therefore, a prerequisite for motor neuron regeneration would be plasticity of relatively quiescent spinal progenitor cells after injury.

These observations prompted us to investigate lesion-induced neuronal regeneration in the heavily myelinated spinal cord of the fully adult zebrafish (>4 months) after complete spinal transection. We focused on motor neurons because this cell type is often lost as a result of injury or neurodegenerative disease in mammals, and differentiation of motor neurons is highly conserved between mammals and zebrafish. For example, HB9 and islet-1/2 are transcription factors found in developing motor neurons of both mammals (Tsuchida et al., 1994; William et al., 2003) and zebrafish (Cheesman et al., 2004; Park et al., 2004).

We find that substantial numbers of new motor neurons are generated after a spinal lesion, some of which show evidence for terminal differentiation and integration into the spinal circuitry. Lineage tracing identifies olig2-positive (olig2$^+$) ependymo-radial glial cells as likely progenitor cells for motor neurons in the lesioned adult spinal cord.

Materials and Methods

Animals. Fish are kept and bred in our laboratory fish facility according to standard methods (Westerfield, 1989), and experiments have been approved by the British Home Office. We used wild-type (wik), HB9:green fluorescent protein (GFP) (Flanagan-Steet et al., 2005), islet-1:GFP (Higashijima et al., 2000), and olig2:GFP (Shin et al., 2003) transgenic fish. Consistency of transgene expression with that of the endogenous genes at the adult stage was verified by immunohistochemistry (HB9: data not shown; islet-1: supplemental Fig. 2, available at www.jneurosci.org as supplemental material) or *in situ* hybridization (olig2; data not shown) for the respective genes.

Spinal cord lesion. As described previously (Becker et al., 2004), fish were anesthetized by immersion in 0.033% aminobenzoic acid ethylmethylester (MS222; Sigma) in PBS for 5 min. A longitudinal incision was made at the side of the fish, and the spinal cord was completely transected under visual control 4 mm caudal to the brainstem–spinal-cord junction.

Electron microscopy. Ultrathin sections (75–100 nm in thickness) were

Received March 19, 2008; revised June 18, 2008; accepted July 11, 2008.

This work was supported by the Deutsche Forschungsgemeinschaft and The Euan MacDonald Centre for Motor Neurone Disease Research. Some of this work is part of the diploma thesis of I.S., performed at the Zentrum für Molekulare Neurobiologie, Hamburg. We thank Drs. B. Appel, D. Meyer, H. Okamato, and J. Scholes for transgenic fish and reagents, Drs. P. Brophy, S. Lowell, and T. Theil for critically reading this manuscript, and Dr. T. Gillespie for expert advice on confocal microscopy.

*C.G.B. and T.B. contributed equally to this work.

Correspondence should be addressed to Thomas Becker, Centre for Neuroscience Research, Royal (Dick) School of Veterinary Studies, University of Edinburgh, Summerhall, Edinburgh EH9 1QH, UK. E-mail: thomas.becker@ed.ac.uk.

DOI:10.1523/JNEUROSCI.1189-08.2008

 0270-6474/08/288510-07$15.00/0

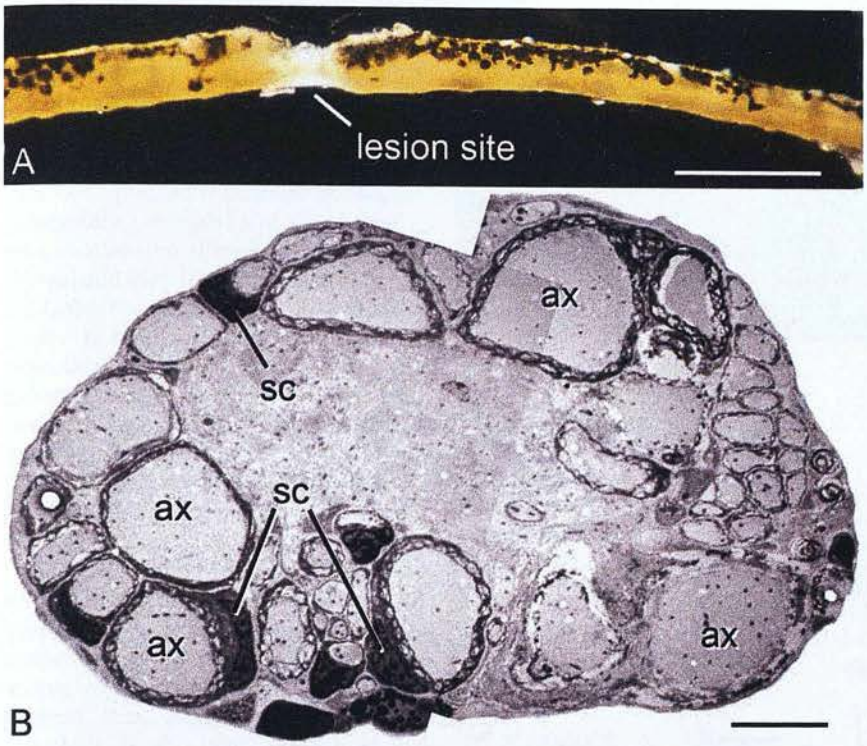

Figure 1. The regenerated spinal cord. ***A***, A lateral stereomicroscopic view of a dissected spinal cord is shown (rostral is left). The tissue bridging the lesion site appears translucent. ***B***, An electron-microscopic cross section through the lesion site is shown. The lesion site consists mainly of axons (ax), some of which are remyelinated by Schwann cells (sc). Scale bars: ***A***, 1 mm; ***B***, 5 μm.

prepared and observed by electron microscopy as published previously (Becker et al., 2004).

Immunohistochemistry. We used rat anti-5-bromo-2-deoxyuridine (BrdU) (BU 1/75, 1:500, AbD Serotec), mouse anti-islet-1/2 (Tsuchida et al., 1994) (40.2D6, 1:1000; Developmental Studies Hybridoma Bank), mouse anti-HB9 (MNR2, 1:400; Developmental Studies Hybridoma Bank), mouse anti-proliferating cell nuclear antigen (PCNA) (PC10, 1:500; DakoCytomation), and goat anti-ChAT (AB144P, 1:250; Millipore Bioscience Research Reagents) antibodies. Secondary cyanine 3 (Cy3)-conjugated antibodies were purchased from Jackson ImmunoResearch. Immunohistochemistry on paraformaldehyde-fixed spinal cord sections (50 μm thickness) has been described previously (Becker et al., 2004). Antigen retrieval was performed by incubating the sections for 1 h in 2 M HCl for BrdU immunohistochemistry or by incubation in citrate buffer (10 mM sodium citrate in PBS, pH 6.0) at 85°C for 30 min for HB9, islet-1/2, and PCNA immunohistochemistry. Double labeling of cells was always determined in individual confocal sections.

Intraperitoneal BrdU application. Animals were anesthetized and intraperitoneally injected with BrdU (Sigma-Aldrich) solution (2.5 mg/ml) at a volume of 50 μl at 0, 2, and 4 d after lesion unless indicated otherwise.

Retrograde axonal tracing. Motor neurons in the spinal cord were retrogradely traced by bilateral application of biocytin to the muscle periphery at the level of the spinal lesion, as described previously (Becker et al., 2005), with the modification that biocytin was detected with Cy3-coupled streptavidin (Invitrogen) in spinal sections. This was followed by immunohistochemistry for BrdU (see above).

Cell counts and statistical analysis. Stereological counts were performed in confocal image stacks of three randomly selected vibratome sections from the region up to 750 μm rostral to the lesion site and three sections from the region up to 750 μm caudal to the lesion site. Cell numbers were then calculated for the entire 1.5 mm surrounding the lesion site.

$PCNA^+$ and $BrdU^+$ nuclear profiles in the parenchyma and the ventricular zone (up to one cell diameter away from the ventricular surface) were counted in the same region of spinal cord. At least six sections were analyzed per animal by fluorescence microscopy, and values were expressed as profiles per section. The observer was blinded to experimental treatments. Variability of values is given as SEM. Statistical significance was determined using the Mann–Whitney *U* test ($p < 0.05$) or ANOVA with Bonferroni's/Dunn's *post hoc* test for multiple comparisons.

Results

A spinal lesion induces widespread ventricular proliferation

To determine the spinal region in which new motor neurons might regenerate, we analyzed the overall organization of the regenerated spinal cord. At 6 weeks after lesion, when functional recovery is complete (Becker et al., 2004), the lesion site itself had not restored normal spinal architecture and consisted mainly of unmyelinated and remyelinated regenerated axons (Fig. 1). Immediately adjacent to this axonal bridge, spinal cross sections showed normal cytoarchitecture, with the exception that white matter tracts were filled with myelin debris of degenerating fibers (Becker and Becker, 2001). This indicated that this tissue existed before the lesion was made. Thus, no significant regeneration of whole spinal cord tissue occurred for up to at least 6 weeks after lesion.

To find newly generated cells in the spinal cord, we used immunohistochemical detection of repeatedly injected BrdU, which labels cells that have divided. This revealed that very few cells proliferated in the unlesioned spinal cord. At 2 weeks after lesion, the number of newly generated cells in the spinal tissue up to 3.6 mm rostral and caudal to the lesion site increased significantly, covering more than one-third of the length of the entire spinal cord. $BrdU^+$ cells were found throughout spinal cross sections but appeared to be concentrated at the midline and in the ventricular zone around the central canal (Fig. 2*A*). Numbers were highest close to the lesion site (Fig. 2*B*).

To localize acutely proliferating cells in the spinal cord, we used immunohistochemistry with the PCNA antibody, which labels cells in early G_1 phase and S phase of the cell cycle. This revealed a significant increase in cell proliferation solely in the ventricular zone. Proliferation peaked at 2 weeks after lesion and returned to values that were similar to those of unlesioned animals by 6 weeks after lesion (Fig. 2*C*,*D*).

Numbers of differentiating motor neurons increased dramatically in the lesioned spinal cord

We determined whether new motor neurons are generated in the core region of proliferation comprising 1.5 mm surrounding the lesion site. We examined the numbers of cells expressing GFP in transgenic lines, in which GFP expression labels motor neurons under the control of the promoters for HB9 (Flanagan-Steet et al., 2005) or islet-1 (Higashijima et al., 2000). In unlesioned HB9:GFP animals, few large (diameter >12 μm) motor neurons and very few smaller (diameter <12 μm) GFP^+ motor neurons (20 ± 7.7 cells; $n = 4$) were observed in the ventral horn. The number of small HB9:GFP^+ cells was nonsignificantly increased at 1 week after lesion (207 ± 84.5 cells; $n = 3$; $p = 0.3$) but was significantly increased at 2 weeks after lesion (870 ± 106.8 cells; $n = 11$; $p = 0.004$) (Fig. 3*A*). Similar observations were made in islet-1:GFP

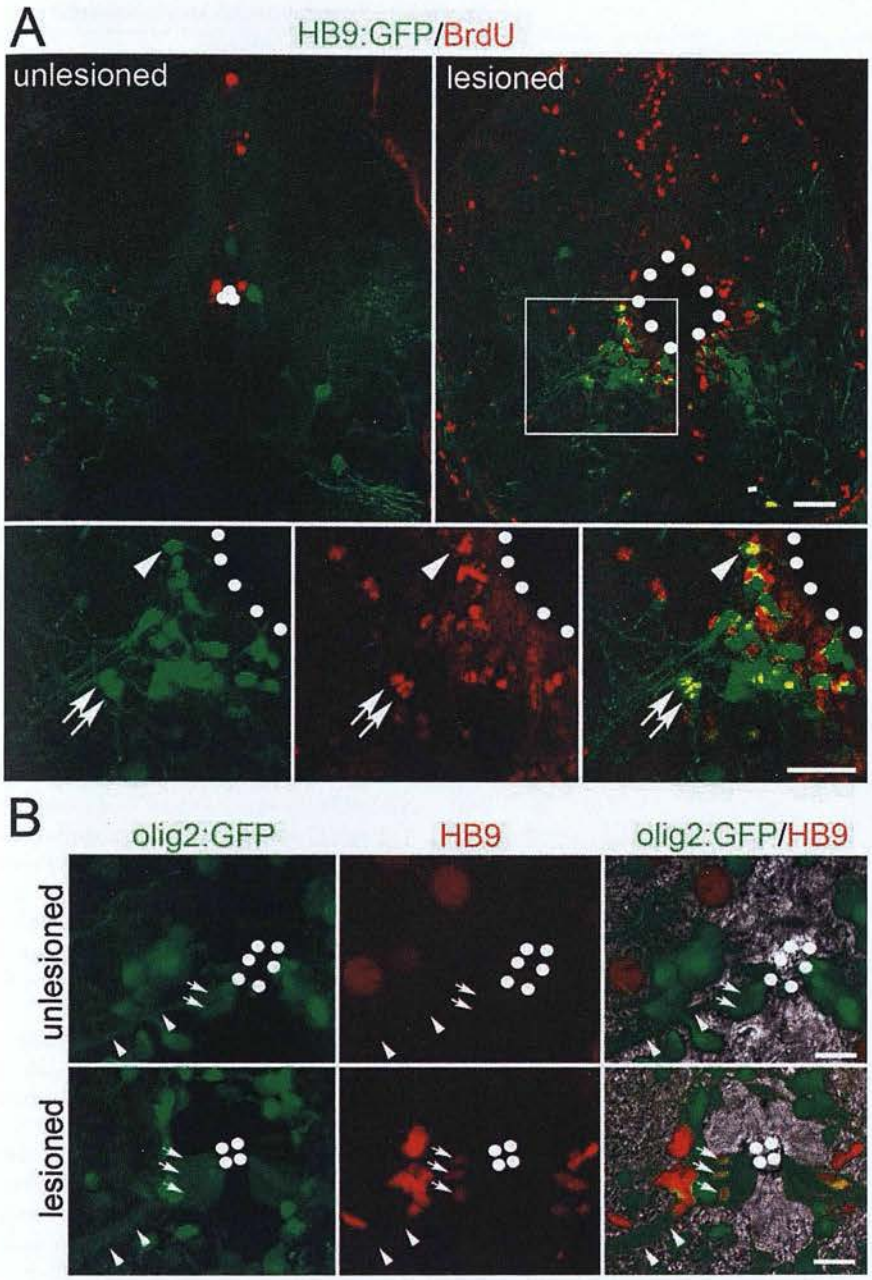

Figure 3. Generation of new motor neurons in the lesioned spinal cord. Confocal images of spinal cross sections at 2 weeks after lesion are shown (dorsal is up; dots outline the ventricle). ***A***, HB9:GFP$^+$/BrdU$^+$ neurons are present in the lesioned, but not the unlesioned, ventral horn. These cells (boxed in top right and shown at higher magnification in bottom row) bear elaborate processes (arrows) or show ventricular contact (arrowhead). ***B***, olig2:GFP$^+$ progenitor cells (arrows) have long radial processes (arrowheads), contact the ventricle, and are HB9$^+$ in the lesioned, but not the unlesioned, spinal cord. Scale bars: ***A***, 25 μm; ***B***, top row, 7.5 μm; ***B***, bottom row, 15 μm.

tracer in transgenic fish to determine the progeny of adult retinal (Bernardos et al., 2007) and tegmental (Chapouton et al., 2006) progenitor cells. In unlesioned animals, no double labeling of GFP and HB9 ($n = 3$) or GFP and islet-1/2 ($n = 4$) was observed. At 2 weeks after lesion, single parenchymal olig2:GFP$^+$ cells did not coexpress either HB9 or islet-1/2, which makes it unlikely that these cells gave rise to motor neurons. In contrast, a substantial subpopulation of olig2:GFP$^+$ ependymo-radial glial cells were HB9$^+$ (204 ± 32.2 cells; $n = 3$) (Fig. 3*B*) or islet-1/2$^+$ (34 ± 8.9 cells; $n = 4$; data not shown). Double labeling indicated that either there was an overlap in the expression of olig2 and HB9 or islet-1/2 during differentiation of motor neurons in the ventricular zone or recently differentiated HB9$^+$ and islet-1/2$^+$ motor neurons had retained the GFP. Differences in the numbers of olig2:GFP$^+$ ependymo-radial glial cells that coexpressed HB9 or islet-1/2 may be related to differences in differentiation stage or subtype of motor neuron produced (William et al., 2003). To demonstrate that HB9$^+$/olig2:GFP$^+$ cells are newly generated, we used HB9, olig2:GFP, and BrdU triple labeling. Indeed, 74 ± 22.7 HB9$^+$/olig2:GFP$^+$/BrdU$^+$ cells ($n = 3$) were found exclusively in the zone continuous with olig2:GFP$^+$ cells at the ventricle at 14 d after lesion (supplemental Fig. 3, available at www.jneurosci.org as supplemental material). In the ventricular zone dorsal and ventral to the olig2:GFP$^+$ region, expression of HB9 or islet-1/2 was rarely observed, suggesting that olig2:GFP$^+$ ependymo-radial glial cells were the main source of new motor neurons (Fig. 3*B*). Thus, olig2 expressing ependymo-radial glial cells proliferate and switch to motor neuron production after a lesion.

To determine whether olig2:GFP$^+$ ependymo-radial glial cells had stem cell characteristics, we determined whether they retained BrdU label and were thus slowly proliferating (Chapouton et al., 2006). Lesioned olig2:GFP animals were injected with a single pulse of BrdU at 14 d after lesion, and the number of olig2:GFP$^+$/BrdU$^+$ cells in the ventricular zone was assessed at 4 h and 14 d after injection. Numbers were not significantly different at the two time points (4 h, 60 ± 11.5 cells, $n = 5$; 14 d, 53 ± 13.3 cells, $n = 4$; $p = 0.6$), indicating that olig2:GFP$^+$ cells did indeed retain label (supplemental Fig. 4, available at www.jneurosci.org as supplemental material). This suggests the possible presence of motor neuron stem cells among the population of olig2:GFP$^+$ ependymo-radial glial cells. However, we cannot exclude that label-retaining olig2:GFP$^+$ cells also give rise to other cell types.

Evidence for terminal differentiation of new motor neurons

Newly generated small motor neurons were not fully differentiated at 2 weeks after lesion. They were either attached to the ventricle with a single slender process or were located farther away from the ventricle with several processes, some of which exceeded 100 μm in length, extending into the gray matter in HB9:GFP and in islet-1:GFP transgenic fish (Figs. 3*A*, 4). However, even the cells with long processes showed very little apposition of somata and processes with SV2$^+$ contacts, an indicator of synaptic coverage (Fig. 4*B*). Moreover, small HB9:GFP$^+$ neurons rarely expressed ChAT (2.7 ± 0.90%; $n = 3$), a marker of

Table 1. Dynamics of motor neuron numbers after spinal cord lesion

	HB9:GFP		Islet-1:GFP		ChAT
	Large cells	Small cells	Large cells	Small cells	Large cells
Unlesioned	133 ± 34.9	20 ± 7.7 ($n = 4$)	78 ± 17.2	27 ± 3.9 ($n = 5$)	478 ± 111.1 ($n = 3$)
1 week	42 ± 15.1*	207 ± 84.5 ($n = 3$)	n.d.	n.d.	n.d.
2 weeks	40 ± 7.3*	870 ± 106.8 ($n = 11$)*	32 ± 9.5	870 ± 244.9 ($n = 4$)	235 ± 40.9 ($n = 3$)
6–8 weeks	91 ± 11.5	251 ± 78.7 ($n = 6$)	n.d.	n.d.	348 ± 67.3 ($n = 4$)

*$p < 0.05$, significantly different from unlesioned control. n.d., Not determined.

mature motor neurons (Arvidsson et al., 1997), at 2 weeks after lesion (Fig. 4*A*).

In contrast to small HB9:GFP$^+$ cells, large HB9:GFP$^+$ cells were mostly ChAT$^+$ in unlesioned animals (80.6 ± 7.99%; $n = 3$), indicating that these were fully differentiated motor neurons. At 1 (42 ± 15.1 cells; $n = 3$; $p = 0.0035$) and 2 (40 ± 7.3 cells; $n = 11$; $p < 0.0003$) weeks after lesion, large-diameter HB9:GFP$^+$ motor neurons were strongly reduced in number compared with unlesioned animals (133 ± 34.9 cells; $n = 4$). This suggests lesion-induced loss of motor neurons, which was confirmed by terminal deoxynucleotidyl transferase-mediated biotinylated UTP nick end labeling of 22.8 ± 11.39% of the HB9:GFP$^+$ motor neurons at 3 d after lesion ($n = 3$) (supplemental Fig. 5, available at www.jneurosci.org as supplemental material).

At 6–8 weeks after lesion, there was an increase in the number of large-diameter HB9:GFP$^+$ cells to 91 ± 11.5 cells ($n = 6$), such that cell numbers were not different from those in unlesioned animals ($p = 0.081$). Large-diameter islet-1:GFP$^+$ and ChAT$^+$ cells showed similar dynamics (Table 1). This suggests that some newly generated motor neurons matured and replaced lost motor neurons. Other newly generated cells might have died, as indicated by increased association with macrophages/microglial cells between 2 and 6 weeks after lesion (supplemental Fig. 6, available at www.jneurosci.org as supplemental material).

To directly demonstrate the presence of newly generated, terminally differentiated motor neurons, we used triple labeling of BrdU, ChAT, and SV2 at 6 weeks after lesion. In the 1500 μm surrounding the lesion site, we found 29 ± 23.1 large BrdU$^+$/ChAT$^+$ cells ($n = 3$) covered with SV2$^+$ contacts at a density that was comparable with that of motor neurons in unlesioned animals (Fig. 4*C*). Application of the axonal tracer biocytin to the muscle periphery labeled one BrdU$^+$ cell in a motor neuron position in the ventromedial spinal cord near the lesion site ($n = 8$; 6–14 weeks after lesion) (Fig. 4*D*). This suggests that some newly generated motor neurons were integrated into the spinal circuitry and grew an axon out of the spinal cord.

Discussion

We show here for the first time that a spinal lesion triggers generation of motor neurons in the spinal cord of adult zebrafish. Lesion-induced proliferation and motor neuron marker expression in olig2$^+$ ependymo-radial glial cells makes these the likely motor neuron progenitor cells. Some of the newly generated motor neurons show markers for terminal differentiation and network integration.

Newly generated motor neurons are added to preexisting spinal tissue adjacent to a spinal lesion site in which normal cytoarchitecture is not restored. Thus, this model differs significantly from tail regeneration paradigms in amphibians in which the entire spinal cord tissue is completely reconstructed from an advancing blastema (Echeverri and Tanaka, 2002).

Our results suggest olig2$^+$ ependymo-radial glial cells to be the progenitor cells for spinal motor neurons, because a lesion induces their proliferation and lineage tracing indicated that a substantial number of newly generated olig2:GFP$^+$ ependymo-radial glial cells coexpressed the motor neuron markers HB9 or islet-1/2. Moreover, parenchymal olig2:GFP$^+$ cells were never, and ependymo-radial glial cells outside the olig2:GFP$^+$ zone were rarely, labeled by HB9 or islet-1/2 antibodies. This supports the hypothesis that olig2:GFP$^+$ ependymo-radial glial cells are the main source of motor neurons after a lesion. However, we cannot exclude the possibility that some motor neurons might have regenerated from as yet unidentified olig2-negative (olig2$^-$) parenchymal progenitors.

During postembryonic development, olig2:GFP$^+$ cells only give rise to oligodendrocytes (Park et al., 2007). Thus, adult neuronal regeneration is not just a continuation of a late developmental process but an indication of significant plasticity of adult spinal progenitor cells in the fully mature spinal cord.

Additionally, olig2$^+$ ependymo-radial glial cells have characteristics of neural stem cells. They are label retaining, and lesion-induced proliferation of these cells leads only to a moderate increase in their number, suggesting asymmetric cell divisions and some potential for self-renewal. Moreover, these cells express brain lipid binding protein, which is also expressed in mammalian radial glial stem cells, and the PAR (partitioning-defective) complex protein atypical PKC, an indicator of asymmetric cell division, at postembryonic stages (Park et al., 2007). A stem cell role for olig2$^+$ ependymo-radial glial cells would be in agreement with that of other radial glia cell types in developing mammals and in adult zebrafish (Pinto and Götz, 2007). For example, Müller cells, the radial glia cell type in the adult retina, can produce different cell types in adult zebrafish depending on which cells are lost after specific lesions (Fausett and Goldman, 2006; Bernardos et al., 2007; Fimbel et al., 2007).

We observed that numbers of differentiated motor neurons, i.e., large HB9:GFP$^+$ cells and ChAT$^+$ cells, were reduced at 2 weeks after lesion and recovered at 6–8 weeks after lesion. This suggests that motor neurons regenerate and is in agreement with previous observations in the guppy (*Poecilia reticulata*), in which large "ganglion cells" disappeared and reappeared after a lesion (Kirsche, 1950). In accordance with this finding, we detected terminally differentiated (ChAT$^+$), newly generated (BrdU$^+$) motor neurons that were covered by SV2$^+$ contacts at 6–8 weeks after lesion, suggesting their integration into the spinal network. The rare observation of one BrdU$^+$ cell that was traced from the muscle periphery indicates that newly generated motor neurons may even be capable of growing their axons out of the spinal cord toward muscle targets. In contrast, at early time points, a transient population of small, newly generated motor neurons (HB9:GFP$^+$, islet-1:GFP$^+$) that were not fully differentiated (ChAT$^-$) and not decorated by SV2$^+$ contacts were present in large numbers. These cells varied in motor neuron marker expression and the extent of process elaboration. Together, these observations suggest that motor neurons are generated and undergo successive

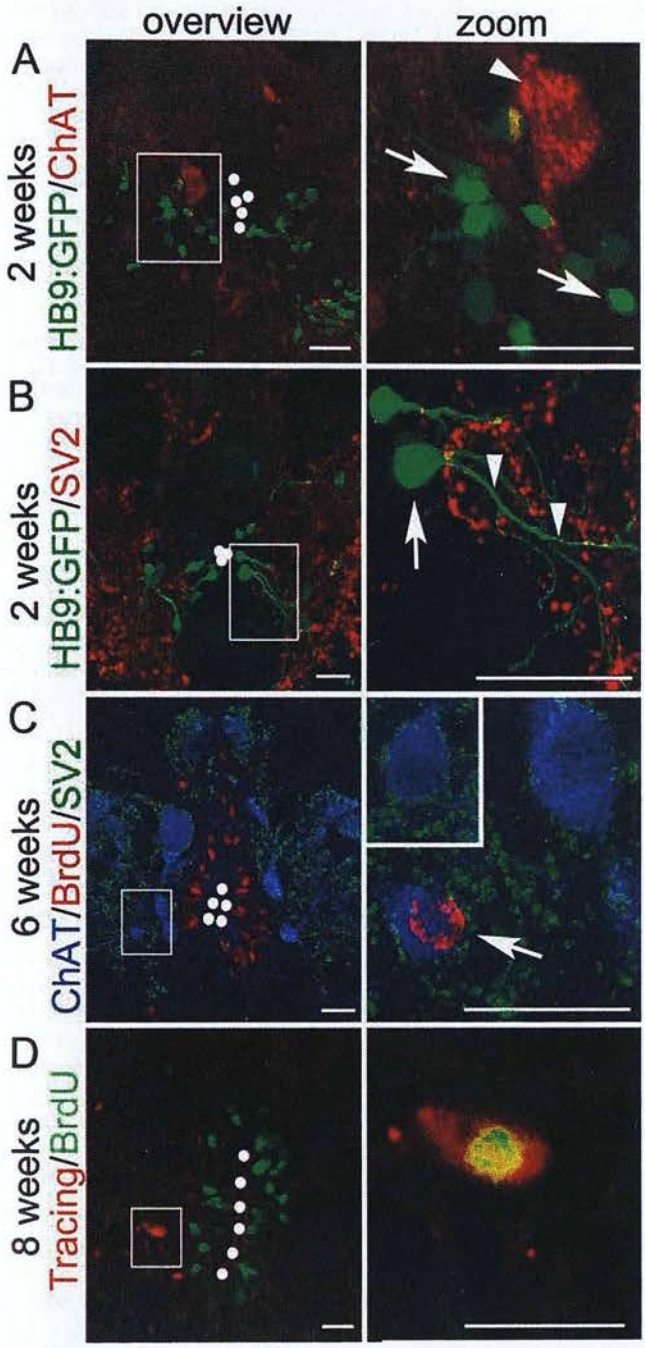

Figure 4. Maturation of newly generated motor neurons. Confocal images of spinal cross sections are shown (dorsal is up, dots outline the ventricle). ***A***, Newly generated HB9:GFP$^+$ motor neurons are ChAT$^-$ (arrows; arrowhead indicates a ChAT$^+$/HB9:GFP$^-$ differentiated motor neuron). ***B***, Somata (arrow) and proximal dendrites (arrowheads) receive few SV2$^+$ contacts at 2 weeks after lesion. ***C***, At 6 weeks after lesion, ChAT$^+$/BrdU$^+$ somata are decorated with SV2$^+$ contacts (arrow). Inset (right) depicts a ChAT$^+$ motor neuron decorated with SV2$^+$ contacts in an unlesioned animal. ***D***, At 8 weeks after lesion, a BrdU$^+$ cell is retrogradely traced from the muscle tissue. Scale bars: ***A–C***, 25 μm; ***D***, 15 μm.

morphological and gene expression differentiation steps toward integration into an existing spinal network after a lesion.

A spinal lesion in mammals leads to proliferation and expression of nestin (Shibuya et al., 2002) as well as Pax6 (Yamamoto et al., 2001), which are markers for progenitor cells, around the ventricle. In addition, parenchymal astrocytes, some of which carry radial processes, express nestin. However, olig2 and several other factors are not re-expressed (Ohori et al., 2006). These observations suggest that spinal progenitors in adult mammals show some plasticity after a lesion and could potentially be induced to produce new motor neurons.

We conclude that the zebrafish, a powerful genetically tractable model, provides an opportunity to identify the evolutionarily conserved signals that trigger massive stem cell-derived regeneration and network integration of motor neurons in the adult spinal cord.

References

Adolf B, Chapouton P, Lam CS, Topp S, Tannhäuser B, Strähle U, Götz M, Bally-Cuif L (2006) Conserved and acquired features of adult neurogenesis in the zebrafish telencephalon. Dev Biol 295:278–293.

Arvidsson U, Riedl M, Elde R, Meister B (1997) Vesicular acetylcholine transporter (VAChT) protein: a novel and unique marker for cholinergic neurons in the central and peripheral nervous systems. J Comp Neurol 378:454–467.

Bareyre FM (2008) Neuronal repair and replacement in spinal cord injury. J Neurol Sci 265:63–72.

Becker CG, Lieberoth BC, Morellini F, Feldner J, Becker T, Schachner M (2004) L1.1 is involved in spinal cord regeneration in adult zebrafish. J Neurosci 24:7837–7842.

Becker T, Becker CG (2001) Regenerating descending axons preferentially reroute to the gray matter in the presence of a general macrophage/microglial reaction caudal to a spinal transection in adult zebrafish. J Comp Neurol 433:131–147.

Becker T, Lieberoth BC, Becker CG, Schachner M (2005) Differences in the regenerative response of neuronal cell populations and indications for plasticity in intraspinal neurons after spinal cord transection in adult zebrafish. Mol Cell Neurosci 30:265–278.

Bernardos RL, Barthel LK, Meyers JR, Raymond PA (2007) Late-stage neuronal progenitors in the retina are radial Muller glia that function as retinal stem cells. J Neurosci 27:7028–7040.

Chapouton P, Adolf B, Leucht C, Tannhäuser B, Ryu S, Driever W, Bally-Cuif L (2006) her5 expression reveals a pool of neural stem cells in the adult zebrafish midbrain. Development 133:4293–4303.

Cheesman SE, Layden MJ, Von Ohlen T, Doe CQ, Eisen JS (2004) Zebrafish and fly Nkx6 proteins have similar CNS expression patterns and regulate motoneuron formation. Development 131:5221–5232.

Echeverri K, Tanaka EM (2002) Ectoderm to mesoderm lineage switching during axolotl tail regeneration. Science 298:1993–1996.

Fausett BV, Goldman D (2006) A role for α1 tubulin-expressing Muller glia in regeneration of the injured zebrafish retina. J Neurosci 26:6303–6313.

Fimbel SM, Montgomery JE, Burket CT, Hyde DR (2007) Regeneration of inner retinal neurons after intravitreal injection of ouabain in zebrafish. J Neurosci 27:1712–1724.

Flanagan-Steet H, Fox MA, Meyer D, Sanes JR (2005) Neuromuscular synapses can form in vivo by incorporation of initially aneural postsynaptic specializations. Development 132:4471–4481.

Gould E (2007) How widespread is adult neurogenesis in mammals? Nat Rev Neurosci 8:481–488.

Grandel H, Kaslin J, Ganz J, Wenzel I, Brand M (2006) Neural stem cells and neurogenesis in the adult zebrafish brain: origin, proliferation dynamics, migration and cell fate. Dev Biol 295:263–277.

Higashijima S, Hotta Y, Okamoto H (2000) Visualization of cranial motor neurons in live transgenic zebrafish expressing green fluorescent protein under the control of the islet-1 promoter/enhancer. J Neurosci 20:206–218.

Kirsche W (1950) The regenerative events on the spinal cord of grown up teleostiers after operative dissection (in German). Z Mikrosk Anat Forsch 56:190–263.

Ohori Y, Yamamoto S, Nagao M, Sugimori M, Yamamoto N, Nakamura K, Nakafuku M (2006) Growth factor treatment and genetic manipulation stimulate neurogenesis and oligodendrogenesis by endogenous neural progenitors in the injured adult spinal cord. J Neurosci 26:11948–11960.

Park HC, Shin J, Appel B (2004) Spatial and temporal regulation of ventral spinal cord precursor specification by Hedgehog signaling. Development 131:5959–5969.

Park HC, Shin J, Roberts RK, Appel B (2007) An olig2 reporter gene marks oligodendrocyte precursors in the postembryonic spinal cord of zebrafish. Dev Dyn 236:3402–3407.

Pinto L, Götz M (2007) Radial glial cell heterogeneity: the source of diverse progeny in the CNS. Prog Neurobiol 83:2–23.

Poss KD, Wilson LG, Keating MT (2002) Heart regeneration in zebrafish. Science 298:2188–2190.

Shibuya S, Miyamoto O, Auer RN, Itano T, Mori S, Norimatsu H (2002) Embryonic intermediate filament, nestin, expression following traumatic spinal cord injury in adult rats. Neuroscience 114:905–916.

Shin J, Park HC, Topczewska JM, Mawdsley DJ, Appel B (2003) Neural cell fate analysis in zebrafish using olig2 BAC transgenics. Methods Cell Sci 25:7–14.

Tsuchida T, Ensini M, Morton SB, Baldassare M, Edlund T, Jessell TM, Pfaff SL (1994) Topographic organization of embryonic motor neurons defined by expression of LIM homeobox genes. Cell 79:957–970.

Westerfield M (1989) The zebrafish book: a guide for the laboratory use of zebrafish (*Brachydanio rerio*). Eugene, OR: University of Oregon Press.

William CM, Tanabe Y, Jessell TM (2003) Regulation of motor neuron subtype identity by repressor activity of Mnx class homeodomain proteins. Development 130:1523–1536.

Yamamoto S, Nagao M, Sugimori M, Kosako H, Nakatomi H, Yamamoto N, Takebayashi H, Nabeshima Y, Kitamura T, Weinmaster G, Nakamura K, Nakafuku M (2001) Transcription factor expression and Notch-dependent regulation of neural progenitors in the adult rat spinal cord. J Neurosci 21:9814–9823.

Zupanc GK, Horschke I (1995) Proliferation zones in the brain of adult gymnotiform fish: a quantitative mapping study. J Comp Neurol 353:213–233.

Zupanc GK, Hinsch K, Gage FH (2005) Proliferation, migration, neuronal differentiation, and long-term survival of new cells in the adult zebrafish brain. J Comp Neurol 488:290–319.

Brief Communications

PlexinA3 Restricts Spinal Exit Points and Branching of Trunk Motor Nerves in Embryonic Zebrafish

Julia Feldner,[2,5] Michell M. Reimer,[1] Jörn Schweitzer,[3] Björn Wendik,[3] Dirk Meyer,[4] Thomas Becker,[1,5] and Catherina G. Becker[1,5]

[1]Centre for Neuroscience Research, Royal (Dick) School of Veterinary Studies, University of Edinburgh, Edinburgh EH9 1QH, United Kingdom, [2]Institute for Molecular Bioscience, University of Queensland, St Lucia QLD 4072, Australia, [3]Institut für Biologie 1, Universität Freiburg, Freiburg, D-79104, Germany, [4]Institut für Molekularbiologie, Leopold-Franzens-Universität Innsbruck, A-6020 Innsbruck, Austria, and [5]Zentrum für Molekulare Neurobiologie, University of Hamburg, D-20246 Hamburg, Germany

The pioneering primary motor axons in the zebrafish trunk are guided by multiple cues along their pathways. Plexins are receptor components for semaphorins that influence motor axon growth and path finding. We cloned plexinA3 in zebrafish and localized plexinA3 mRNA in primary motor neurons during axon outgrowth. Antisense morpholino knock-down led to substantial errors in motor axon growth. Errors comprised aberrant branching of primary motor nerves as well as additional exit points of axons from the spinal cord. Excessively branched and supernumerary nerves were found in both ventral and dorsal pathways of motor axons. The trunk environment and several other types of axons, including trigeminal axons, were not detectably affected by plexinA3 knock-down. RNA overexpression rescued all morpholino effects. Synergistic effects of combined morpholino injections indicate interactions of plexinA3 with semaphorin3A homologs. Thus, plexinA3 is a crucial receptor for axon guidance cues in primary motor neurons.

Key words: primary motor neurons; pioneer axons; neuropilin; semaphorin; zebrafish; development

Introduction

Axonal path finding during development is determined by an array of overlapping pathway cues and receptors. PlexinA1 to A4 are coreceptors for axon-repelling or -attracting class 3 extracellular semaphorins. It is thought that neuropilin-1 (NRP1) or NRP2 are the ligand-binding part, and plexins are the signal-transducing part of semaphorin class 3 receptors (for a recent review, see Kruger et al., 2005). Removing individual components from this guidance network leads to specific defects of nerve growth (Giger et al., 2000; Huber et al., 2005; Yaron et al., 2005), indicating distinct roles for different ligand/receptor combinations in the path finding of different axon populations.

Studying the outgrowth of primary motor axons in zebrafish offers the opportunity to unravel the role of individual guidance cues and receptors at the level of single pioneer axons *in vivo*. Three primary motor neurons per trunk hemisegment grow axons out of the spinal cord along a common pathway in the middle of each segment up to the horizontal myoseptum. The axon of the caudal primary motor neuron (CaP) is the first to grow, followed by the axons of the middle (MiP) and rostral primary motor neurons (RoP). At the horizontal myoseptum, the CaP axon continues its growth toward the ventral somite, pioneering the ventral motor nerve, whereas the MiP axon retracts and grows toward the dorsal somite. The RoP axon takes a lateral path from the horizontal myoseptum (for review, see Beattie, 2000).

Semaphorin 3A1 (sema3A1) and sema3A2 (zebrafish homologs of mammalian sema3A) are expressed in the trunk environment. Overexpression of either ligand reduces growth of primary motor axons (Roos et al., 1999; Halloran et al., 2000). Antisense morpholino oligonucleotide knock-down of sema3A1 leads mainly to aberrant branching of the CaP axon (Sato-Maeda et al., 2006). Knock-down of NRP1a alone or in double knock-down experiments with semaphorin ligands leads to nerve branching, additional exit points of axons from the spinal cord, and ventral displacement of neuronal somata along the extraspinal motor axon pathway (Feldner et al., 2005). This suggests that semaphorins guide primary motor axons by repellent mechanisms via NRP1a-containing axonal receptors. Although this powerful system has attracted significant attention, for example in forward genetic screens for axon guidance molecules (Birely et al., 2005; Gulati-Leekha and Goldman, 2006), the role of plexins has not been examined. The only class A member of the plexin family characterized in zebrafish so far is plexinA4, which is not expressed in primary trunk motor neurons (Miyashita et al., 2004).

Here, we clone plexinA3 in zebrafish and show by antisense morpholino knock-down that plexinA3 is necessary for unbranched nerve growth and to restrict spinal exit points of primary motor axons to a midsegmental position. Morpholino coinjection experiments suggest that plexinA3 belongs to a receptor complex for semaphorins in primary motor neurons.

Received Dec. 25, 2006; accepted March 30, 2007.

This work was supported by the Deutsche Forschungsgemeinschaft and the Royal Society. We thank Dr. Melitta Schachner for support, Dr. Peter Brophy for support and use of his microscope, Laura Sander for correction of the English, and Bénédicte Autin for excellent technical assistance.

Correspondence should be addressed to Catherina G. Becker at the above address. E-mail: catherina.becker@ed.ac.uk.

DOI:10.1523/JNEUROSCI.1132-07.2007

 0270-6474/07/274978-06$15.00/0

Materials and Methods

Zebrafish. Zebrafish were bred under standard conditions (Kimmel et al., 1995). The transgenic fish in which the promoter for hb9 drives expression of green fluorescent protein (GFP) in primary motor neurons has been described previously (Flanagan-Steet et al., 2005).

Cloning procedure. A search of the Ensembl database (www.ensembl.org/Danio_rerio/) predicted ENSDARG00000016216 (Ensembl release 19) on zebrafish chromosome 8 to be most closely related to mouse and human plexinA3. The predicted transcript lacked part of the 5′ region, which was included in the expressed sequenced-tagged clone 24185179. Based on this information, the entire gene could be isolated from cDNA prepared from adult zebrafish brains using PCR with the proofreading polymerase PfuUltra (Stratagene, Cambridge, UK). The GenBank accession number for plexinA3 is EF538743.

Injection of mRNA and morpholinos. Two morpholinos of nonoverlapping sequence for plexinA3 (plexinA3 morpholino1, ATACCAGCAGCCACAAGGACCT*CAT*; plexinA3 morpholino2, AGCTCTTCCCTCAAGCGTATTCCAG) and a morpholino in which five bases were mismatched based on morpholino1 (PlexinA3 5 mm morpholino, ATACCACCACCCAGAACGACCTGAT) were purchased from Gene Tools (Philomath, OR). Morpholinos against sema3A1, sema3A2 (Feldner et al., 2005), and NRP1a (Lee et al., 2002) have been described previously.

Messenger RNAs for injection experiments were synthesized as described previously (Feldner et al., 2005). Partial sequences of plexinA3 that contained untranslated 5′ sequences followed by a myc-tag were used to determine binding efficiency of the morpholinos. Full-length plexinA3 mRNA followed by a myc-tag was synthesized for rescue experiments. This construct did not contain the recognition sequence of morpholino2.

For injections, rhodamine dextran (0.8%; $M_r = 10 \times 10^3$; Invitrogen, Paisley, UK) was added to mRNA or morpholino solutions. A glass micropipette was filled with the mRNA (1–2 $\mu g/\mu l$) or morpholino solutions ($\leq$2 mM), and a volume of 0.5 to 1 nl per egg (one-to-four-cell stage) was injected as described previously (Feldner et al., 2005). All injected animals showed normal overall growth and differentiation of nervous structures, such as head commissures, the dorsoventral diencephalic tract, and peripheral nerves, as indicated by anti-tubulin immunohistochemistry. Development was not retarded by any experimental procedures, as indicated by segmental positions of the lateral line nerve primordium (prim-stage) (Kimmel et al., 1995) that were not altered, compared with uninjected embryos (data not shown). Viability was not compromised by RNA or morpholino injections compared with uninjected embryos.

In situ *hybridization.* A full-length PlexinA3 probe was labeled with digoxigenin using the Megascript kit (Ambion, Warrington, UK) and used on 16 and 24 h post fertilization (hpf) whole-mounted embryos as described previously (Feldner et al., 2005).

Immunohistochemistry. Whole-mount immunohistochemistry was performed as described previously (Feldner et al., 2005). Ventral motor axons were labeled with a monoclonal antibody against acetylated tubulin (6-11B-1; Sigma-Aldrich, Poole, UK). GFP was immunodetected after *in situ* hybridization with a polyclonal antibody (AB3080P; Millipore, Bedford, MA). Different antibodies were used to label trunk structures in morpholino-injected animals (1 mM PlexinA3 morpholino1) (supplemental Fig. 3, available at www.jneurosci.org as supplemental material). The 412 monoclonal antibody to the HNK-1 epitope labels motor axons, as described previously (Becker et al., 2001). Monoclonal antibody (mAb) CS-56 to chondroitin sulfates labels the spinal floor plate and vertical myosepta (Bernhardt and Schachner, 2000) and was purchased from Sigma-Aldrich. A polyclonal antibody against tenascin-C of zebrafish (Tongiorgi, 1999) is used as a marker of the horizontal myoseptum region (Schweitzer et al., 2005). The 40.2D6 antibody to islet-1/-2 that labels motor neuron somata and Rohon-Beard cells (Feldner et al., 2005) and the antibody 3A10 to a neurofilament-associated antigen that labels commissural primary ascending interneurons and Mauthner axons in the spinal cord (Feldner et al., 2005) were both developed by Dr. T. M. Jessell (Columbia University, New York, NY). These antibodies, as well as the 4D9 antibody to engrailed that labels muscle pioneer cells at the horizontal myoseptum (Patel et al., 1989), were obtained as cell culture supernatants from the Developmental Studies Hybridoma Bank maintained by The University of Iowa, Department of Biological Sciences (Iowa city, IA). To reveal potential alterations in the trunk environment in those segments in which nerve growth was aberrant, anti-tenascin-C and anti-engrailed immunolabeling was combined with the axonal markers anti-HNK-1 and anti-tubulin, respectively. For each antibody or combination of antibodies, 11–28 embryos were analyzed. Secondary antibodies were purchased from Dianova (Hamburg, Germany).

Analysis of nerve growth. Anti-tubulin immunolabeled peripheral nerves were analyzed in whole-mounted 24 hpf embryos as described previously (Feldner et al., 2005). Briefly, embryos were scored as affected by nerve branching when at least two of the ventral motor nerves were branched at or above the level of the ventral edge of the notochord. Embryos were scored as affected by multiple exits when at least one hemisegment showed more than one exit point of ventral motor axons from the spinal cord. The rostral 12 pairs of motor nerves were examined. Numbers of peripheral trigeminal axons were assessed as described previously (Becker et al., 2002).

To analyze the dorsal motor axon pathway in 31 hpf hb9:GFP transgenic fish, trunk regions at the level of the yolk extension were scanned on a confocal microscope. Seven segments on both sides of the embryos were assessed for more than one nerve present in the dorsal somite and for excessive branching. For the latter, we scored branching of the nerve ventral to the level of the GFP-positive neuronal somata in the spinal cord. Values for affected embryos are given as mean ± SEM. Statistical analyses were done using Fisher's exact test unless indicated otherwise.

Results

Cloning of plexinA3 in zebrafish

Zebrafish plexinA3 was cloned as described in Materials and Methods. The general domain structure of the deduced protein (1892 aa) is identical to that of plexinA3 in other vertebrate species: a semaphorin domain, followed by three Met-related sequence domains, four IPT (immunoglobulin-like fold shared by plexins and transcription factors) motifs, and the characteristic intracellular plexin domain at the C terminus. The transmembrane domain of the zebrafish protein is located between the IPT motifs and the Plexin domain and comprises amino acids 1241–1263 (Fig. 1*A*).

The cloned protein has significant structural homology (supplemental Fig. 1, available at www.jneurosci.org as supplemental material) and overall amino acid identity (73%) with human (Maestrini et al., 1996) and mouse (Kameyama et al., 1996) plexinA3. In a phylogenetic tree constructed using the Clustal method (Chenna et al., 2003), zebrafish plexinA3 segregated with plexinA3 homologs of other species (Fig. 1*B*). These data strongly suggest that we cloned a species homolog of plexinA3. A search for a second paralog of plexinA3 using BLAST analysis of the cloned sequence on the zebrafish genome (Ensembl release 43) had a negative result.

PlexinA3 is expressed in primary motor neurons during axon outgrowth

In situ hybridization indicated expression of plexinA3 mRNA mainly in the developing nervous system but also in the developing heart (data not shown) and the non-neural tissue at the tip of the tail. Conspicuous expression was detected in the telencephalon, epiphysis, tegmentum, and regular cell clusters in the hindbrain at 24 hpf, suggesting expression in differentiating neurons. Low-level expression was found in cranial ganglia and the spinal cord (supplemental Fig. 2*A*,*B*, available at www.jneurosci.org as supplemental material). However, a particularly strong signal was found in regular clusters of cells at the ventral edge of the spinal cord at 16 and 24 hpf (i.e., during the time of axon out-

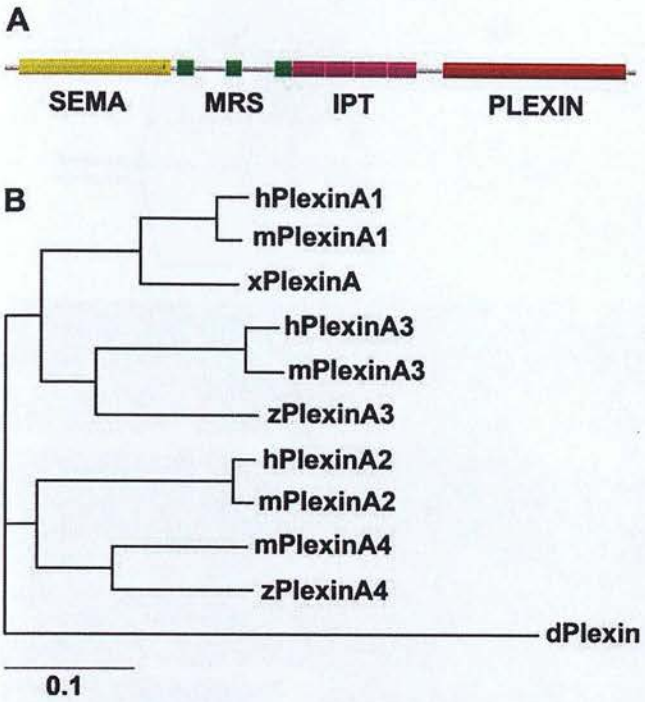

Figure 1. Structural features and identity of plexinA3 in zebrafish. ***A***, Domain structure of plexinA3. SEMA, Semaphorin domain; PLEXIN, plexin domain; MRS, Met-related sequence. ***B***, Multiple comparisons in a phylogenetic tree group zebrafish plexinA3 with plexinA3 homologs in other vertebrates. *Drosophila* plexinA was added as an outgroup. The scale bar represents 10 substitutions per 100 aa. z, Zebrafish; m, mouse; h, human; x, *Xenopus*; d, *Drosophila*.

growth of primary motor neurons) (Fig. 2*A*,*B*). Axons and somata of motor neurons are labeled by GFP in an hb9:GFP transgenic fish (Flanagan-Steet et al., 2005). *In situ* hybridization of the motor neuron markers islet-1 and islet-2 in these transgenic fish confirmed GFP expression in primary motor neurons (data not shown). Double labeling of plexinA3 mRNA with GFP immunohistochemistry in hb9:GFP transgenic embryos at 24 hpf revealed colocalization of the mRNA in GFP-positive motor neuron clusters from which the CaP axon had just started to grow in developmentally younger caudal segments. Conspicuous plexinA3 mRNA expression was also found in more dorsal GFP-negative spinal neurons (Fig. 2*C–E*). In more rostral segments in which the MiP axon could be seen to grow out, the mRNA was detectable in adjacent cells that are likely the CaP and MiP primary motor neurons (Fig. 2*F–H*). The extra-spinal pathway of motor axons did not express detectable levels of plexinA3 mRNA. Thus, plexinA3 mRNA is expressed in primary motor neurons during axon outgrowth.

Reduction of plexinA3 expression leads to aberrant branching and multiple exits of motor nerves

Two translation-blocking plexinA3 morpholinos of nonoverlapping sequence significantly reduced expression of a coinjected myc-tagged plexinA3 mRNA that included the binding sites for both morpholinos. This was determined in immunohistochemistry for the myc epitope (data not shown). Thus, both plexinA3 morpholinos efficiently bind to their target sequence *in vivo*.

Ventral motor nerve growth in plexinA3 morpholino-injected embryos was analyzed at 24 hpf using anti-tubulin immunohistochemistry (Fig. 2*I–N*). Injection of 1 mM plexinA3 morpholino1 led to abnormal growth of primary motor axons. Aberrations of ventral motor nerves, which normally grow as one unbranched nerve beyond the ventral edge of the notochord at 24 hpf (Fig. 2*I*,*L*), can be grouped into two categories: hemisegments that showed an additional nerve exiting the spinal cord (Fig. 2*M*,*N*) or nerves that were abnormally branched (Fig. 2*J*,*K*).

In 64% of the affected hemisegments, mostly one additional nerve of variable length grew ventrally from an additional exit point in the ventral spinal cord (Fig. 2*M*,*N*). The additional nerve ran parallel to the main nerve or joined it at variable positions dorsal of the horizontal myoseptum. In 68% of the hemisegments showing additional exit points, it could not be resolved whether the nerve emanated rostral or caudal to the segment border because the nerves grew very close to it. In the remaining hemisegments, 73% of the additional exit points were located in the posterior half of the somites and 25% were in the anterior half of the somites or in both the anterior and posterior somite half (2%). On average, 4.7 ± 0.4 hemisegments per embryo had multiple exits in affected embryos.

Ventral motor nerves were aberrantly branched in 35% of the affected hemisegments (Fig. 2*J*,*K*). The vast majority of these branches (82%) were directed caudally. Bifurcated (10%), rostrally (5%), and bilaterally (3%) branched nerves were observed less frequently. On average, 3.4 ± 0.2 hemisegments per embryo showed aberrant branching in affected embryos.

The effects were dose dependent with 26, 43, and 64% of the embryos showing aberrant nerve branching and 18, 56, and 94% of the embryos showing additional exit points from the spinal cord after injections of 0.25, 0.5, and 1 mM morpholino1, respectively. Injecting 1 mM morpholino2 phenocopied these effects (83% of embryos were affected by abnormal branching; 95% of embryos were affected by additional exits). Injections of 1 mM of a morpholino in which five bases were mismatched (5 mm morpholino) had no effect (14% of embryos were affected by branching; 12% of embryos were affected by additional exits) (for statistical significance, see Table 1). Thus, knock-down of plexinA3 induces both branching of ventral motor nerves and additional exit points from the spinal cord, preferentially in the posterior half of the trunk segments.

To determine whether dorsal motor axons, which are obscured in anti-tubulin-labeled embryos, were affected by the morpholino treatment, we analyzed hb9:GFP transgenic fish at 31 hpf. At this time point, GFP-positive axons had grown into the dorsal MiP pathway at the level of the yolk extension in uninjected animals (Fig. 2*O*). In 1 mM plexinA3 morpholino1- (n = 10 embryos) or morpholino2- (n = 13 embryos) injected hb9:GFP embryos, axons were also present in the MiP pathway, including the segments with multiple exits (n = 47 segments). Interestingly, in nine of these segments, the additional exit points of ventral motor axons also produced additional axons that grew dorsally (Fig. 2*P*). Most of these dorsally growing axons were located more laterally than the normal MiP axons as determined from confocal image stacks (data not shown). This indicates that these ectopic axons did not simply follow an MiP pathway. Branching away from the normal MiP pathway was also slightly increased by morpholino treatment (Fig. 2*P*). The frequency of dorsal motor nerves that were branched ventral to the level of GFP-positive ventral spinal neurons was 33.4 ± 2.84% hemisegments per embryo (n = 327 hemisegments) in morpholino-treated animals and 12.1 ± 2.04% hemisegments per embryo (n = 215 hemisegments; Mann–Whitney U test; $p < 0.0001$) in hb9:GFP embryos injected with 5 mm morpholino (n = 14 embryos). Thus, additional nerves and increased nerve branching occur in both ventral and dorsal primary motor axon paths.

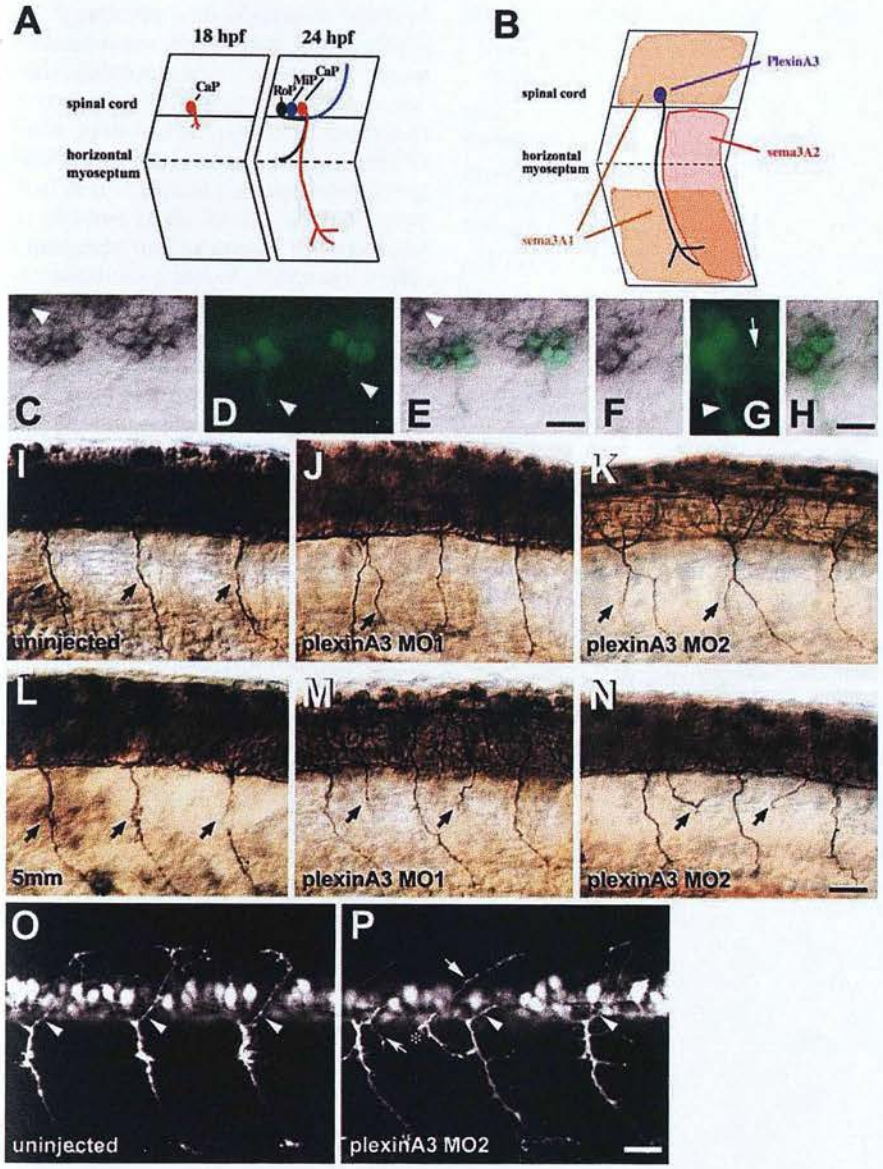

Figure 2. Expression and function of plexinA3 in primary motor neurons. ***A***, ***B***, A schematic representation of the outgrowth of primary motor axons, which is preceded by the CaP axon at ~18 hpf, is given in a lateral view of one trunk segment in ***A***. ***B***, The distribution of semaphorin ligands relative to the ventral motor axon pathway. ***C–H***, *In situ* hybridization of plexinA3 mRNA shows expression in clusters of GFP-immunopositive motor neurons of hb9:GFP transgenic fish in lateral views at 24 hpf. ***C–E***, A caudal region in which CaP axons (***D***, arrowheads) are just growing out. The arrowhead in ***C*** and ***E*** depicts a more dorsal, GFP-immunonegative cell that shows strong expression of plexinA3 mRNA. At higher magnification in ***F–H***, two adjacent intensely plexinA3 mRNA-positive neurons in a more rostral segment are depicted. These are likely the CaP (right cell) and MiP (left cell) motor neurons, judging by the trajectories of the GFP-positive MiP (arrow) and CaP (arrowhead) axons. ***I–N***, Lateral views at midtrunk levels of anti-tubulin-labeled whole-mounted 24 hpf embryos are shown. In uninjected embryos (***I***) or those injected with 1 mM plexinA3, 5 mm morpholino (5 mm; ***L***), single unbranched motor nerves (arrows in ***I*** and ***L***) grow ventrally out of the spinal cord. Injection of 1 mM plexinA3 morpholino1 (MO1) induces branching (arrow in ***J***) or a second spinal exit point for motor nerves per hemisegment (arrows indicate additional nerves in ***M***). Injection of 1 mM plexinA3 morpholino2 (MO2) also induced aberrant branching (***K***, arrows) of the ventral motor nerve and additional nerves exiting the spinal cord (***N***, arrows). ***O***, ***P***, Axons in the dorsal MiP pathway are visualized in hb9:GFP transgenic fish in selected confocal image stacks at 31 hpf, indicating normal growth in uninjected embryos (***O***, arrowheads), and excessive branching (curved arrow in ***P***) and supernumerary nerves (straight arrow in ***P***) in 1 mM plexinA3 morpholino2-injected embryos. The asterisk in ***P*** indicates an additional nerve exit point with a dorsal and ventral nerve branch exiting the spinal cord. Arrowheads in ***P*** point to normal appearance of axons in the dorsal motor axon pathway. Rostral is left in ***A*** to ***P***. Scale bars (in ***E***) ***C–E***, 25 μm; (in ***H***) ***F–H***, 12.5 μm; (in ***N***) ***I–N***, 25 μm; (in ***P***) ***O***, ***P***, 25 μm.

Several other axonal structures labeled in anti-tubulin immunohistochemistry, such as commissures and the dorsoventral diencephalic tract in the head, as well as the posterior lateral line nerve and sensory Rohon-Beard axons, appeared unaffected by plexinA3 knock-down (data not shown). The trigeminal ganglion, which shows defasciculation in its ophthalmic branch in plexinA3 deficient mice (Cheng et al., 2001; Yaron et al., 2005), appeared normal and contained 15.3 ± 0.61 (1 mM morpholino1) and 15.7 ± 0.64 (1 mM morpholino2) primary axon branches in morpholino-treated animals, which was not significantly different from embryos injected with 5 mm morpholino (16.4 ± 0.65; $p > 0.1$) (supplemental Fig. 2*C–E*, available at www.jneurosci.org as supplemental material).

Morpholino phenotypes are rescued by RNA overexpression and are not because of alterations of the trunk environment

Overexpression of a full-length myc-tagged plexinA3 mRNA had no effect on motor axon growth as determined by anti-tubulin immunohistochemistry at 24 hpf (data not shown). However, coinjection of plexinA3 morpholino2 (titrated to 0.3 mM) with mRNA that does not have a binding sequence for the morpholino, led to a strong and significant reduction in the frequency of both abnormal branching (13% affected embryos) and additional exits (16% affected embryos). This was compared with injection of 0.3 mM plexinA3 morpholino2 alone at 24 hpf (embryos affected by branching: 87%, $p < 0.0001$; embryos affected by additional exits: 49%, $p < 0.01$) (Table 1).

Analysis of markers of the horizontal and vertical myosepta, as well as spinal floorplate, motor neuron somata, commissural primary ascending interneurons in the spinal cord, and Mauthner neurons with their spinal axons, indicated normal differentiation of these structures after injection of 1 mM plexinA3 morpholino1 (supplemental Fig. 3, available at www.jneurosci.org as supplemental material).

Genetic interactions of plexinA3 with sema3A1 and sema3A2

To show synergisms of plexinA3 with potential ligands and coreceptors, we performed pairwise coinjections of morpholinos at subthreshold concentrations that did not elicit a phenotype in single-injection experiments. Coinjections of sema3A1 (2 mM) and sema3A2 (2 mM) morpholinos with plexinA3 morpholino1 (0.1 mM) at subthreshold concentrations induced significant branching (sema3A1, 60% affected embryos; sema3A2, 34% affected embryos) and additional exits (sema3A1, 38% affected embryos; sema3A2, 52% affected embryos) compared with embryos coinjected with 0.1 mM plexinA3 5 mm morpholino and 2 mM sema3A1 morpholino

(20% embryos with aberrantly branched ventral motor nerves and 19% embryos with additional exits of ventral motor nerves) (Fig. 3). Coinjections of morpholinos against the potential coreceptor NRP1a (0.1 mM) and against plexinA3 (0.1 mM) at subthreshold concentrations (Fig. 3) (Feldner et al., 2005) were ineffective. These experiments suggest the possibility that plexinA3 is part of a receptor complex for sema3A1 and sema3A2. Differences in the magnitude of synergistic effects that are strongest for branching when sema3A1 morpholinos are coinjected with plexinA3 morpholinos or multiple exits when sema3A2 morpholinos are used suggest specific roles of the two sema3A paralogs.

Table 1. Effects of morpholino treatment on ventral motor nerves

Injection type (plexinA3 morpholinos)	*n*	Embryos with aberrant ventral motor nerve branching (%)	Embryos with additional exits of ventral motor nerves (%)
Vehicle	53	11.5 ± 7.3	4.4 ± 2.4
PlexinA3 5 mm MO (1 mM)	51	13.8 ± 5.3	12.0 ± 0.3
PlexinA3 MO1 (0.25 mM)	53	26.0 ± 10.4	17.5 ± 5.2
PlexinA3 MO1 (0.5 mM)	65	43.2 ± 14.7**	56.0 ± 11.7***
PlexinA3 MO1 (1 mM)	68	63.8 ± 7.3***	93.9 ± 2.7***
PlexinA3 MO2 (1 mM)	66	82.9 ± 6.5***	94.7 ± 2.5***
Rescue experiments			
PlexinA3 MO2 (0.3 mM) alone	42	87.3 ± 3.5	48.8 ± 12.5
PlexinA3 MO2 (0.3 mM) plus plexinA3 mRNA	47	12.7 ± 4.4***	15.7 ± 15.7**

Morpholino doses are indicated in parentheses. *n*, Numbers of embryos analyzed; MO, morpholino; plexinA3 MO1/MO2, morpholino1/2 against plexinA3; plexinA3 5 mm MO, morpholino with five mismatched bases based on plexinA3 morpholino1. $^{**}p < 0.01$; $^{***}p < 0.001$; Fisher's exact test.

Discussion

Relatively little is known about the contribution of the plexin coreceptors to the guidance of pioneer axons by semaphorins *in vivo*. Here, we identify plexinA3 as a key player for correct spinal exit of primary motor axons and unbranched growth of primary nerves in the trunk of zebrafish. Double knock-down experiments suggest a complex interplay of ligands in the trunk environment and receptor components in primary motor neurons.

PlexinA3 expression in motor neurons is pivotal for motor axon growth. Up to 95% of plexinA3 morpholino-injected embryos showed specific types of aberrations, and 30% of all hemisegments analyzed were aberrant. This effect is larger than that found in comparable studies of other proteins in motor axon growth (Feldner et al., 2005; Sato-Maeda et al., 2006). Two sequence-independent morpholinos yielded identical results, and all of the phenotypes were almost completely rescued by supplementing plexinA3 by overexpression. Using various markers, we could not find detectable changes in other axons or the spinal cord and trunk structures of morpholino-treated embryos. This suggests a major and specific function of plexinA3 in primary motor neurons.

PlexinA3 in dorsal and ventral motor axons may be necessary to correctly integrate repellent cues from semaphorins during axon outgrowth. The receptor knock-down phenotypes observed showed additional exits from the spinal cord and branching of the ventral and dorsal motor nerve that are consistent with a release of axon growth from environmental restrictions. Indeed, class 3 semaphorins are expressed in the trunk environment (Fig. 2*B*) and are thought to signal through plexin receptors. Synergistic effects in double morpholino injections of plexinA3 with sema3A homologs support a role for plexinA3 as a signal-transducing receptor component for repellent sema3A signals. Also consistent with such an interaction, knock-down of sema3A1 alone induces similar phenotypes to plexinA3 knock-down, including aberrant branching. However, shortened axons were also observed to a lesser extent (Sato-Maeda et al., 2006). Conversely, overexpression of sema3A1 or sema3A2 mainly induces reduced growth of motor axons (Roos et al., 1999; Halloran et al., 2000). In mammals, plexinA3 also mediates semaphorin-induced pruning of axonal branches (Bagri et al., 2003). However, pruning appears not to be prominent during primary motor axon differentiation (Liu and Westerfield, 1990).

We provide evidence for subtle differences in the function of the two zebrafish homologs of sema3A for ventral motor nerve growth. Coinjections of plexinA3 and sema3A1 morpholinos primarily induced nerve branching, whereas coinjections of plexinA3 and sema3A2 morpholinos primarily induced additional nerve exits. This may be explained by differential distribution of the ligands (schematically shown in Fig. 2*B*). Sema3A mRNA is only expressed in the dorsal and ventral myotome, leaving a corridor free of sema3A1 mRNA expression that includes the ventral edge of the spinal cord. Sema3A1 may therefore be more important during ventral growth when axons have ex-

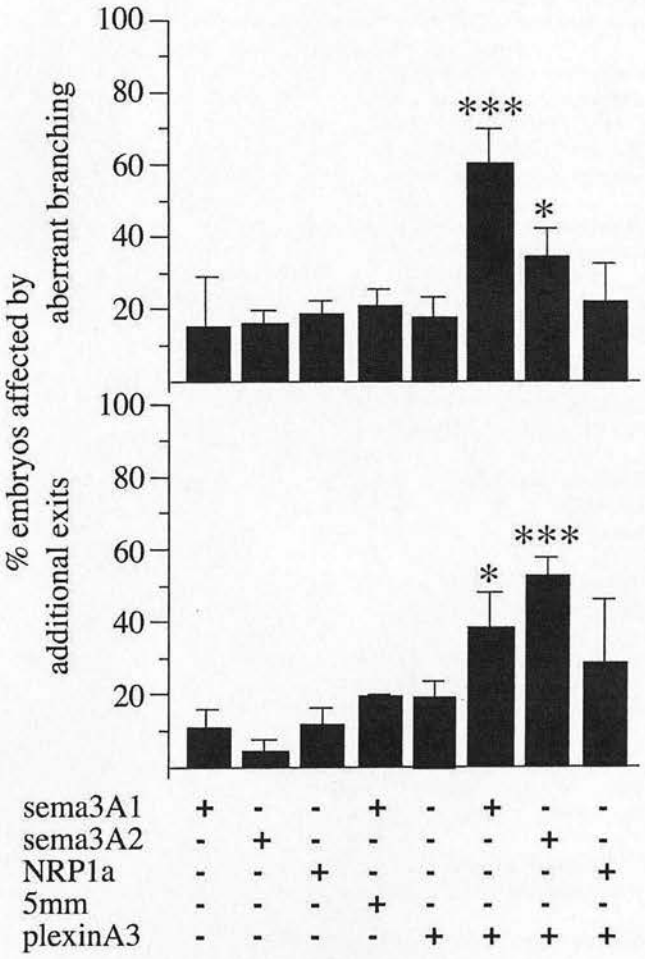

Figure 3. Combining plexinA3 with semaphorin morpholinos has synergistic effects. 5 mm, Control morpholino based on plexin morpholino 1 with five mismatched bases. For concentrations, see Results. $^{*}p < 0.05$; $^{***}p < 0.001$.

ited the spinal cord (Sato-Maeda et al., 2006). In contrast, sema3A2 mRNA is expressed continuously along the dorsoventral axis of the somite, including the level of nerve exit from the spinal cord but only in the caudal part of the somite (Roos et al., 1999). Thus, sema3A2 could restrict additional spinal exit points of motor nerves in the caudal part of the somite. Under plexinA3 knock-down conditions, consequently, 73% of the additional exits that were not exactly at the border between two segments occurred in the caudal half of the somite. Moreover, most aberrant nerve branches (82%) were also directed caudally. This bias may indicate a loss of sensitivity to a repellent sema3A2 activity in the caudal half of the somite under plexinA3 knock-down conditions. However, it is still unknown what keeps nerves from branching rostrally and from exiting the spinal cord in the rostral half of the somite (Bernhardt et al., 1998).

Interestingly, combined injections of morpholinos to NRP1a and plexinA3 did not produce synergistic effects, although single knock-down of plexinA3 and NRP1a did induce partially overlapping phenotypes (nerve branching, additional exits). It is possible that efficiency/concentrations of morpholinos were not suitable to reveal such a possible interaction. However plexinA3 appears to preferentially associate with NRP2 in mammals (Cheng et al., 2001). A homolog of NRP2, NRP2b, is also expressed in primary motor neurons in zebrafish (gene expression database: http://zfin.org/cgi-bin/webdriver?MIval=aa-xpatselect.apg). Moreover, there is at least one additional class 3 semaphorin expressed in the trunk of zebrafish, sema3G, which could influence motor axon growth (Stevens and Halloran, 2005). PlexinA1, which has not yet been cloned in zebrafish, may also play a role in the motor neuron system. Interestingly, the requirement for plexinA3 in specific axons in zebrafish appears to differ from that in mice: a plexinA3-deficient mouse shows fasciculation defects of trigeminal axons but apparently normal motor axon growth (Cheng et al., 2001; Yaron et al., 2005), whereas in zebrafish, motor axons but not trigeminal axons are affected by plexinA3 knock-down.

The anatomical simplicity of the primary motor system in zebrafish makes it an excellent tool to unravel the *in vivo* interactions of several ligands and their receptors that determine the outgrowth of pioneer axons. It will, for example, be interesting to find out whether mutations in the semaphorin signaling cascade will be discovered in genetic screens (Birely et al., 2005; Gulati-Leekha and Goldman, 2006). We conclude that growth and path finding of primary motor axons in zebrafish is governed by a complex interplay of different semaphorin ligands and receptors of which plexinA3 is a crucial component. Forward and reverse genetic approaches have the potential to elucidate path finding of pioneer axons in this *in vivo* model in unprecedented detail.

References

Bagri A, Cheng HJ, Yaron A, Pleasure SJ, Tessier-Lavigne M (2003) Stereotyped pruning of long hippocampal axon branches triggered by retraction inducers of the semaphorin family. Cell 113:285–299.

Beattie CE (2000) Control of motor axon guidance in the zebrafish embryo. Brain Res Bull 53:489–500.

Becker T, Becker CG, Schachner M, Bernhardt RR (2001) Antibody to the HNK-1 glycoepitope affects fasciculation and axonal pathfinding in the developing posterior lateral line nerve of embryonic zebrafish. Mech Dev 109:37–49.

Becker T, Ostendorff HP, Bossenz M, Schlüter A, Becker CG, Peirano RI, Bach I (2002) Multiple functions of LIM domain-binding CLIM/NLI/Ldb cofactors during zebrafish development. Mech Dev 117:73–83.

Bernhardt RR, Schachner M (2000) Chondroitin sulfates affect the formation of the segmental motor nerves in zebrafish embryos. Dev Biol 221:206–219.

Bernhardt RR, Goerlinger S, Roos M, Schachner M (1998) Anterior-posterior subdivision of the somite in embryonic zebrafish: implications for motor axon guidance. Dev Dyn 213:334–347.

Birely J, Schneider VA, Santana E, Dosch R, Wagner DS, Mullins MC, Granato M (2005) Genetic screens for genes controlling motor nerve-muscle development and interactions. Dev Biol 280:162–176.

Cheng HJ, Bagri A, Yaron A, Stein E, Pleasure SJ, Tessier-Lavigne M (2001) Plexin-A3 mediates semaphorin signaling and regulates the development of hippocampal axonal projections. Neuron 32:249–263.

Chenna R, Sugawara H, Koike T, Lopez R, Gibson TJ, Higgins DG, Thompson JD (2003) Multiple sequence alignment with the Clustal series of programs. Nucleic Acids Res 31:3497–3500.

Feldner J, Becker T, Goishi K, Schweitzer J, Lee P, Schachner M, Klagsbrun M, Becker CG (2005) Neuropilin-1a is involved in trunk motor axon outgrowth in embryonic zebrafish. Dev Dyn 234:535–549.

Flanagan-Steet H, Fox MA, Meyer D, Sanes JR (2005) Neuromuscular synapses can form in vivo by incorporation of initially aneural postsynaptic specializations. Development 132:4471–4481.

Giger RJ, Cloutier JF, Sahay A, Prinjha RK, Levengood DV, Moore SE, Pickering S, Simmons D, Rastan S, Walsh FS, Kolodkin AL, Ginty DD, Geppert M (2000) Neuropilin-2 is required in vivo for selective axon guidance responses to secreted semaphorins. Neuron 25:29–41.

Gulati-Leekha A, Goldman D (2006) A reporter-assisted mutagenesis screen using alpha 1-tubulin-GFP transgenic zebrafish uncovers missteps during neuronal development and axonogenesis. Dev Biol 296:29–47.

Halloran MC, Sato-Maeda M, Warren JT, Su F, Lele Z, Krone PH, Kuwada JY, Shoji W (2000) Laser-induced gene expression in specific cells of transgenic zebrafish. Development 127:1953–1960.

Huber AB, Kania A, Tran TS, Gu C, De Marco Garcia N, Lieberam I, Johnson D, Jessell TM, Ginty DD, Kolodkin AL (2005) Distinct roles for secreted semaphorin signaling in spinal motor axon guidance. Neuron 48:949–964.

Kameyama T, Murakami Y, Suto F, Kawakami A, Takagi S, Hirata T, Fujisawa H (1996) Identification of plexin family molecules in mice. Biochem Biophys Res Commun 226:396–402.

Kimmel CB, Ballard WW, Kimmel SR, Ullmann B, Schilling TF (1995) Stages of embryonic development of the zebrafish. Dev Dyn 203:253–310.

Kruger RP, Aurandt J, Guan KL (2005) Semaphorins command cells to move. Nat Rev Mol Cell Biol 6:789–800.

Lee P, Goishi K, Davidson AJ, Mannix R, Zon L, Klagsbrun M (2002) Neuropilin-1 is required for vascular development and is a mediator of VEGF-dependent angiogenesis in zebrafish. Proc Natl Acad Sci USA 99:10470–10475.

Liu DW, Westerfield M (1990) The formation of terminal fields in the absence of competitive interactions among primary motoneurons in the zebrafish. J Neurosci 10:3947–3959.

Maestrini E, Tamagnone L, Longati P, Cremona O, Gulisano M, Bione S, Tamanini F, Neel BG, Toniolo D, Comoglio PM (1996) A family of transmembrane proteins with homology to the MET-hepatocyte growth factor receptor. Proc Natl Acad Sci USA 93:674–678.

Miyashita T, Yeo SY, Hirate Y, Segawa H, Wada H, Little MH, Yamada T, Takahashi N, Okamoto H (2004) PlexinA4 is necessary as a downstream target of Islet2 to mediate Slit signaling for promotion of sensory axon branching. Development 131:3705–3715.

Patel NH, Martin-Blanco E, Coleman KG, Poole SJ, Ellis MC, Kornberg TB, Goodman CS (1989) Expression of engrailed proteins in arthropods, annelids, and chordates. Cell 58:955–968.

Roos M, Schachner M, Bernhardt RR (1999) Zebrafish semaphorin Z1b inhibits growing motor axons in vivo. Mech Dev 87:103–117.

Sato-Maeda M, Tawarayama H, Obinata M, Kuwada JY, Shoji W (2006) Sema3a1 guides spinal motor axons in a cell- and stage-specific manner in zebrafish. Development 133:937–947.

Schweitzer J, Becker T, Lefebvre J, Granato M, Schachner M, Becker CG (2005) Tenascin-C is involved in motor axon outgrowth in the trunk of developing zebrafish. Dev Dyn 234:550–566.

Stevens CB, Halloran MC (2005) Developmental expression of sema3G, a novel zebrafish semaphorin. Gene Expr Patterns 5:647–653.

Tongiorgi E (1999) Tenascin-C expression in the trunk of wild-type, cyclops and floating head zebrafish embryos. Brain Res Bull 48:79–88.

Yaron A, Huang PH, Cheng HJ, Tessier-Lavigne M (2005) Differential requirement for Plexin-A3 and -A4 in mediating responses of sensory and sympathetic neurons to distinct class 3 Semaphorins. Neuron 45:513–523.